Using Induced Pluripotent Stem Cells to model the Pathophysiology of Schizophrenia

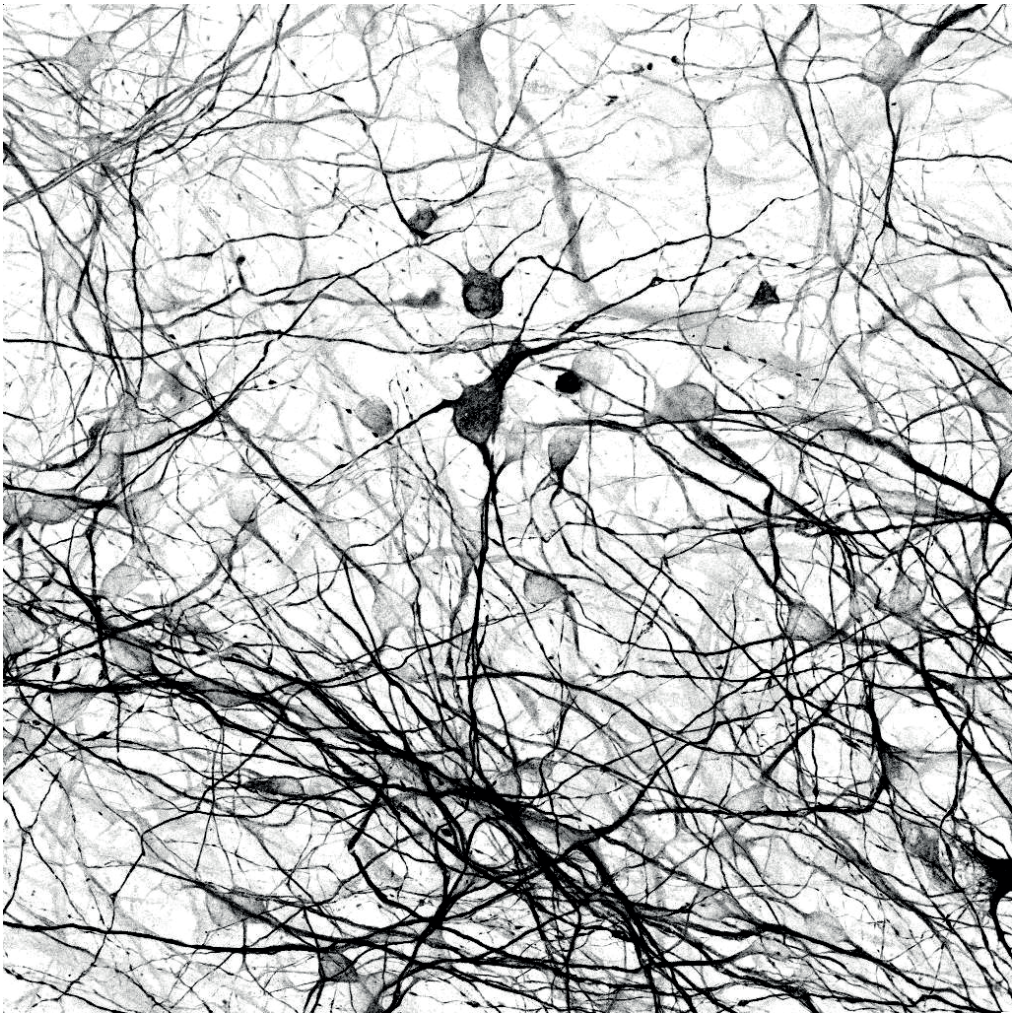

Nilhan Günhanlar

Using Induced Pluripotent Stem Cells to model the Pathophysiology of Schizophrenia

Nilhan Günhanlar

Cover shows Induced Pluripotent Stem Cell derived neurons (front) and Oligodendrocyte Precursor Cells (back)
Cover and Layout design: Nilhan Günhanlar

Printing of this thesis was kindly supported by Erasmus MC, University Medical Center Rotterdam

ISBN: 978-94-6299-333-4
Printing: Ridderprint B.V., Ridderkerk

Using Induced Pluripotent Stem Cells to model the Pathophysiology of Schizophrenia

Het gebruik van geïnduceerde pluripotente stamcellen om de pathofysiologie van schizofrenie te modeleren

Thesis

to obtain the degree of Doctor from the
Erasmus University Rotterdam
by command of the rector magnificus

Prof.dr. H.A.P. Pols

and in accordance with the decision of the Doctorate Board

The public defense shall be held on
Wednesday 18 May 2016 at 15.30 o'clock

by

Nilhan Günhanlar
born in Nicosia, Cyprus

Erasmus University Rotterdam

Doctoral Committee

Promotor:	Prof.dr. S.A. Kushner
Co-promoter:	Dr. F.M.S. de Vrij
Other Members:	Prof.dr. J.H. Gribnau Prof.dr. Y. Elgersma Prof.dr. E.M. Hol

“anneme ve babama”

...for my parents...

CONTENTS

Abbreviations

iPSC	Induced Pluripotent Stem Cell
hiPSC	Human Induced Pluripotent Stem Cell
NPC	Neural Precursor Cell
OPC	Oligodendrocyte Precursor Cell
GPC	Glial Precursor Cell
CNS	Central Nervous System
GWAS	Genome-Wide Association Study
DISC1	Disrupted in Schizophrenia 1
NRG1	Neuroregulin 1
SNP	Single Nucleotide Polymorphism
ER	Endoplasmic Reticulum
mRNA	Messenger RNA
ES cells	Embryonic Stem cells
EBs	Embryoid bodies
hNuc	Human Nuclear Antigen
MBP	Myelin Basic Protein
bFGF/FGF-2	Basic Fibroblast Growth Factor
PDGFRa	Platelet-Derived Growth Factor Receptor, Alpha
CSPG4	Chondroitin Sulfate Proteoglycan 4
CS-GAG	Chondroitin Sulfate Glycosaminoglycan
NG2	Neural/Glial antigen 2
MHC	Major Histocompatibility Complex
TF	Transcription Factor
XCI	X Chromosome Inactivation
XCR	X Chromosome Reactivation
2D	Two-Dimensional
3D	Three-Dimensional
PD	Parkinson’s disease
ALS	Amyotrophic Lateral Sclerosis
MS	Multiple Sclerosis
BAC	Bacterial Artificial Chromosome

Aim and Scope of the Thesis

Schizophrenia is a quite common psychotic disorder, affecting ~1% of the general population. However, there is yet no satisfying explanation for the underlying biological mechanism due to the extraordinary complexity of the brain and the difficulties inherent in studying human neurophysiology. The overall aim of this thesis is to create a cellular model for schizophrenia using induced pluripotent stem cells (iPSCs). Applying iPSC technology in psychiatry allows for the first time the opportunity to study living patient-specific neural cells that has the potential to be implemented across a wide range of psychiatric and neurological disorders.

Chapter 1 of this thesis is a general introduction on the clinical features and cellular pathophysiology of schizophrenia. It includes a review of genetic studies and iPSC technology to study schizophrenia together with the recent development of differentiation protocols for generating neural cells from iPSCs. **Chapter 2** describes the development of a neural differentiation protocol from iPSCs that results in spontaneously active networks of neurons and glia, confirmed by electrophysiology and confocal imaging. **Chapter 3** describes generation of oligodendrocyte precursor cells (OPCs) from iPSCs-derived neural precursor cells. In several studies, schizophrenia has been associated with white matter abnormalities; therefore generation of oligodendrocyte lineage cells might provide insight into the mechanisms underlying these disorders. **Chapter 4** utilizes patient-specific iPSCs to model the cellular neuropathology of schizophrenia in a family with a high incidence of schizophrenia. High-resolution exome sequencing on DNA isolated from blood samples of patients and their healthy siblings identifies a missense coding mutation in the *CSPG4* gene as the causal genetic variant, which has particularly abundant expression in OPCs. Characterization of iPSC-derived neural cells of patients and their healthy siblings demonstrated a highly specific alteration in OPCs. Finally, **Chapter 5** provides a general discussion of the findings, together with future perspectives.

Chapter 1

Introduction

SCHIZOPHRENIA AS A PSYCHOTIC DISORDER

Psychotic disorders are severe mental illnesses in which the underlying etiology remains largely unknown. Symptoms of psychotic disorders can be clustered into three main categories: (i) positive symptoms; psychosis e.g. delusions and hallucinations (ii) negative symptoms; lack of motivation, reduction in spontaneous speech, and social withdrawal (iii) cognitive symptoms; alterations in neurocognition e.g. difficulties in memory, attention, and executive functioning[1].

Schizophrenia affects ~1% of the general population for which the primary pathophysiology is enigmatic. The illness develops in adolescence and early adulthood between the ages of 16 and 30 years and persists throughout the patient's lifetime[2,3]. The incidence rate of schizophrenia is similar across different countries, cultures and sexes. Genetic, early environmental, neurobiological, psychological and social factors are important influences for the onset[4–7]. In some cases, social and cognitive impairments can be noticeable earlier than the first episode[8]. On the other hand, the onset can also manifest suddenly in well functioning individuals. Antipsychotic treatment with dopamine receptor 2 antagonists are well demonstrated to have efficacy for delusions and hallucinations, but not for cognitive impairments and negative symptoms[1,9,10]. In addition, psychosocial treatments are supportive for patients. Examples include family intervention, supported employment, cognitive-behavior therapy for psychosis, social and self-management skills training and integrated treatment for co-occurring substance misuse.

Several studies indicate that schizophrenia is a complex neurodevelopmental disorder that might arise from a variety of functional abnormalities. Initially, a study reporting psychosis associated with temporal lobe epilepsy mimicking schizophrenia[11] was used to support a neurodevelopmental model of schizophrenia[12]. In addition, several subsequent post mortem, brain imaging and genetic studies have together implied the model that schizophrenia is a neurodevelopmental disorder[9]. In a neurodevelopmental model, changes occur in the Central Nervous System (CNS) througout development that have long-term effects during the entire lifespan of schizophrenia patients. Remarkably, one of the key neuropathological findings in schizophrenia research was reported by post mortem studies showing distinguished features such as reduced synaptic spine densities on neurons[13–15] and grey matter loss[8,16] which might be the result of excessive synaptic pruning during adolescence. In addition, multiple neurodevelopmental factors such as season of birth, maternal influenza, obstetric complications and CT/MRI scans confirm correlations with the incidence of schizophrenia[1]. There are also other models, e.g. the dopamine hypothesis, white matter abnormalities and genetic findings explaining the pathophysiology of schizophrenia.

Overall, findings indicate that schizophrenia is a complex disorder that might arise from a variety of functional abnormalities. The following paragraphs discuss further about the possible pathophysiological models of schizophrenia.

PATHOPHYSIOLOGICAL MODELS OF SCHIZOPHRENIA

The role of dopamine and glutamate dysfunction

An altered excitatory-inhibitory balance during neurodevelopment has been widely hypothesized as a possible disease mechanism of schizophrenia[17]. Excitatory-inhibitory balance alterations have been explained by two possible mechanisms: a) changes in dopaminergic signaling, and b) NMDA-dependent inhibitory GABA interneuron malfunctioning[18,19].

The Dopamine 2 receptor (D2) is known for its affinity for antipsychotics. Increased dopamine production was observed during psychosis in the striatum of a patient with schizophrenia[20]. Blocking D2 receptors is not a

disease-modifying treatment for schizophrenia, however it functions to reduce the severity of positive symptoms, such as hallucinations and delusions but not the negative or cognitive symptoms. Also, most patients with schizophrenia are supersensitive to dopamine, which correlates with findings in animal models of psychosis that show genetic risk factors related to dopamine[20].

Even though D2 receptor antagonists reduce positive symptoms, negative symptoms and the cognitive deficits of schizophrenia patients such as attention problems and working memory deficits cannot be improved. Lower glutamate levels related to impaired cognitive functioning were shown in patients with schizophrenia in whom glutamate levels predicted task performance[21]. Thus, cognitive symptoms might imply dysfunctioning of glutamatergic neurons in schizophrenia. A possible mechanism is reduced activity of the NMDA-type glutamate receptor, which reduces the excitation of GABA inhibitory interneurons in the prefontal cortex[19,22]. Reduced excitation of GABA inhibitory interneurons disinhibits glutamatergic pyramidal neurons, thereby resulting in excessive stimulation by glutamate, which might cause neuronal damage by exocytosis.

Dopamine and glutamate dysfunction possibly converge[18]. In this scenario, augmented signals travel along glutamatergic pyramidal neurons to the brainstem and over-stimulate dopamine neurons and GABA inhibitory interneurons. Over-stimulated dopamine neurons carry enhanced signals to the midbrain, which results in high dopamine levels in the Nucleus Accumbens leading to "positive symptoms" such as hallucinations. Inversely, hypo-active dopamine neurons that are suppressed by over-stimulated GABA inhibitory interneurons carry discontinuous dopamine to the prefrontal cortex which results in low amounts of dopamine released, leading to "negative symptoms" such as anxiety or social withdrawal. Overall, it is not well defined if the effects linked to dopamine D2 receptors or interneuron NMDA receptors are the effect or the cause of schizophrenia.

White Matter abnormalities and schizophrenia

Neuroimaging techniques suggest evidence for the involvement of glial biology in the pathophysiology of schizophrenia, such as alterations in oligodendrocytes, myelination and white matter integrity[23–30]. White matter of the brain is composed of neuronal axons and myelin. Oligodendrocytes myelinate axons thereby providing metabolic support to surrounding neurons. Oligodendrocytes support axonal integrity and defects in oligodendrocytes can cause axonal degeneration[31]. Oligodendrocyte dysfunctioning has been associated with severe lethal neurological disorders such as multiple sclerosis[32] and amyotrophic lateral sclerosis (ALS)[33] and with psychiatric disorders such as bipolar disorder and schizophrenia[34,35]. Interestingly, some myelin defects trigger neuroinflammation that might further lead to neurodegeneration[36,37]. In the last decade, an increasing number of studies hypothesize that oligodendrocyte and oligodendrocyte-related myelin dysfunctioning can cause schizophrenia[34,35,38,39]. In line with these hypotheses, the late adolescent critical period for cerebral cortex myelination overlaps closely with the age of onset for schizophrenia[40–42]. Overall, these studies have diverged from the long-standing neuronal synapse and neurotransmitter-based hypothesis as the predominant cause of schizophrenia. Nevertheless, not much is known about the definitive mechanism of alterations in white matter integrity associated with schizophrenia.

The role of inflammation in schizophrenia

It has been long hypothesized that the immune system may be involved in the pathology of schizophrenia. Remarkably, an increased inflammatory status of the brain was shown in patients with schizophrenia. For instance, increased pro-inflammatory substances that activate microglia, which are the phagocytic

immune cells of the CNS, have been defined in brain tissue and cerebrospinal fluid of schizophrenia patients[43,44]. Moreover, ~15% of CNS-residing cells are microglia and in schizophrenia patients, there is a shift from resting to activated microglia[45,46]. Activated microglia produce cytokines, radical oxygen species and other neurotoxic substances that can damage the neural cells[47], thereby creating a microenvironment that might result in a disease phenotype. On the other hand, increased inflammation might be a result of infectious agents, genetic defects, reactions to lesions from traumata and toxins[48]. Remarkably, the major histocompatibility complex (MHC) locus has been consistently the top Genome-Wide Association Study (GWAS) finding in the largest schizophrenia studies of common genetic variation. This locus has a role in immunity, containing genes that encode antigen-presenting molecules. Recently, increased expression of the MHC gene locus gene C4A was found in the brains of patients with schizophrenia[49]. C4A protein is known for its role in mediating synapse elimination in mice. Thus, C4A overexpression might lead to overstimulation of microglia and elimination of synapses during adolescence that ultimately might results in schizophrenia pathogenesis.

GENETIC STUDIES IN SCHIZOPHRENIA RESEARCH

In many cases positive family history is the strongest predictor for developing schizophrenia[50–52]. The risk of having schizophrenia among identical twins is much higher than fraternal twins, which further supports the genetic contribution of the disorder[53]. Remarkably, recent meta-analysis based on fifty years of twin studies found a monozygotic twin correlation of 0.76 ± 0.018 and a heritability estimate of 0.77 ± 0.051 whereas limited contribution of shared environmental influences was found (0.013 ± 0.025)[54].

Genetic epidemiology studies have identified chromosomal variations related to schizophrenia[55]. Single nucleotide polymorphism (SNP) data from several studies show variation in genes on different chromosomes from patients with schizophrenia such as in the MHC region on chromosome 6, neuregulin 1 (NRG1) on chromosome 8, ZNF804A on chromosomes 2 and TCF4 on 18[56,57]. Also, 43 candidate genes have been identified, showing evidence for high heritability[58,59]. A recent paper of the Psychiatric Genomics Consortium identified 128 genome-wide significant SNPs in 108 independent genomic loci from 36,989 cases and 113,075 controls, however the odds ratios remain small[60]. In contrast, rare variants may have stronger causative effects such as copy number variants and translocations[61]. Replication for such variants can be difficult as shown for example by the DISC1 translocation that was found in one Scottish family[62]. Nevertheless, these rare variants can provide important understanding of the pathophysiology of the disorder. Interestingly, some of these variants are known as neurodevelopmental genes that have a role in neuronal proliferation, migration or synapse formation[63]. For instance, NRG1 and DISC1 control the expression of splice variants in the prefrontal cortex during brain development[64–66]. Also, a mouse model in which DISC1 is transiently knocked down, shows behavioral changes related to the frontal cortex and neurochemical abnormalities[67]. Interestingly, there exists considerable overlap with the genetics of autism and schizophrenia[68,69] which proposes some genomic modifiers or environmental factors that determine the specific syndrome. Together with genetic studies, cohort studies also indicate that schizophrenia is a developmental disorder, reporting that patients show problems at earlier ages[70,71] for example early-reduced IQ and a history of delayed maturation.

Various schizophrenia mouse models exist as reviewed in Jones et al.[72] to study the effect of specific genes on drug testing and behavioural tests. For example, the DISC1 mouse model has been used for studying gene-environment interactions in schizophrenia[73]. Nevertheless, even though some memory, social behavior and motivation tests can be applied, it is challenging to measure human specific symptoms in animal models.

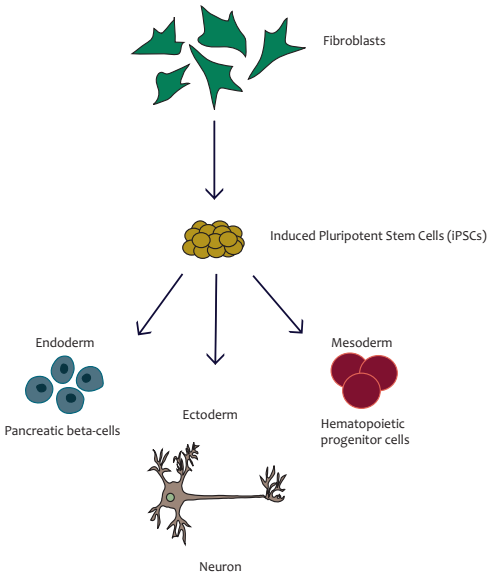

Figure 1. Generation of Induced Pluripotent Stem Cells (iPSCs)
iPSCs are generated from somatic cells, e.g. adult fibroblast by introduction of pluripotency transcription factor. iPSCs are able to differentiate into all three germ-layers cells, endoderm (pancreatic beta cells), mesoderm (hematopoietic progenitor cells) and ectoderm (neurons).

INDUCED PLURIPOTENT STEM CELLS TO MODEL PSYCHIATRIC DISORDERS

Due to the extraordinary complexity of the brain and the difficulties inherent in studying the pathology of the CNS, psychiatry in general has suffered tremendously from a lack of good research models. Induced pluripotent stem cell (iPSC) technology provides for the first time an opportunity to study the development of the disorder by using living neural cells of patients with schizophrenia.

During development, all types of cells in the body are generated from a pluripotent state to a differentiated state of the cells. Previously, terminal differentiation was considered to be an irreversible developmental process, in which differentiated cells are unable to return to the pluripotent state. However, reprogramming of mature cells to a pluripotency state can be achieved by forced overexpression of pluripotency factors. iPSC technology achieves dedifferentiation from differentiated cells (somatic cells) back to the undifferentiated state (pluripotent stem cells) by induced expression of pluripotency transcription factors (TFs) Oct4, Sox2, Klf4 and c-Myc **(Figure 1)**. Pluripotency TFs are expressed in stem cells and upon differentiation to somatic cells their expression level is downregulated. iPSC technology was first described in 2006 by Takahashi and Yamanaka[74] which was acknowledged with the Nobel Prize in Medicine or Physiology in 2012. Due to the ability for self-renewal and differentiation into all three germ layers (mesoderm, endoderm and ectoderm), iPSCs are considered embryonic-like stem cells.

iPSCs were first generated by reprogramming mouse fibroblasts, which was later reproduced in human fibroblasts followed by the development of the technique from different somatic cells lines such as peripheral blood cells, NSCs, keratinocytes and amniotic cells by using different reprogramming vectors[75].

Nevertheless, in many studies, fibroblasts from skin biopsies are still the standard cell type for reprogramming. In Takahashi and Yamanaka et al.(2006), lentiviral vectors for each TF were used for reprogramming[74]. However, integration of the viral vectors into the host genome creates a risk of tumor formation in iPSCs[76]. Because the pluripotency TF c-Myc is an oncogene, several strategies were developed to avoid tumor formation, such as reprogramming without c-Myc[77], with another Myc family member L-Myc[78], and by using inducible lentiviral vectors[79]. In addition, reprogramming techniques have been developed using non-viral vectors such as cDNA plasmids[80], episomal vectors[81], mini-circle vectors[82], RNAs, small molecules and chemical compounds[83,84] to prevent tumor formation in iPSCs. Even though reprogramming by non-viral/non integrating vectors has much lower reprogramming efficiency than by viral vectors, for clinical purposes aimed at replacement therapy, nonviral/non-integrating vectors are preferred to circumvent any chance of modifying the genetic integrity of the patient cells[85].

Protocols for generation of iPSCs-derived neural lineages

The derivation of neurons from iPSCs was first described by Takahashi and Yamanaka[74]. In this study, early neuronal structures were observed after 2 weeks of differentiation, which were positive for Tyrosine Hyrdoxylase and βIII tubulin, however not for GFAP+ astrocytes and late neuronal markers. Protocols for the generation of human iPSCs-derived neural cells were adapted from embryonic stem (ES) cells based protocols leading to the generation of dopaminergic neurons[86], motoneurons[87], GABA-ergic and glutamatergic neurons[88], astrocytes[89] and OPCs and myelinating oligodendrocytes[90,91].

Limited access to living human brain samples and neural cells for the study of neurodegenerative and psychiatric disorders has positioned iPSC-based studies as being a uniquely promising approach. The generation of the first human iPSCs-derived neurons therefore boosted disease-related neuroscience research and was quickly followed by studies of iPSC-derived neural cells from patients with various diseases. Not only protocols for different neuronal subtypes such as serotonergic neurons[92], midbrain dopamine neurons from Parkinson patients[93] and motoneurons from Amyotrophic Lateral Sclerosis (ALS) patients[94], but also glial protocols for the generation of astrocytes[95] and oligodendrocyte lineages[96,97] to study myelin disorders, e.g. Multiple Sclerosis (MS)[98,99] were designed to shed new light on these complex disorders.

At present, most neural induction strategies for iPSCs still have considerable disadvantages, e.g. poorly defined culture conditions, a long timeline and a low yield of differentiation. Over the last few years, several protocols have been optimized for generating improved quality of neural cultures. The most well known method for neural induction from iPSCs is based on embryoid body (EB) formation that mostly yields glutamatergic neurons[100,101]. iPSCs are first grown as EBs in cell suspension and later as neurospheres, followed by plating the neurospheres for neural differentiation. With slight modifications to an EB-based protocol timeline, cell culture conditions and the addition of regional growth and transcription factors, such as retinoic acid or FGF, different subtypes of neurons can be obtained from specific brain regions such as forebrain, hindbrain and midbrain[100,102]. Another way of neural induction is to use Noggin and SB431542, which are two inhibitors of the TGFb-SMAD signaling pathway. These inhibitors provide complete neural conversion of iPSCs into midbrain dopamine and spinal motor neurons under adherent culture conditions where single iPSCs are plated on Matrigel-coated dishes[93,103].

Direct conversion of somatic cells to neural lineages

Some somatic cells can be converted into another somatic cell type without a pluripotent state, which is called direct reprogramming. The first study to prove this for neurons was performed by Wernig

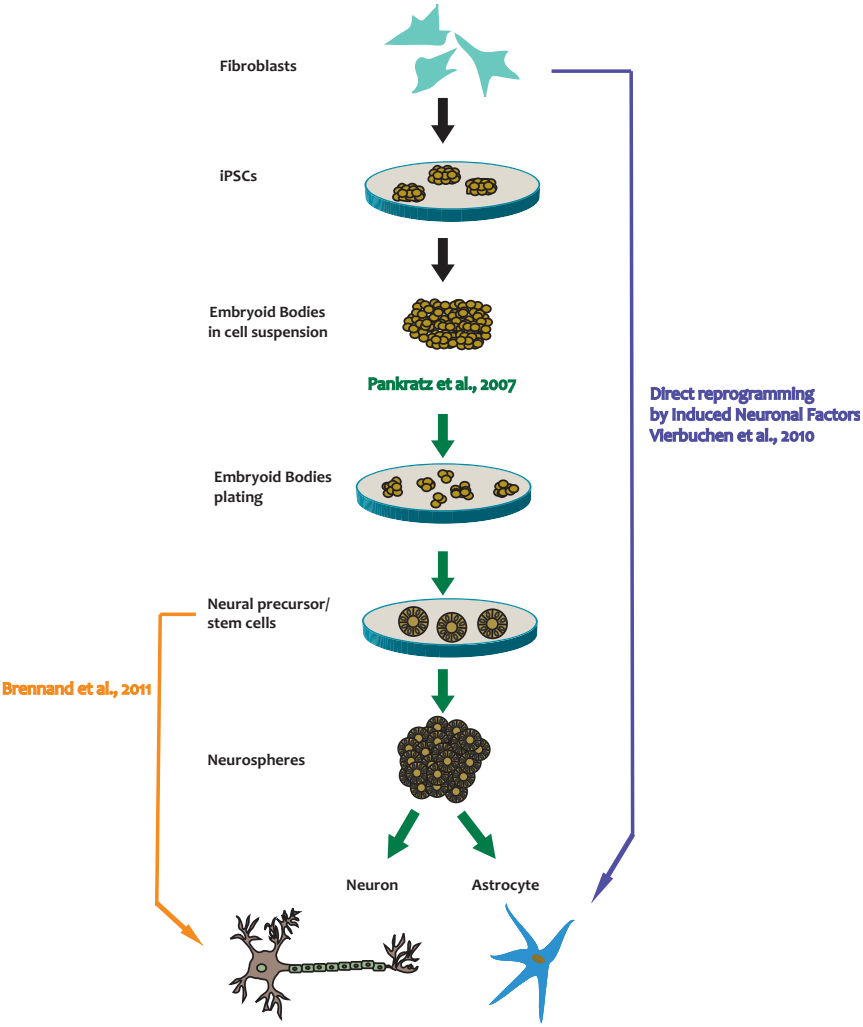

Figure 2. Protocols for generation of iPSC derived neural cells
Both direct reprogramming and IPSCs- based protocols yield neural cells, neurons and astrocytes.

and his colleagues where three factors Ascl1, Brn2 and Myt1l, termed induced neuronal (iN) factors, were sufficient to convert mouse embryonic and postnatal fibroblasts into functional neurons **(Figure 2)**[104]. Likewise, direct somatic lineage conversion of terminally differentiated cells to astrocytes and oligodendrocyte lineages was reported both from human and mouse cells by various groups. A summary of the studies on direct reprogramming to specific neural subtypes is reviewed in Tanabe et al.[105]. Even though the direct conversion method is faster, since it skips the pluripotency state, it yields only one cell type and the efficiency of reprogramming to neural cells is lower than generation of neural cells from iPSCs-derived protocols. Also, it is debated whether the maturity of neurons from direct reprogramming is as good as iPSC-derived neurons[106] and therefore usually astrocyte co-culturing is required to generate neurons with better electrophysiological properties[107]. To conclude, the direct conversion method can be an

efficient way to generate a specific kind of neural cell type, which can be useful for addressing specific questions regarding intrinsic properties of a subtype of neural cells.

Generation of iPSC-derived neural cells from psychiatric patients

The first iPSC-derived neural cells from patients with schizophrenia were described in Brennand et al.[108]. This study used a neural differentiation protocol based on EB formation. NPCs were generated after plating EBs instead of neurospheres **(Figure 2)**. Later, NPCs were plated for further differentiation into neurons of different subtypes, e.g. glutamatergic, GABA-ergic and Tyrosine Hydroxylase-positive neurons. Designing a protocol that yields a mixed culture of neurons and glia would allow a cell culture model that more closely resembles *in vivo* conditions than pure populations of neurons or glia. Because it remains unclear which neural cell types may be affected in different brain regions in schizophrenia patients, a neural protocol, which yields both neurons and glia, provides the opportunity to investigate different neural lineages in the same culture. On the other hand, microglia, which are also implicated in schizophrenia pathology, are absent from iPSCs-derived neural cell cultures since they have a hematopoietic origin, therefore would require a co-culture system.

An increasing number of studies have used iPSC-derived neural cells from psychiatric patients. Studies of iPSC-derived neural cells from schizophrenia patients have suggested a synaptic pathophysiology of the disorder[108,109]. In Brennand et al.[108], a comparison of iPSC-derived neurons from unrelated schizophrenia patients and unrelated healthy control individuals showed differences in synaptic transmission, pointing towards neuronal dysfunction as the major pathophysiological mechanism of schizophrenia. Likewise, in Wen et al., iPSC-derived forebrain neurons from a patient with schizophrenia having a DISC1 mutation showed deficits in synaptic vesicle release and transcriptional dysregulation of synapse-relates genes[109]. Interestingly, hippocampal dentate gyrus-like neurons derived from iPSCs of patients with bipolar disorder showed mitochondrial abnormalities in young neurons such as hyperactive action potential firing[110]. In another study, a slower migration rate of iPSC-derived NPCs was reported from patients with schizophrenia[111].

CAVEATS TO THE USE OF INDUCED PLURIPOTENT STEM CELL TECHNOLOGY

Genetic and epigenetic variables within and between cell lines are important to consider in disease modelling by iPSCs. Family-based research in studying psychiatric disorders would reduce the genetic heterogeneity and would help to find candidate genes in psychiatric patients. In addition, having iPSCs from family members and comparing the effect of candidate genes would allow determination of the molecular genetic etiology of the disorder.

Dramatic epigenetic changes occur after reprogramming as well as during differentiation from a pluripotency state to somatic cells. One of the major changes is silencing of one of the two X chromosomes in female cells upon differentiation, which is called X chromosome inactivation (XCI). Conversely, during reprogramming of somatic cells to a pluripotency state, the inactive X chromosome is reactivated, called X chromosome reactivation (XCR). Importantly, the reprogramming process might not be fully complete in iPSCs, thereby retaining some of the epigenetic features of the somatic cell source, a process that differs from human to mouse iPSCs. Analysis of the XCI process in human and mouse iPSCs shows important differences, which must be considered in disease modelling studies. As reviewed in Pasque et al.,[112] there are conflicting studies; multiple groups reported XCR in human iPSCs and activation of X-linked genes[113–115] whereas other findings do not show reactivation of the X chromosome[116,117]. In contrast, mouse iPSCs clearly show XCR, which might be explained by the fact

that mouse iPSCs have a more naïve stem cell state whereas hiPSCs reside in a primed state. In addition, the X chromosome is unstable and might "erode" when iPSCs are subjected to long-term culture[117]. Thus, erosion of XCI in hiPSCs can affect X-linked disease modelling, for instance modelling Lesch-Nyhan syndrome[117]. Erosion of XCI may also lead to upregulation of X-linked oncogenes, differences in proliferation and differentiation potential, altogether resulting in a lower quality of iPSC lines[118]. Recently, a method has been developed for generating hiPSC in a naïve ground state that maintained them undifferentiated by a combination of small molecules[119]. Naïve state hiPSCs maintain pluripotency through more than 50 passages and are equivalent to mouse iPSCs in their molecular and functional features.

In summary, epigenetic changes due to reprogramming can cause variability in iPSC cultures. As epigenetic changes may influence the quality of iPSCs and thereby the neural differentiation potential, the heterogeneity of the neural cells might cause false positive or negative results. Thus, it is crucial to use multiple clones per cell line when modelling by iPSCs. Also, as XCI implies the epigenetic stability of the iPSCs, checking the XCI state can be used to monitor the epigenetic state of human iPSCs.

REFERENCES

1 van Os J, Kapur S. Schizophrenia. Lancet 2009; 374: 635–45.

2 Lieberman JA, Perkins D, Belger A, Chakos M, Jarskog F, Boteva K et al. The early stages of schizophrenia: speculations on pathogenesis, pathophysiology, and therapeutic approaches. Biol Psychiatry 2001; 50: 884–97.

3 Addington J, Heinssen R. Prediction and prevention of psychosis in youth at clinical high risk. Annu Rev Clin Psychol 2012; 8: 269–89.

4 Jablensky A V, Morgan V, Zubrick SR, Bower C, Yellachich L-A. Pregnancy, delivery, and neonatal complications in a population cohort of women with schizophrenia and major affective disorders. Am J Psychiatry 2005; 162: 79–91.

5 Kirov G, O'Donovan MC, Owen MJ. Finding schizophrenia genes. J Clin Invest 2005; 115: 1440–8.

6 Tsuang M. Schizophrenia: genes and environment. Biol Psychiatry 2000; 47: 210–20.

7 St Clair D, Xu M, Wang P, Yu Y, Fang Y, Zhang F et al. Rates of adult schizophrenia following prenatal exposure to the Chinese famine of 1959-1961. JAMA 2005; 294: 557–62.

8 Lewandowski KE, Cohen BM, Ongur D. Evolution of neuropsychological dysfunction during the course of schizophrenia and bipolar disorder. Psychol Med 2011; 41: 225–41.

9 Graff-Guerrero A, Mizrahi R, Agid O, Marcon H, Barsoum P, Rusjan P et al. The dopamine D2 receptors in high-affinity state and D3 receptors in schizophrenia: a clinical [11C]-(+)-PHNO PET study. Neuropsychopharmacology 2009; 34: 1078–86.

10 Seeman P. Dopamine D2 receptors as treatment targets in schizophrenia. Clin Schizophr Relat Psychoses 2010; 4: 56–73.

11 BEARD AW, SLATER E. The schizophrenic-like psychoses of epilepsy. Proc R Soc Med 1962; 55: 311–6.

12 Murray RM. Neurodevelopmental schizophrenia: the rediscovery of dementia praecox. Br J Psychiatry Suppl 1994; : 6–12.

13 Glausier JR, Lewis DA. Dendritic spine pathology in schizophrenia. Neuroscience 2013; 251: 90–107.

14 Glantz LA, Lewis DA. Decreased dendritic spine density on prefrontal cortical pyramidal neurons in schizophrenia. Arch Gen Psychiatry 2000; 57: 65–73.

15 Garey LJ, Ong WY, Patel TS, Kanani M, Davis A, Mortimer AM et al. Reduced dendritic spine density on cerebral cortical pyramidal neurons in schizophrenia. J Neurol Neurosurg Psychiatry 1998; 65: 446–53.

16 Cannon TD, Thompson PM, van Erp TGM, Toga AW, Poutanen V-P, Huttunen M et al. Cortex mapping reveals regionally specific patterns of genetic and disease-specific gray-matter deficits in twins discordant for schizophrenia. Proc Natl Acad Sci U S A 2002; 99: 3228–33.

17 Yoon JH, Minzenberg MJ, Raouf S, D'Esposito M, Carter CS. Impaired prefrontal-basal ganglia functional connectivity and substantia nigra hyperactivity in schizophrenia. Biol Psychiatry 2013; 74: 122–9.

18 Elert E. Aetiology: Searching for schizophrenia's roots. Nature 2014; 508: S2–3.

19 Insel TR. Rethinking schizophrenia. Nature 2010; 468: 187–93.

20 Carlsson A. The current status of the dopamine hypothesis of schizophrenia. Neuropsychopharmacology 1988; 1: 179–86.

21 Falkenberg LE, Westerhausen R, Craven AR, Johnsen E, Kroken RA, L Berg E-M et al. Impact of glutamate levels on neuronal response and cognitive abilities in schizophrenia. NeuroImage Clin 2014; 4: 576–84.

22 Coyle JT. Glutamate and schizophrenia: beyond the dopamine hypothesis. Cell Mol Neurobiol; 26: 365–84.

23 White T, Ehrlich S, Ho B-C, Manoach DS, Caprihan A, Schulz SC et al. Spatial characteristics of white matter abnormalities in schizophrenia. Schizophr Bull 2013; 39: 1077–86.

24 Zalesky A, Fornito A, Seal ML, Cocchi L, Westin CF, Bullmore ET et al. Disrupted axonal fiber connectivity in schizophrenia. Biol Psychiatry 2011; 69: 80–89.

25 Davis KL, Stewart DG, Friedman JI, Buchsbaum M, Harvey PD, Hof PR et al. White matter changes in schizophrenia: evidence for myelin-related dysfunction. Arch Gen Psychiatry 2003; 60: 443–456.

26 Andreasen NC, Nopoulos P, Magnotta V, Pierson R, Ziebell S, Ho BC. Progressive brain change in schizophrenia: A prospective longitudinal study

of first-episode schizophrenia. Biol Psychiatry 2011; 70: 672–679.

27 Terwisscha Van Scheltinga AF, Bakker SC, Van Haren NEM, Derks EM, Buizer-Voskamp JE, Boos HBM et al. Genetic schizophrenia risk variants jointly modulate total brain and white matter volume. Biol Psychiatry 2013; 73: 525–531.

28 van den Heuvel MP, Sporns O, Collin G, Scheewe T, Mandl RCW, Cahn W et al. Abnormal rich club organization and functional brain dynamics in schizophrenia. JAMA psychiatry 2013; 70: 783–92.

29 Nave K-A, Ehrenreich H. Myelination and oligodendrocyte functions in psychiatric diseases. JAMA psychiatry 2014; 71: 582–4.

30 Goudriaan A, de Leeuw C, Ripke S, Hultman CM, Sklar P, Sullivan PF et al. Specific Glial Functions Contribute to Schizophrenia Susceptibility. Schizophr Bull 2013; : 1–11.

31 Nave K-A. Myelination and support of axonal integrity by glia. Nature 2010; 468: 244–252.

32 Nave K-A, Trapp BD. Axon-Glial Signaling and the Glial Support of Axon Function. Annu Rev Neurosci 2008; 31: 535–561.

33 Philips T, Bento-Abreu A, Nonneman A, Haeck W, Staats K, Geelen V et al. Oligodendrocyte dysfunction in the pathogenesis of amyotrophic lateral sclerosis. Brain 2013; 136: 471–82.

34 Tkachev D, Mimmack ML, Ryan MM, Wayland M, Freeman T, Jones PB et al. Mechanisms of disease Oligodendrocyte dysfunction in schizophrenia and bipolar disorder. Lancet; : 798–805.

35 Tkachev D, Mimmack ML, Ryan MM, Wayland M, Freeman T, Jones PB et al. Oligodendrocyte dysfunction in schizophrenia and bipolar disorder. Lancet (London, England) 2003; 362: 798–805.

36 Ip CW, Kroner A, Bendszus M, Leder C, Kobsar I, Fischer S et al. Immune cells contribute to myelin degeneration and axonopathic changes in mice overexpressing proteolipid protein in oligodendrocytes. J Neurosci 2006; 26: 8206–16.

37 Kassmann CM, Lappe-Siefke C, Baes M, Brügger B, Mildner A, Werner HB et al. Axonal loss and neuroinflammation caused by peroxisome-deficient oligodendrocytes. Nat Genet 2007; 39: 969–76.

38 Ren Y, Wang H, Xiao L. Improving myelin/oligodendrocyte-related dysfunction: a new mechanism of antipsychotics in the treatment of schizophrenia? Int J Neuropsychopharmacol 2013; 16: 691–700.

39 Roussos P, Haroutunian V. Schizophrenia: susceptibility genes and oligodendroglial and myelin related abnormalities. Front Cell Neurosci 2014; 8: 5.

40 Fields RD. White matter in learning, cognition and psychiatric disorders. Trends Neurosci. 2008; 31: 361–370.

41 Paus T, Keshavan M, Giedd JN. Why do many psychiatric disorders emerge during adolescence? Nat Rev Neurosci 2008; 9: 947–57.

42 Haroutunian V, Katsel P, Roussos P, Davis KL, Altshuler LL, Bartzokis G. Myelination, oligodendrocytes, and serious mental illness. Glia 2014; 62: 1856–77.

43 Körschenhausen DA, Hampel HJ, Ackenheil M, Penning R, Müller N. Fibrin degradation products in post mortem brain tissue of schizophrenics: a possible marker for underlying inflammatory processes. Schizophr Res 1996; 19: 103–9.

44 Wildenauer DB, Körschenhausen D, Hoechtlen W, Ackenheil M, Kehl M, Lottspeich F. Analysis of cerebrospinal fluid from patients with psychiatric and neurological disorders by two-dimensional electrophoresis: identification of disease-associated polypeptides as fibrin fragments. Electrophoresis; 12: 487–92.

45 van Berckel BN, Bossong MG, Boellaard R, Kloet R, Schuitemaker A, Caspers E et al. Microglia activation in recent-onset schizophrenia: a quantitative (R)-[11C]PK11195 positron emission tomography study. Biol Psychiatry 2008; 64: 820–2.

46 Bayer TA, Buslei R, Havas L, Falkai P. Evidence for activation of microglia in patients with psychiatric illnesses. Neurosci Lett 1999; 271: 126–8.

47 Matute C, Alberdi E, Domercq M, Sánchez-Gómez M-V, Pérez-Samartín A, Rodríguez-Antigüedad A et al. Excitotoxic damage to white matter. J Anat 2007; 210: 693–702.

48 Müller N, Weidinger E, Leitner B, Schwarz MJ. The role of inflammation in schizophrenia. Front Neurosci 2015; 9: 372.

49 Sekar A, Bialas AR, de Rivera H, Davis A, Hammond TR, Kamitaki N et al. Schizophrenia risk from complex variation of complement component 4. Nature 2016; advance on. doi:10.1038/nature16549.

50 Kety SS. The significance of genetic factors in the etiology of schizophrenia: results from the national study of adoptees in Denmark. J Psychiatr Res 1987; 21: 423–9.

51 McGuffin P, Gottesman II. Risk factors for schizophrenia. N Engl J Med 1999; 341: 370–1; author reply 372.

52 Austin JC, Peay HL. Applications and limitations of empiric data in provision of recurrence risks for schizophrenia: a practical review for healthcare professionals providing clinical psychiatric genetics consultations. Clin Genet 2006; 70: 177–87.

53 Cardno AG, Marshall EJ, Coid B, Macdonald AM, Ribchester TR, Davies NJ et al. Heritability estimates for psychotic disorders: the Maudsley twin psychosis series. Arch Gen Psychiatry 1999; 56: 162–8.

54 Polderman TJC, Benyamin B, de Leeuw CA, Sullivan PF, van Bochoven A, Visscher PM et al. Meta-analysis of the heritability of human traits based on fifty years of twin studies. Nat Genet 2015; 47: 702–709.

55 Riley BP, McGuffin P. Linkage and associated studies of schizophrenia. Am J Med Genet 2000; 97: 23–44.

56 Stefansson H, Ophoff RA, Steinberg S, Andreassen OA, Cichon S, Rujescu D et al. Common variants conferring risk of schizophrenia. Nature 2009; 460: 744–7.

57 Purcell SM, Wray NR, Stone JL, Visscher PM, O'Donovan MC, Sullivan PF et al. Common polygenic variation contributes to risk of schizophrenia and bipolar disorder. Nature 2009; 460: 748–52.

58 McClellan J, King M-C. Genetic heterogeneity in human disease. Cell 2010; 141: 210–7.

59 Need AC, Ge D, Weale ME, Maia J, Feng S, Heinzen EL et al. A genome-wide investigation of SNPs and CNVs in schizophrenia. PLoS Genet 2009; 5: e1000373.

60 Ripke S, Neale BM, Corvin A, Walters JTR, Farh K-H, Holmans P a. et al. Biological insights from 108 schizophrenia-associated genetic loci. Nature 2014. doi:10.1038/nature13595.

61 Bassett AS, Scherer SW, Brzustowicz LM. Copy number variations in schizophrenia: critical review and new perspectives on concepts of genetics and disease. Am J Psychiatry 2010; 167: 899–914.

62 Brandon NJ, Millar JK, Korth C, Sive H, Singh KK, Sawa A. Understanding the role of DISC1 in psychiatric disease and during normal development. J Neurosci 2009; 29: 12768–75.

63 Walsh T, McClellan JM, McCarthy SE, Addington AM, Pierce SB, Cooper GM et al. Rare structural variants disrupt multiple genes in neurodevelopmental pathways in schizophrenia. Science 2008; 320: 539–43.

64 Tan W, Wang Y, Gold B, Chen J, Dean M, Harrison PJ et al. Molecular cloning of a brain-specific, developmentally regulated neuregulin 1 (NRG1) isoform and identification of a functional promoter variant associated with schizophrenia. J Biol Chem 2007; 282: 24343–51.

65 Colantuoni C, Hyde TM, Mitkus S, Joseph A, Sartorius L, Aguirre C et al. Age-related changes in the expression of schizophrenia susceptibility genes in the human prefrontal cortex. Brain Struct Funct 2008; 213: 255–71.

66 Nakata K, Lipska BK, Hyde TM, Ye T, Newburn EN, Morita Y et al. DISC1 splice variants are upregulated in schizophrenia and associated with risk polymorphisms. Proc Natl Acad Sci U S A 2009; 106: 15873–8.

67 Niwa M, Kamiya A, Murai R, Kubo K, Gruber AJ, Tomita K et al. Knockdown of DISC1 by in utero gene transfer disturbs postnatal dopaminergic maturation in the frontal cortex and leads to adult behavioral deficits. Neuron 2010; 65: 480–9.

68 Guilmatre A, Dubourg C, Mosca A-L, Legallic S, Goldenberg A, Drouin-Garraud V et al. Recurrent rearrangements in synaptic and neurodevelopmental genes and shared biologic pathways in schizophrenia, autism, and mental retardation. Arch Gen Psychiatry 2009; 66: 947–56.

69 Rujescu D, Ingason A, Cichon S, Pietiläinen OPH, Barnes MR, Toulopoulou T et al. Disruption of the neurexin 1 gene is associated with schizophrenia. Hum Mol Genet 2009; 18: 988–96.

70 Sørensen HJ, Mortensen EL, Schiffman J, Reinisch JM, Maeda J, Mednick SA. Early developmental milestones and risk of schizophrenia: a 45-year follow-up of the Copenhagen Perinatal Cohort. Schizophr Res 2010; 118: 41–7.

71 Woodberry KA, Giuliano AJ, Seidman LJ. Premorbid IQ in schizophrenia: a meta-analytic review. Am J Psychiatry 2008; 165: 579–87.

72 Jones CA, Watson DJG, Fone KCF. Animal models of schizophrenia. Br J Pharmacol 2011; 164: 1162–94.

73 Cash-Padgett T, Jaaro-Peled H. DISC1 mouse models as a tool to decipher gene-environment interactions in psychiatric disorders. Front Behav Neurosci 2013; 7: 113.

74 Takahashi K, Yamanaka S. Induction of pluripotent stem cells from mouse embryonic and adult fibroblast cultures by defined factors. Cell 2006; 126: 663–76.

75 Zhao J, Jiang W, Sun C, Hou C, Yang X-M, Gao J. Induced pluripotent stem cells: origins, applications, and future perspectives. J Zhejiang Univ Sci B 2013; 14: 1059–69.

76 Okita K, Ichisaka T, Yamanaka S. Generation of germline-competent induced pluripotent stem cells. Nature 2007; 448: 313–7.

77 Nakagawa M, Koyanagi M, Tanabe K, Takahashi K, Ichisaka T, Aoi T et al. Generation of induced pluripotent stem cells without Myc from mouse and human fibroblasts. Nat Biotechnol 2008; 26: 101–6.

78 Nakagawa M, Takizawa N, Narita M, Ichisaka T, Yamanaka S. Promotion of direct reprogramming by transformation-deficient Myc. Proc Natl Acad Sci U S A 2010; 107: 14152–7.

79 Stadtfeld M, Nagaya M, Utikal J, Weir G, Hochedlinger K. Induced Pluripotent Stem Cells Generated Without Viral Integration. Science (80-) 2008; 322: 945–949.

80 Okita K, Nakagawa M, Hyenjong H, Ichisaka T, Yamanaka S. Generation of mouse induced pluripotent stem cells without viral vectors. Science 2008; 322: 949–53.

81 Yu J, Hu K, Smuga-Otto K, Tian S, Stewart R, Slukvin II et al. Human induced pluripotent stem cells free of vector and transgene sequences. Science 2009; 324: 797–801.

82 Jia F, Wilson KD, Sun N, Gupta DM, Huang M, Li Z et al. A nonviral minicircle vector for deriving human iPS cells. Nat Methods 2010; 7: 197–9.

83 Shi Y, Tae Do J, Desponts C, Hahm HS, Schöler HR, Ding S. A Combined Chemical and Genetic Approach for the Generation of Induced Pluripotent Stem Cells. Cell Stem Cell 2008; 2: 525–528.

84 Desponts C, Ding S. Using small molecules to improve generation of induced pluripotent stem cells from somatic cells. Methods Mol Biol 2010; 636: 207–18.

85 O'Doherty R, Greiser U, Wang W. Nonviral methods for inducing pluripotency to cells. Biomed Res Int 2013; 2013: 705902.

86 Wichterle H, Lieberam I, Porter JA, Jessell TM. Directed differentiation of embryonic stem cells into motor neurons. Cell 2002; 110: 385–97.

87 Miles GB, Yohn DC, Wichterle H, Jessell TM, Rafuse VF, Brownstone RM. Functional properties of motoneurons derived from mouse embryonic stem cells. J Neurosci 2004; 24: 7848–58.

88 Strübing C, Ahnert-Hilger G, Shan J, Wiedenmann B, Hescheler J, Wobus AM. Differentiation of pluripotent embryonic stem cells into the neuronal lineage in vitro gives rise to mature inhibitory and excitatory neurons. Mech Dev 1995; 53: 275–87.

89 Sandhu JK, Sikorska M, Walker PR. Characterization of astrocytes derived from human NTera-2/D1 embryonal carcinoma cells. J Neurosci Res 2002; 68: 604–14.

90 Liu S, Qu Y, Stewart TJ, Howard MJ, Chakrabortty S, Holekamp TF et al. Embryonic stem cells differentiate into oligodendrocytes and myelinate in culture and after spinal cord transplantation. Proc Natl Acad Sci U S A 2000; 97: 6126–31.

91 Brüstle O, Jones KN, Learish RD, Karram K, Choudhary K, Wiestler OD et al. Embryonic stem cell-derived glial precursors: a source of myelinating transplants. Science 1999; 285: 754–6.

92 Alenina N, Bashammakh S, Bader M. Specification and differentiation of serotonergic neurons. Stem Cell Rev 2006; 2: 5–10.

93 Nguyen HN, Byers B, Cord B, Shcheglovitov A, Byrne J, Gujar P et al. LRRK2 mutant iPSC-derived DA neurons demonstrate increased susceptibility to oxidative stress. Cell Stem Cell 2011; 8: 267–80.

94 Dimos JT, Rodolfa KT, Niakan KK, Weisenthal LM, Mitsumoto H, Chung W et al. Induced pluripotent stem cells generated from patients with ALS can be differentiated into motor neurons. Science 2008; 321: 1218–21.

95 Emdad L, D'Souza SL, Kothari HP, Qadeer ZA, Germano IM. Efficient differentiation of human embryonic and induced pluripotent stem cells into functional astrocytes. Stem Cells Dev 2012; 21: 404–10.

96 Czepiel M, Balasubramaniyan V, Schaafsma W, Stancic M, Mikkers H, Huisman C et al. Differentiation of induced pluripotent stem cells into functional oligodendrocytes. Glia 2011; 59: 882–92.

97 Wang S, Bates J, Li X, Schanz S, Chandler-Militello D, Levine C et al. Human iPSC-derived oligodendrocyte progenitor cells can myelinate and rescue a mouse model of congenital hypomyelination. Cell Stem Cell 2013; 12: 252–264.

98 Song B, Sun G, Herszfeld D, Sylvain A, Campanale N V, Hirst CE et al. Neural differentiation of patient specific iPS cells as a novel approach to study the pathophysiology of multiple sclerosis. Stem Cell Res 2012; 8: 259–73.

99 Herszfeld D, Payne NL, Sylvain A, Sun G, Bernard CC, Clark J et al. Fine structure of neurally differentiated iPS cells generated from a multiple sclerosis (MS) patient: a case study. Microsc Microanal 2014; 20: 1869–75.

100 Pankratz MT, Li X-J, LaVaute TM, Lyons EA, Chen X, Zhang S-C. Directed Neural Differentiation of Human Embryonic Stem Cells via an Obligated Primitive Anterior Stage. Stem Cells 2007; 25: 1511–1520.

101 Shi Y, Kirwan P, Livesey FJ. Directed differentiation of human pluripotent stem cells to cerebral cortex neurons and neural networks. Nat Protoc 2012; 7: 1836–46.

102 Du Z-W, Zhang S-C. Neural differentiation from embryonic stem cells: which way? Stem Cells Dev 2004; 13: 372–81.

103 Chambers SM, Fasano C a, Papapetrou EP, Tomishima M, Sadelain M, Studer L. Highly efficient neural conversion of human ES and iPS cells by dual inhibition of SMAD signaling. Nat Biotechnol 2009; 27: 275–80.

104 Vierbuchen T, Ostermeier A, Pang ZP, Kokubu Y, Südhof TC, Wernig M. Direct conversion of fibroblasts to functional neurons by defined factors. Nature 2010; 463: 1035–41.

105 Tanabe K, Haag D, Wernig M. Direct somatic lineage conversion: Table 1. Philos Trans R Soc B Biol Sci 2015; 370: 20140368.

106 Gopalakrishnan S, Hor P, Ichida JK. New approaches for direct conversion of patient fibroblasts into neural cells. Brain Res 2015. doi:10.1016/j.brainres.2015.10.012.

107 Bardy C, van den Hurk M, Eames T, Marchand C, Hernandez R V., Kellogg M et al. Neuronal medium that supports basic synaptic functions and activity of human neurons in vitro. Proc Natl Acad Sci 2015; : 201504393.

108 Brennand KJ, Simone A, Jou J, Gelboin-Burkhart C, Tran N, Sangar S et al. Modelling schizophrenia using human induced pluripotent stem cells. Nature 2011; 473: 221–5.

109 Wen Z, Nguyen HN, Guo Z, Lalli MA, Wang X, Su Y et al. Synaptic dysregulation in a human iPS cell model of mental disorders. Nature 2014; 515: 414–418.

110 Mertens J, Wang Q-W, Kim Y, Yu DX, Pham S, Yang B et al. Differential responses to lithium in hyperexcitable neurons from patients with bipolar disorder. Nature 2015; 527: 95–99.

111 Brennand K, Savas JN, Kim Y, Tran N, Simone A, Hashimoto-Torii K et al. Phenotypic differences in hiPSC NPCs derived from patients with schizophrenia. Mol Psychiatry 2015; 20: 361–8.

112 Pasque V, Plath K. X chromosome reactivation in reprogramming and in development. Curr Opin Cell Biol 2015; 37: 75–83.

113 Tomoda K, Takahashi K, Leung K, Okada A, Narita M, Yamada NA et al. Derivation conditions impact X-inactivation status in female human induced pluripotent stem cells. Cell Stem Cell 2012; 11: 91–9.

114 Barakat TS, Ghazvini M, de Hoon B, Li T, Eussen B, Douben H et al. Stable X chromosome reactivation in female human induced pluripotent stem cells. Stem cell reports 2015; 4: 199–208.

115 Kim K-Y, Hysolli E, Tanaka Y, Wang B, Jung Y-W, Pan X et al. X Chromosome of female cells shows dynamic changes in status during human somatic cell reprogramming. Stem cell reports 2014; 2: 896–909.

116 Pomp O, Dreesen O, Leong DFM, Meller-Pomp O, Tan TT, Zhou F et al. Unexpected X chromosome skewing during culture and reprogramming of human somatic cells can be alleviated by exogenous telomerase. Cell Stem Cell 2011; 9: 156–65.

117 Mekhoubad S, Bock C, de Boer AS, Kiskinis E, Meissner A, Eggan K. Erosion of dosage compensation impacts human iPSC disease modeling. Cell Stem Cell 2012; 10: 595–609.

118 Anguera MC, Sadreyev R, Zhang Z, Szanto A, Payer B, Sheridan SD et al. Molecular signatures of human induced pluripotent stem cells highlight sex differences and cancer genes. Cell Stem Cell 2012; 11: 75–90.

119 Gafni O, Weinberger L, Mansour AA, Manor YS, Chomsky E, Ben-Yosef D et al. Derivation of novel human ground state naive pluripotent stem cells. Nature 2013; 504: 282–6.

Chapter 2

A robust differentiation protocol for human induced pluripotent stem cell derived neural networks with improved electrophysiological maturity

N. Gunhanlar, G. Shpak, M. van der Kroeg, L.A. Gouty-Colomer, S.T. Munshi, B. Lendemeijer, C. Dupont, J. Gribnau, J.G. Borst, F.M.S. de Vrij and S.A. Kushner

Manuscript in preparation

A robust differentiation protocol for human induced pluripotent stem cell derived neural networks with improved electrophysiological maturity

N. Gunhanlar[1,], G. Shpak[1,*], M. van der Kroeg[1], L.A. Gouty-Colomer[1,3], S.T. Munshi[1], B. Lendemeijer[1], C. Dupont[4], J. Gribnau[4,5], J.G. Borst[2], F.M.S. de Vrij[1,#] and S.A. Kushner[1,#]*

[*] These authors contributed equally to this work
[#] These authors contributed equally to this work

[1] Department of Psychiatry, Erasmus University Medical Center, Rotterdam, The Netherlands.
[2] Department of Neuroscience, Erasmus University Medical Center, Rotterdam, The Netherlands.
[3] Present address: Institut national de la Recherche Médicale et de la Santé Inserm, INMED UMR 901, Marseille, France.
[4] Department of Reproduction and Development Erasmus University Medical Center, Rotterdam, The Netherlands
[5] Erasmus MC Stem Cell Institute, Rotterdam, The Netherlands

ABSTRACT

Progress in elucidating the molecular and cellular pathophysiology of neuropsychiatric disorders has been hindered by the limited availability of living human brain tissue. Therefore, the emergence of induced pluripotent stem cell (iPSC) technology has offered a unique alternative strategy for investigating the pathophysiology of disease initiation and progression using patient-derived functional neural networks. However, it has been challenging to develop methods that reliably generate iPSC-derived neurons with mature electrophysiological characteristics. Here, we report an optimized protocol that yields neurons with substantially improved electrophysiological properties, including high rates of spontaneous action potential firing and synaptic activity. This protocol generates a very consistent ratio of neurons and astrocytes that arise from a common neural progenitor without the need for astrocyte co-culture or specialized media, offering an important tool for modelling neuropsychiatric disorders.

INTRODUCTION

A detailed knowledge of the pathogenesis and pathophysiology of the majority of human neuropsychiatric disorders remains largely enigmatic. However, recent genetic and functional studies have begun to offer novel insights into many forms of severe mental illness[1–4]. There is widespread consensus that validated and robust human cellular models for brain disorders, and severe mental illness in particular, would be of considerable benefit[5,6].

The discovery of induced pluripotent stem cells (iPSCs) has provided the opportunity to investigate the physiology of living human neurons derived from individual patients[7]. Several protocols have been reported for generating iPSC-derived neurons based on a variety of different methods. One of the most commonly employed approaches is neural induction through embryoid body (EB) formation, which predominantly yields glutamatergic neurons[8,9]. The addition of regional patterning factors, such as retinoic acid or FGF, allows the derivation of distinct neuronal subtypes and brain region identities[8,10]. Another widely implemented method for neural induction is inhibition of the TGFβ-SMAD signaling pathway by Noggin and SB431542, which provides highly efficient neural conversion of iPSCs into midbrain dopamine and spinal motor neurons[11,12]. More recently, protocols have been developed for generating three-dimensional (3D) neural cultures using cerebral organoids cultured in a spinning bioreactor[13], cortical spheroids in free-floating conditions[14], or in 3D Matrigel culture[15].

In establishing optimized and

standardized methods for neuronal differentiation from iPSCs, one of the most important questions is the functional maturity of the iPSC-derived neurons. The design of robust neural differentiation protocols is critical for the generation of functional neurons that can form active networks and demonstrate mature electrophysiological properties. Bardy et al. recently reported an important advance in achieving functionally mature iPSC-derived neural networks suitable for whole-cell patch-clamp electrophysiological recordings[16]. However, the major limitation with this approach is the requirement for non-standard culture media and intracellular solution during the differentiation process and electrophysiological recordings.

Neuron-astrocyte interactions are critical both during early neurodevelopment and in the adult brain[17,18]. Astrocytes are involved in the guidance of neuronal precursors and in lengthening neuronal fiber projections during the development. In addition, astrocytes support neurite outgrowth and dynamically modulate synaptic transmission. Consequently, co-cultures of human pluripotent stem cell-derived neurons with astrocytes significantly enhance their functional maturation and synaptic transmission[19]. For the derivation of iPSC-derived neural networks, astrocytes can either be introduced through co-culture[20] or differentiated from a common neural progenitor which gives rise to both neurons and astrocytes as occurs *in vivo*[9]. The co-culture approach allows more flexibility in having experimental control over the neuron-to-astrocyte ratio and the source of the co-cultured astrocytes. The major drawback, however, is the potential for introducing a source of variability, especially concerning species differences when using co-cultures of rodent astrocytes with human iPSC-derived neurons. In contrast, differentiation protocols based on a common progenitor, giving rise to both neurons and astrocytes proceed more similarly to *in vivo* neurodevelopment and without the requirement for co-culture[8,9].

Using the latter approach, we now report an optimized differentiation protocol for deriving functionally mature neural networks suitable for whole-cell patch-clamp recordings and without the need for co-cultures or specialized media.

RESULTS

Generation of forebrain-patterned NPCs from iPSCs

Neural Precursor Cells (NPCs) are capable of generating a diversity of neural lineages, including both neurons and astrocytes. To generate NPCs, fully characterized iPSCs **(Supplementary Figure 1)** were detached from feeder cells using collagenase and suspended colonies were transferred to non-adherent plates. Suspended colonies were cultured on a shaker, which promoted the formation of spherical embryoid bodies (EBs) **(Figure 1A)**. EBs were cultured for six days (d1-d6), of which the first two days (d1-d2) were in human embryonic stem cell (hESC) medium (Knock-out serum based) supplemented with fibroblast growth factor 2 (FGF2) and then four days (d3-d7) in neural induction medium (Advanced DMEM with heparin and N-2 supplement). On the seventh day of differentiation (d7), EBs were gently dissociated and plated onto laminin-coated dishes in neural induction medium for eight days (d7-d15), resulting in a population of pre-NPCs (passage one). At d15 pre-NPCs were dissociated by collagenase and replated onto laminin-coated dishes in NPC medium (Advanced DMEM with N-2, B-27 supplement and laminin) containing FGF2 to promote selection and proliferation of precursor cells. The medium was changed every other day from the beginning of differentiation. Once confluent, cells were passaged 1:4 and could be cryopreserved in liquid nitrogen. At passage five, the cells appeared more homogeneous with a morphology and marker profile of NPCs, expressing general NPCs markers Sox2, Nestin and Vimentin and forebrain specific NPC marker FoxG1 **(Figure 1B).**

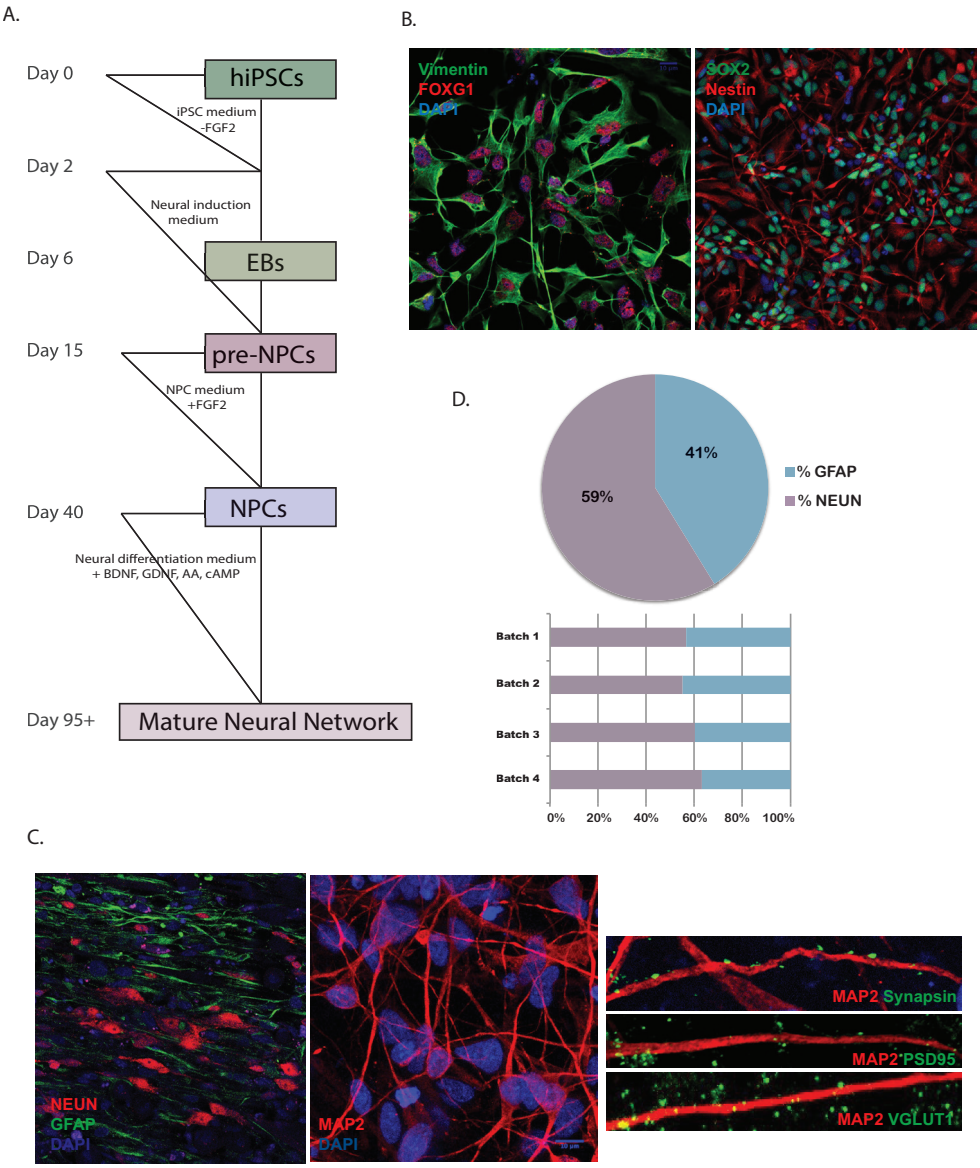

Figure 1. Generation and characterization of NPCS and neural networks from iPSCs. (A) Scheme illustrating the main developmental stages of the protocol for generating NPCs and neural networks. **(B)** Immunostaining for NPCs markers Nestin, SOX2, Vimentin and FOXG1. **(C)** Immunostaining for neural markers, GFAP+ glia, MAP2+ and NeuN+ mature neurons, pre and post synaptic markers Synapsin and PSD95 and VGLUT1+ glutamatergic neurons. **(D)** Proportion of NeuN+ and GFAP expressing cells at day 56-70 *in vitro*.

Differentiation of a mixed neuronal/glial culture

NPCs were utilized between passages 5-10 for neural differentiation. In addition to NPCs derived using the protocol above, we also used commercially-available NPCs (Axol Biosciences, line ax0015) derived using the protocol reported by Shi et al.,[9] to examine the general applicability of our neural differentiation protocol. NPCs were plated onto polyornithine/laminin-coated coverslips in neural differentiation medium (Neurobasal medium with N-2, B27-RA) supplemented with growth factors BDNF, GDNF, db-cAMP and ascorbic acid. Throughout the entire period of neural differentiation, medium was replaced 3 times per week. From week 6 onwards, only half of the medium was replaced per exchange. Electrophysiological recordings and confocal imaging were performed after 8-10 weeks of neural differentiation that yielded a mixed culture of neurons and glia **(Figure 1C)**. Neurons were positive for MAP2, beta-tubulin, pre and postsynaptic markers Synapsin and PSD95 **(Figure 1C)**. The ratio of $NeuN^+$ (neurons) to $GFAP^+$ (astrocytes) was consistently 59.5% to 40.5% **(Figure 1D)**. Overall, $NeuN^+$ cells constituted 15.5% of the total DAPI nuclei, whereas cells expressing the astrocytic and radial glial marker GFAP were 10.5%. Among the remaining cells were Sox2 expressing NPCs (60.3%), and doublecortin expressing (dcx) (13.7%) young

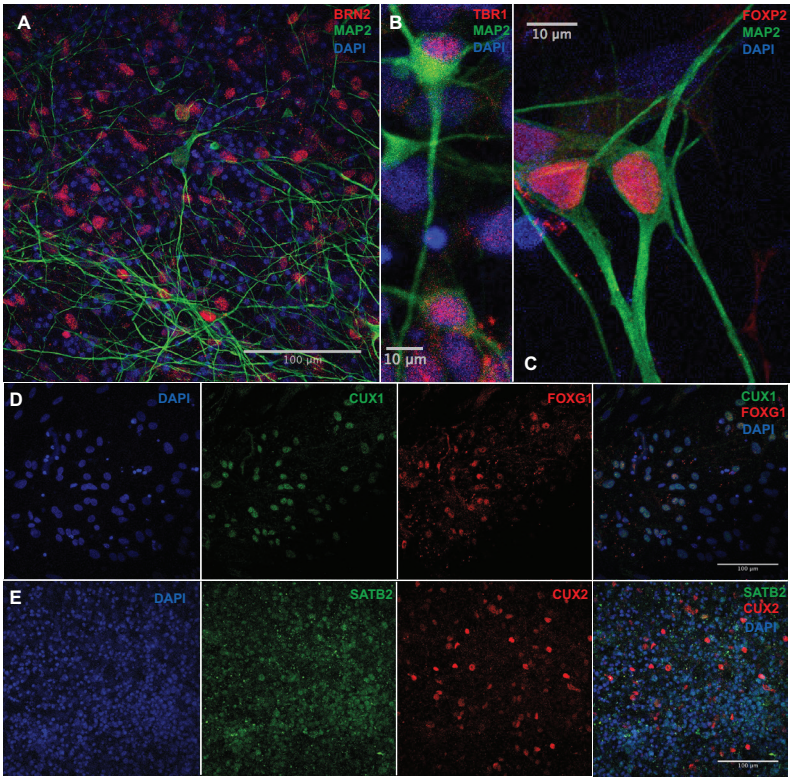

Figure 2. Cortical layer markers in neural networks. Cultures were stained at day 56 for **(A)** transcription factor BRN2 for layer II-IV neurons and and MAP2 for neurons in general **(B)** TBR1 which is expressed by subtypes of corticofugal neurons in deep layers and in cortical layer II **(C)** FOXP2 which is expressed in cortical precursors in layer V and VI **(D)** CUX1 corresponding to upper layer neurons in layers II–IV, and FOXG1 expressed in forebrain progenitors **(E)** CUX2 for upper layer neurons and SATB2 which defines corticocortical projecting neurons and callosal neurons from layers V and upper layers.

neurons **(Supplementary Figure 2)**.

We next studied the expression of cortical layer-specific markers in the differentiated neurons **(Figure 2)**[21,22]. Subsets of neurons were positive for the transcription factor BRN2, which is expressed in late cortical progenitors and migrating neurons **(Figure 2A)**, the cortical-layer marker TBR1 which is expressed by subtypes of corticofugal neurons in deep layers (IV-VI) and layer II **(Figure 2B)**, Foxp2 which is expressed among cortical precursors in layer V/VI **(Figure 2C)**, CUX1 and CUX2 expressed in upper layer neurons (II–IV), SATB2 which defines corticocortical projecting neurons also corresponding to callosal neurons from layer V and upper layer neurons, and FoxG1 expressed in forebrain progenitors **(Figure 2D and E).**

Electrophysiology results

Whole-cell patch-clamp electrophysiological recordings confirmed the functional maturity of the neurons, including repetitive firing of action potentials, sodium and potassium currents, spontaneous spiking activity and synaptic transmission. We compared the electrophysiological properties of neurons differentiated from multiple independent batches of each of the 3 distinct lines of iPSC-derived NPCs reprogrammed from different individuals.

Most protocols that have been reported for neuronal differentiation of human pluripotent stem cells employ a semi-defined culture medium, while electrophysiological recordings are performed either in the same culture medium or transferred directly from the culture medium into a defined artificial cerebrospinal fluid (aCSF). Importantly, the use of culture medium for electrophysiological recordings of neurons has previously been found to impair spontaneous and evoked firing of action potentials, network spontaneous calcium activity, and both excitatory and inhibitory synaptic activity[16]. Notably however, those experiments relied upon an immediate switch from culture medium to aCSF, for which a substantial acute increase in extracellular osmolarity (from ~220 mOsm/kg in culture medium to ~305 mOsm/kg in aCSF) is known to be highly stressful for neurons[23]. Therefore, we implemented a gradual transition from the culture medium to the aCSF recording medium over 25 minutes by 5 serial partial exchanges of medium with aCSF (see Methods section for specific details). Following this equilibration procedure, neurons significantly improved morphology, viability, and electrophysiological characteristics. When comparing the electrophysiological properties of neurons recorded with either instantaneous transition to aCSF or using a gradual equilibration, significant differences were found in the proportion of neurons that exhibited spontaneous action potential (AP) firing and synaptic activity, with notable alterations in the activity dynamics among those neurons with spontaneous APs **(Supplementary Figure 3).**

In order to evaluate the stability of our differentiation and patch clamping protocol between different cell lines, recordings were obtained from neurons derived from three independent iPSC lines. We defined AP maturity as those events with an overshooting amplitude (>0 mV), with a fast depolarization (≤5ms rise time) and fast repolarization (≤10ms decay time). Nearly all cells were capable of firing mature APs in response to depolarizing current injection (111/114 cells, 97.4%). Among these cells, 80.2% (89/111) of the active neurons exhibited repetitive firing with a sequence of mature APs **(Figure 3A and B)** with average maximum frequency of around 13 Hz **(Figure 3C)**. The remaining 19.8% (22/111) fired either a single mature AP or followed by a short sequence of 2-3 APs which exhibited rapid accommodation**.**

Detailed electrophysiological analysis of membrane parameters was performed among the group of neurons that were defined as mature based on their ability to fire mature APs repetitively in response to a current injection. Eight standard membrane parameters were quantified: input resistance, resting membrane potential and capacitance as passive properties, and action potential threshold, amplitude, half

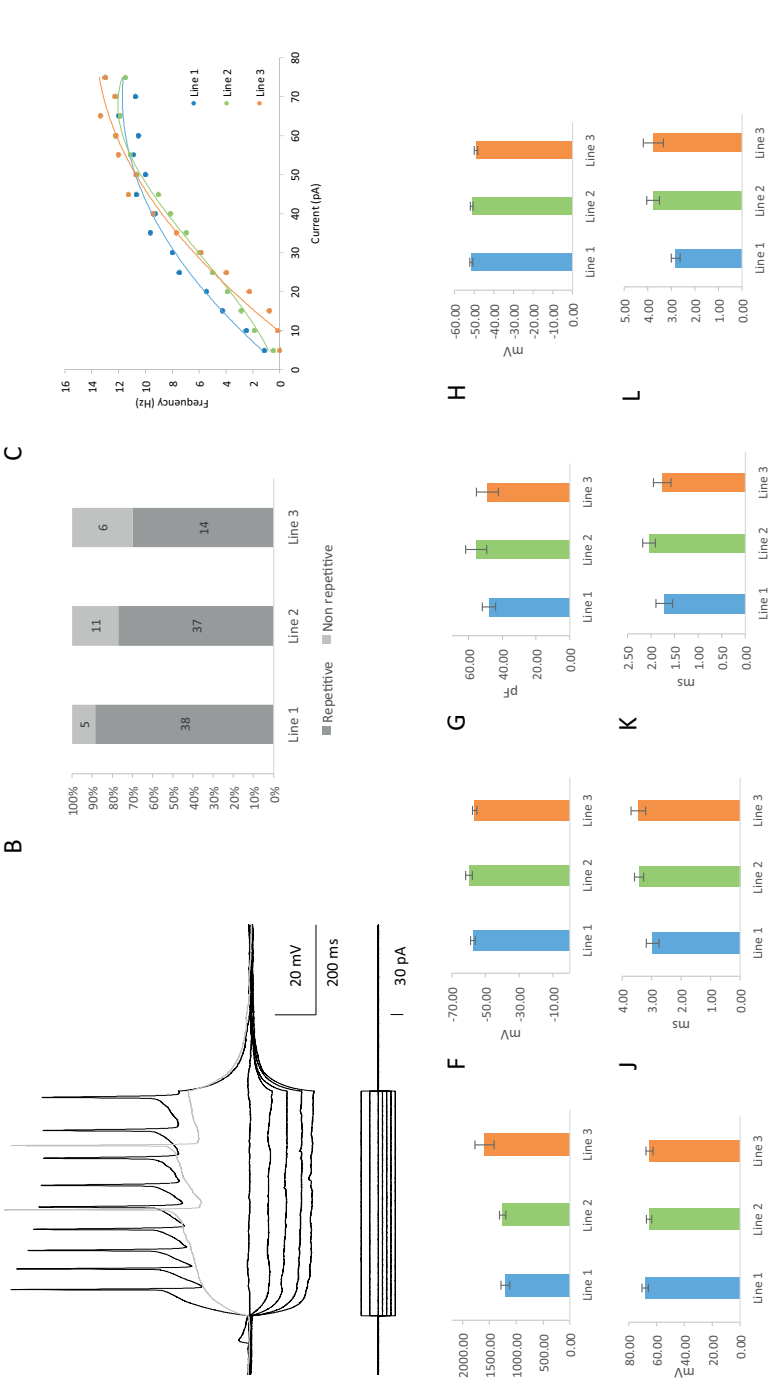

Figure 3. Active and passive properties of neurons from 3 different cell lines. All the data presented (except for B) was measured from repetitive cells in equilibrated cultures. **(A)** A representative trace from a repetitive neuron, stimulated with 5 hyperpolarized current steps and two depolarizing steps (minimal current needed to evoke an action potential and response frequency saturation. Stimulations at the bottom panel). All the action potential parameters were calculated from the first evoked spike. **(B)** The ratios of non-repetitive vs. repetitive cells in the 3 equilibrated cells lines. **(C)** F-I plot of the repetitive neurons population. **(E-L)** Active and passive membrane properties: **(E)** input resistance ($p=0.03$, $F=3.6$), **(F)** resting membrane potential ($p=0.44$, $F=0.82$,) and **(G)** capacitance ($p=0.84$, $F=0.18$,), **(H)** action potential threshold ($p=0.29$, $F=1.25$), **(I)** amplitude ($p=0.37$, $F=1.0$), **(J)** half width ($p=0.01$, $F=4.7$), **(K)** Rise time ($p=0.3$, $F=1.23$) and **(L)** decay time ($p=0.01$, $F=4.61$).

width and rise and decay time as parameters of the action potential kinetics. Of all the membrane properties we measured, the input resistance and AP decay time were the only parameters in which we observed a small but statistically significant difference between lines. The average value of the input resistance for all 3 lines was 1277.7±52.75 MΩ **(Figure 3E),** showing a significant difference between lines 1 and 3 (Tukey HSD, p=0.03). The resting membrane potential was -58.17±1.0 mV on average **(Figure 3F)**. The average capacitance of the 3 lines was 49.07±2.9 pF **(Figure 3G)**. Regarding the action potential characteristics, the average voltage threshold was 50.85±0.48 mV **(Figure 3H)**. The action potential amplitude was 66.54±1.32 mV, measured from voltage threshold to peak **(Figure 3I)**. The average half-width, which represents the speed of the onset and termination of the action potential, was 3.18±0.11 ms **(Figure 3J)**, showing a significant difference between lines 1 and 2 (Tukey HSD, p=0.02). Looking into the APs kinetics, we measured the AP rise and decay time. The average rise time was 1.86±0.10 ms **(Figure 3K)** and average decay time was 3.36±0.16 **(Figure 3L)**. According to the post-hoc test, there was a significant difference in decay time between lines 1 and 2 (Tukey HSD, p=0.02).

Another aspect of neuronal network maturity is spontaneous AP firing. Notably, more than 50% of neurons exhibited spontaneous APs while recording at sub-threshold membrane potentials **(Figure 4A and B)**. As a standard measurement, recordings were acquired for 3 consecutive minutes. However, cells were consistently capable of being maintaining high-quality whole-cell recordings for more than 30 minutes. Trains of low-frequency APs could be sustained without alteration in membrane potential or of AP characteristics **(Supplementary Figure 4A)**. Moreover, spontaneous firing of APs was also evident in non-permeating cell-attached recordings, confirming that the frequency of spontaneous APs is not an artifact of the patch-clamp procedure **(Supplementary Figure 4B)**.

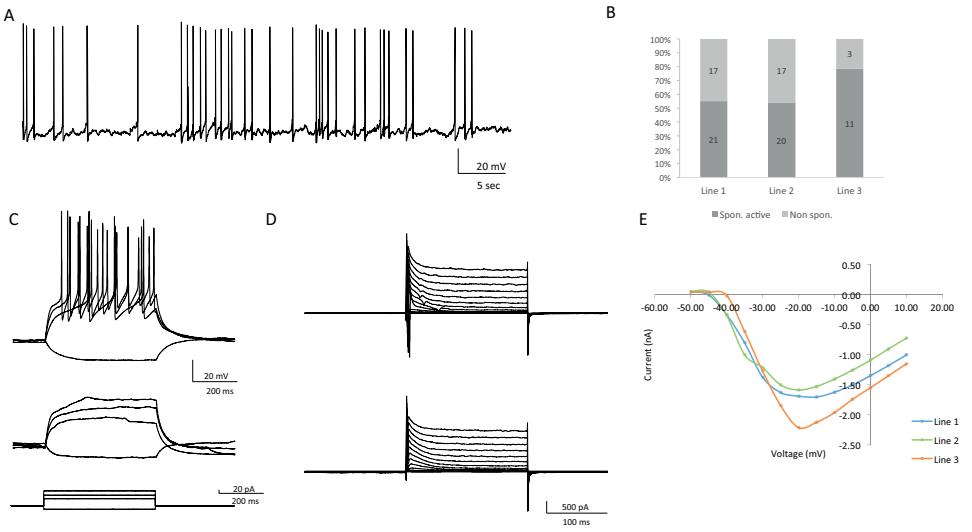

Figure 4. iPSC-derived neurons exhibit spontaneous firing of sodium-mediated action potentials. (A) A 50 seconds representative trace from a spontaneously active neuron. **(B)** The ratios of non-spontaneous Vs. spontaneous cells in the 3 equilibrated cells lines. **(C)** The voltage responses of the same cell to 1 hyperpolarizing and 3 depolarizing (bottom panel), before and after TTX application. **(D)** The sodium currents in voltage-clamp recording were also abolished by the application of TTX. The peak amplitude of the observed sodium currents in varying membrane potentials (-50 - +10 mV, in 5 mV increments).

In order to confirm whether the observed APs are driven by active sodium conductance, we blocked voltage-gated sodium channels by applying TTX to the bath solution in a subset of recordings. As expected, all action potentials were eliminated **(Figure 4C)**.

Neurons from all 3 lines demonstrated the presence of fast sodium currents in voltage clamp recording, as was evident from the fast inward current observed in response to depolarized membrane potentials **(Figure 4D, upper panel and 4E)**. The inward sodium currents were also completely blocked by TTX application **(Figure 4D, lower panel)**.

Another important aspect of neuronal maturity is synaptic connectivity. Spontaneous post-synaptic currents (sPSCs) are characterized by a rapid onset (rise time) and slower, more variable decay time. In all lines, low-frequency (~1 Hz) spontaneous synaptic activity was evident in at least 70% of the cells **(Figure 5A-C)**. The average frequency of these events was 1.09±0.17 Hz **(Figure 5D)**. The average amplitude of the events was 16.03±0.82 mV **(Figure 5E)**, where according to the post-hoc test, there were significant differences between lines 1 and 2, and line 2 and 3 (Tukey HSD p=0.01 and p=0.004, respectively). The kinetics of these events resembled the expected shape of sPSCs from neuronal recordings in acute ex vivo slices with an average rise time of 1.66±0.07 ms **(Figure 5F)** and decay time of 5.59±0.48 ms **(Figure 5G)**. For decay time, a statistically significant difference was observed between lines 2 and 3 (Tukey HSD, p=0.03).

DISCUSSION

Our results describe a robust protocol for neural network differentiation from human iPSCs, focused on improved electrophysiological maturity. Importantly, this differentiation protocol starts from a common iPSC-derived neural progenitor without requirement for exogenous glial cell co-culture. We observed a highly consistent ratio of neurons-to-glia of

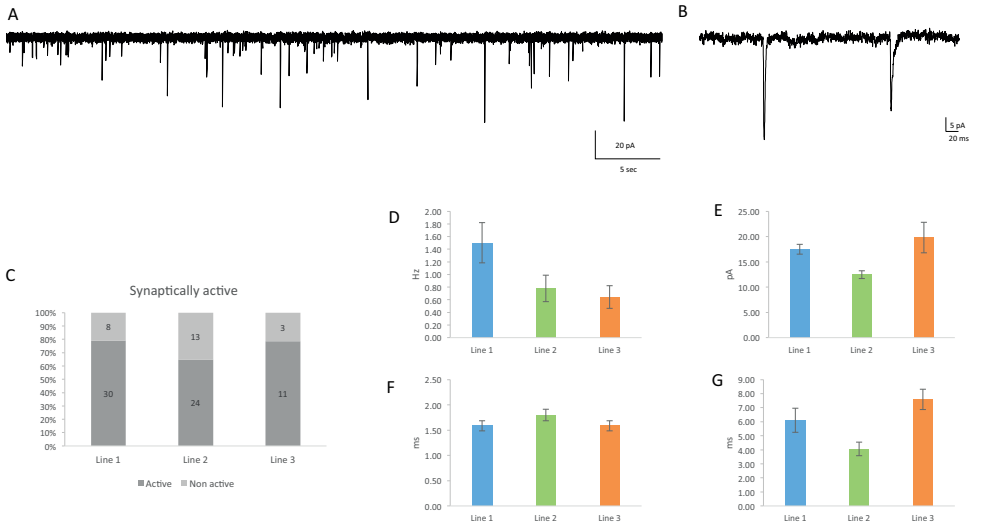

Figure 5. Synaptic activity in 3 different cell lines (A) A 50 seconds representative trace from a synaptically active cell. **(B)** A zoom in of the trace in (A) which shows 2 post-synaptic events. **(C)** The ratios between synaptically non active Vs. active cells. **(D-G)** the PSCs characteristics: **(D)** The frequency of PSCs (p=0.09, F=2.55), **(E)** amplitude (p=0.001, F=7.25), **(F)** rise (p=0.3, F=1.24) and **(G)** decay time (p=0.02, F=4.01).

60:40 with low inter-individual and batch-to-batch variability in a network with emergence of cortical layer markers. The versatility of this neural network was further shown by reducing the volume of medium changes during the course of differentiation, following the rationale that the cultures are increasingly self-supportive. Regarding the physiological maturity of the neurons generated, various electrophysiological parameters can be considered to define neuronal maturity, most of which progressively change during neurodevelopment. For example, over the course of development the resting membrane potential tends to become progressively more hyperpolarized and stabilizes around -70mV, and input resistance tends to decrease, both as a result of the changing complement of membrane ion channels and cell morphology[24]. AP kinetics also change during development, as APs become more rapid and with larger amplitudes. The presence of post-synaptic current events and their kinetics are important measurements of pre-synaptic neurotransmitter release, as well as the repertoire of post-synaptic receptors[25–29]. The values of these parameters depend on the species, type of cell, and tissue origin[30]. Of all the different parameters we assessed, three membrane properties and two synaptic parameters showed significant differences between cell lines. However, when assessing the maturity of each of these lines individually, they all show equally high proportions of repetitive neurons, spontaneously firing and synaptically active cells, as well as overall similar membrane properties. In light of the developing nature of the above parameters, we intentionally set a high standard for the definition of neuronal maturity, essentially using only the population of repetitive neurons for analysis. This high standard for neuronal maturity ensures characterization of the electrophysiological properties of functional iPSC-derived neurons which strengthens the use of iPSC-derived neurons as a valid model. The values of the different cellular parameters we assessed are highly comparable to many neurophysiological characterizations from both acute slices and neuronal cultures from human and rodent origin. Notably, the vast majority of these parameters were highly similar of differentiation of the same iPSC-derived NPCs and between iPSC lines reprogrammed from different individuals. This low variability can also be observed by the relatively low coefficient of variation for the measured parameters. Taken together, these results support the validity of this protocol for yielding functionally mature iPSC-derived neuronal networks.

Importantly, in this protocol no specialized media are required to obtain high standard electrophysiological recordings from iPSC-derived neurons with mature electrophysiological properties, using a gradual equilibration procedure to move cultures from standard neural differentiation medium to aCSF. The significance of the osmotic environment to the physiology of cultured neurons was recently demonstrated by Bardy et al., that introduced a designated medium for both culturing and electrophysiological recordings[16]. While the use of a specialized medium did support the differentiation of mature neurons, our approach was to use standard neural differentiation media, yet to minimize the physiological response of the cells to osmotic changes by introducing a gradual equilibration. This equilibrium stage led to improved stability and reproducibility of the electrophysiological results, as demonstrated by the higher ratios of cells exhibiting the ability to fire APs repetitively in response to depolarizing current injections, as well as spontaneous firing of APs and synaptic activity (**Supplementary Figure 3**) compared with other studies using different protocols[16,28,31,32] . Therefore, this protocol represents a significant improvements towards the validity of iPSC use in modeling both healthy and diseased conditions.

Many genetic, molecular and physiological considerations are required for iPSC-derived functional neural network modeling. For example, physical environmental aspects in different three-dimensional cell culture models have suggested differences between the traditional 2D approach and a 3D environment[15,16,34]. Issues such as the density of plated cells were found to affect several neuronal properties[34] and

the composition of a mixture of different cell types present in the culture is important for functional maturity of the network[19]. Together, the presence of high ratios of repetitive, spontaneously active and synaptically connected cells should serve as a sign of functional maturity of neurons in culture, together with appropriate membrane properties.

In summary, we have described the development of a reliable differentiation protocol that generates a consistent ratio of neurons and astrocytes that arise from a common neural progenitor without the need for astrocyte co-culture or specialized media. The ability to generate a healthy cellular environment that supports many different cell types to mature and function as an active neural network with detailed electrophysiological characterization is a key feature and essential requirement for using this technology as a valid model for psychiatric disorders.

METHODS

Reprogramming and characterization of iPSCs

Reprogramming of human primary skin fibroblasts from two different donors (one male, age 57 and one female, age 54) was performed as described previously[35]. Briefly, fibroblasts were infected with a single, multicistronic lentiviral vector encoding OCT4, SOX2, KLF4, and MYC and cultured on g-irradiated mouse embryonic feeder (MEF) cells. All participants gave informed consent, and the Medical Ethics Committee of the Erasmus University Medical Centre approved the study. Quality control of iPSC clones was performed by karyotyping, realtime quantitative PCR and classic embryoid differentiation into the three different germ layers, confirmed by immunohistochemistry, as performed previously[36].

Differentiation from iPSCs to neural networks

Generation of Embryoid Bodies and Neural Precursor Cells

Human iPSCs were differentiated according to Brennand et al.,[20] with modifications and without astrocyte co-culture. iPSC colonies were dissociated from MEFs with collagenase (100 U/ml) for 7 minutes at 37°C/5% CO_2. For Embryoid Body (EB) formation, iPSC colonies were transferred to non-adherent plates in hES medium on a shaker in an incubator at 37°C/5% CO_2. EBs were grown for two days in hES medium and after two days, EBs were changed to neural induction medium (DMEM/F12, 1x N2, 2 µg/ml heparin, 1% Pen/Strep) (d2) and cultured for another four days in suspension (d6). For generation of NPCs, at d7 EBs were slightly dissociated by trituration to prevent formation of EB clumps and plated onto laminin coated 10cm dishes (1µg/ml laminin in DMEM for 30min at 37°C) first in neural induction medium for eight days and then at d15 in NPC medium (DMEM/F12, 1x N2, 1x B27-RA, 1µg/ml laminin and 20 ng/ml FGF_2). At d15, cells are defined as pre-NPCs stage (passage one) and they can be passaged (1:4) and frozen, as they get confluent. At passage five, cells reach a homogeneious NPC stage and are considered mature for initiation of neural differentiation.

Neural Differentiation

For neural differentiation, NPCs (passage five to eleven) are plated on sterile coverslips in 6 or 12-well plates, coated with 1ml/well polyornithine for 1 hour at RT. After coating, coverslips were washed 3 times with sterile water and dried for 30min. Subsequently, 100ul drops of laminin solution (2.5ug/ml in water) were placed in the middle of the coverslip and incubated for 15-30min at 37°C/5% CO_2 and then replaced with a drop of DMEM until plating of cells. In the meantime, NPCs were washed with DPBS and dissociated with collagenase (100 U/ml). One full (100% confluent) 10cm dish of NPCs (passage 5-11) was divided over one 12-well plate. A 100ul drop of NPC cell suspension was placed on the laminin-

coated spot for 1 hour for attachment of NPCs on coverslips in neural differentiation medium (Neurobasal medium, 1x N2, 1x B27-RA, 20ug/ml, 1x NEAA with growth factors (20ng/ml BDNF, 20ng/ml GDNF, 1uM db-cAMP, 200uM ascorbic acid). After 1hr, 900ul neural differentiation medium was added to each well. Plated cells were refreshed 3 times per week. After 5 weeks of neural differentiation, replenishments were performed with only half the volume of medium. Electrophysiology and confocal imaging were performed on neural networks between 8-10 weeks.

Immunocytochemistry and quantification

Cell cultures were fixed using 4% formaldehyde in PBS. Primary antibodies were incubated overnight at 4°C in labelling buffer containing 0.05 M Tris, 0.9% NaCl, 0.25% gelatin, and 0.5% Triton-X-100 (pH 7.4). The following primary antibodies were used: Sox2, Nestin, MAP2, NeuN, GFAP, FoxG1 [ProSci], Vimentin [Santa Cruz Biotechnology], AFP [R&D Systems], TRA-1-81, Nanog [Beckton Dickinson], Oct4 [Abcam], BRN2, Satb2, Tbr1, Cux1 and Cux2 [kindly provided by Janssen Pharmaceuticals]. The following secondary antibodies were used: Alexa-488, Alexa-546, Alexa-555 and Cy3 antibodies [Jackson ImmunoResearch]. Samples were imbedded in Mowiol 4-88 (Fluka) after which confocal imaging was performed with a Zeiss LSM510 confocal microscope using ZEN software (Zeiss, Germany).

Statistical analysis

All statistical comparisons were performed using one-way ANOVA with post-hoc Tukey's test, using SPSS (Version 21, IBM). The threshold for significance was set at $P<0.05$ for all statistical comparisons.

Electrophysiology

Culture slides were collected from 6 or 12 well culture plates. Slides in which the tissue was detached where excluded from the electrophysiology experiments. Whole-cell patch clamp recordings were performed at 8-10 weeks post neural differentiation. The recording micropipettes (tip resistance 3–6 MΩ) were filled with internal solution composed of (mM): 130 K-gluconate, 0.1 EGTA, 1 $MgCl_2$, 2 MgATP, 0.3 NaGTP, 10 HEPES, 5 NaCl, 11 KCl, 5 phosphocreatine (pH 7.4). Recordings were made using a MultiClamp 700B amplifier (Molecular Devices). Signals were sampled and filtered at 10 kHz and 3 kHz, respectively. The whole-cell capacitance was compensated and series resistance was monitored throughout the experiment. Voltage was corrected for liquid junction potential (14 mV). The bath was constantly perfused with fresh saline composed of (mM): 110 NaCl, 2.5 KCl, 2 $CaCl_2$, 10 glucose and 1 NaH_2PO_4, 25 $NaHCO_3$, 0.2 ascorbic acid, 2 $MgCl_2$ (pH 7.4). For voltage-clamp recordings, cells were clamped at −80 mV; sPSCs were measured for 3 minutes. For current-clamp recordings neurons were held at -75mV. Hyperpolarized and depolarized voltage responses were stimulated by 500 msec current steps varied from −20 to +150 pA in 5 or 10 pA increments (varied according to the cell's input resistance and firing pattern). Single action potential properties were calculated from the first evoked action potential in response to a depolarizing step. Spontaneous spiking activity was measured at resting potential or at threshold potential in cases that the spontaneous frequency was very high and the APs were compromised. Importantly, this holding current was in all cases minimal and didn't exceed 10 pA. The holding current needed for keeping the membrane at a sub-threshold potential was fixed at the beginning of the recording, and was not changed throughout the recording. Action potential threshold was calculated by the first point to exceed noise levels of the second derivative of the action potential wave form. AP rise and decay times were calculated from 10%-90% of AP amplitude. All recordings were performed at room temperature. Data analysis was performed by Clampfit 10.2 (Molecular devices). sPSCs were analyzed by MiniAnalysis software (Synaptosoft).

Equilibrium stage–before inserting the culture slide into the recording chamber, the culture medium was gradually replaced with fresh external solution in the following manner: to the

total volume of 1 ml culture medium in the well, 300 µl of fresh oxygenated aCSF was added and then 300 µl of the total mixture was removed. This stage was repeated 5 times, with 5-minute intervals between changes. During this phase the cells were kept at room temperature. At the end of this stage the slide was placed within the recording chamber with perfused aCSF. The osmolarity of fresh culture medium was 220 mOsm/kg, differing substantially from the 305 mOsm/kg of the external solution. All recordings were performed using this equilibrium procedure, unless indicated otherwise.

SUPPLEMENTARY FIGURES

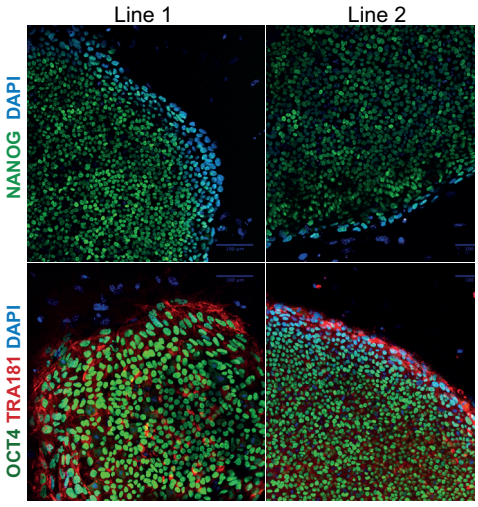

Supplementary Figure 1. Characterization of iPSCs. iPSCs express pluripotency markers NANOG, TRA181 and Oct4 which confirms the pluripotency state of the cells.

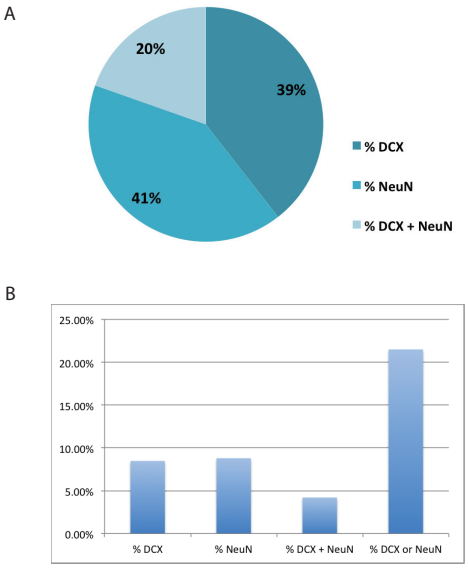

Supplementary Figure 2. Neuronal cell type distribution. **(A)** Distribution of neuronal lineage cells subdivided in DCX+ immature and NeuN+ mature neurons. **(B)** Distribution of neuronal lineage cells in the entire cell population.

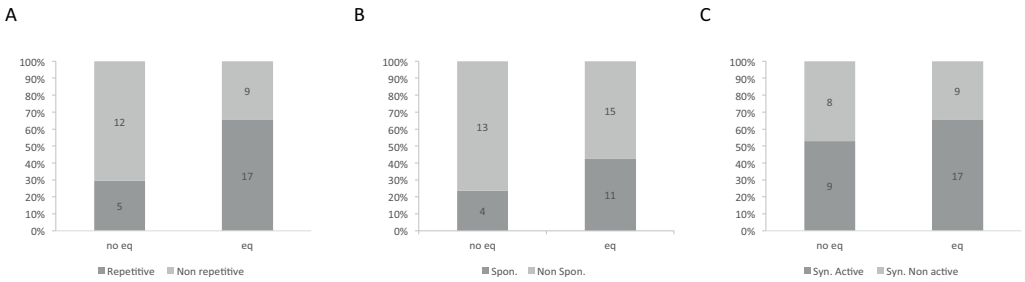

Supplementary Figure 3. Non equilibrated vs. equilibrated cultures. The advantage of the equilibrium stage was already evident by the ability to find and maintained patched neurons. From a similar number of slides it was possible to successfully record from many more cells from the equilibrated cultures (26 Vs. 17). **(A)** The ratio between repetitive and non-repetitive cells is much higher in the equilibrated culture conditions. **(B)** The same tendency can be seen also in the number of spontaneously spiking cells and **(C)** synaptically active cells.

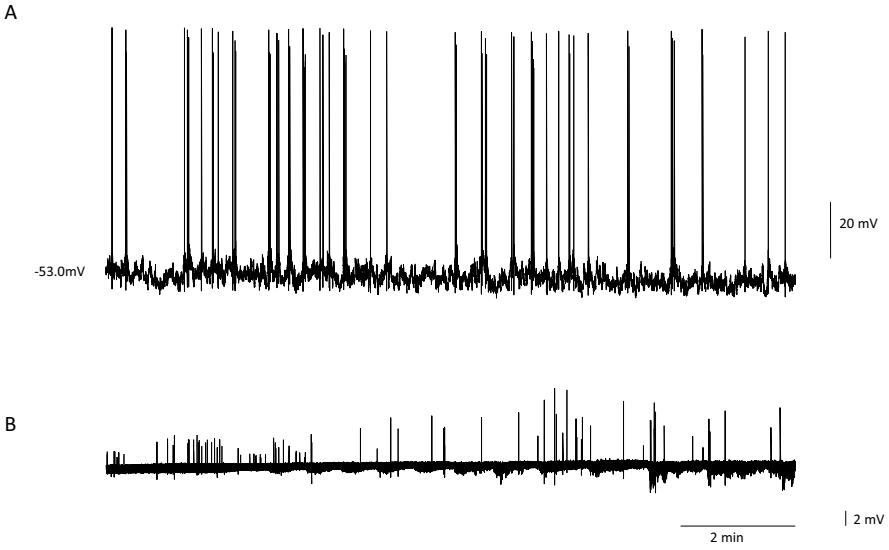

Supplementary Figure 4. Spontaneous firing of action potential in patch-clamp configuration could be maintained for more than 30 min. A) A representative 12 minute long whole-cell recording. Cell was held at sub-threshold potential. **B)** 12 minutes of spontaneous activity recorded in cell-attached configuration.

REFERENCES

1 Ripke S, Neale BM, Corvin A, Walters JTR, Farh K-H, Holmans P a. et al. Biological insights from 108 schizophrenia-associated genetic loci. Nature 2014; 511: 421–427.

2 Bassett AS, Scherer SW, Brzustowicz LM. Copy number variations in schizophrenia: critical review and new perspectives on concepts of genetics and disease. Am J Psychiatry 2010; 167: 899–914.

3 Ng MYM, Levinson DF, Faraone S V, Suarez BK, DeLisi LE, Arinami T et al. Meta-analysis of 32 genome-wide linkage studies of schizophrenia. Mol Psychiatry 2009; 14: 774–85.

4 Riley BP, McGuffin P. Linkage and associated studies of schizophrenia. Am J Med Genet 2000; 97: 23–44.

5 Watmuff B, Berkovitch SS, Huang JH, Iaconelli J, Toffel S, Karmacharya R. Disease signatures for schizophrenia and bipolar disorder using patient-derived induced pluripotent stem cells. Mol Cell Neurosci 2016. doi:10.1016/j.mcn.2016.01.003.

6 Young-Pearse TL, Morrow EM. Modeling developmental neuropsychiatric disorders with iPSC technology: challenges and opportunities. Curr Opin Neurobiol 2016; 36: 66–73.

7 Takahashi K, Yamanaka S. Induction of pluripotent stem cells from mouse embryonic and adult fibroblast cultures by defined factors. Cell 2006; 126: 663–76.

8 Pankratz MT, Li X-J, LaVaute TM, Lyons EA, Chen X, Zhang S-C. Directed Neural Differentiation of Human Embryonic Stem Cells via an Obligated Primitive Anterior Stage. Stem Cells 2007; 25: 1511–1520.

9 Shi Y, Kirwan P, Livesey FJ. Directed differentiation of human pluripotent stem cells to cerebral cortex neurons and neural networks. Nat Protoc 2012; 7: 1836–46.

10 Du Z-W, Zhang S-C. Neural differentiation from embryonic stem cells: which way? Stem Cells Dev 2004; 13: 372–81.

11 Nguyen HN, Byers B, Cord B, Shcheglovitov A, Byrne J, Gujar P et al. LRRK2 mutant iPSC-derived DA neurons demonstrate increased susceptibility to oxidative stress. Cell Stem Cell 2011; 8: 267–80.

12 Chambers SM, Fasano C a, Papapetrou EP, Tomishima M, Sadelain M, Studer L. Highly efficient neural conversion of human ES and iPS cells by dual inhibition of SMAD signaling. Nat Biotechnol 2009; 27: 275–80.

13 Lancaster MA, Renner M, Martin C-A, Wenzel D, Bicknell LS, Hurles ME et al. Cerebral organoids model human brain development and microcephaly. Nature 2013; 501: 373–9.

14 Paşca AM, Sloan S a, Clarke LE, Tian Y, Makinson CD, Huber N et al. Functional cortical neurons and astrocytes from human pluripotent stem cells in 3D culture. Nat Methods 2015; 12. doi:10.1038/nmeth.3415.

15 Kim YH, Choi SH, D'Avanzo C, Hebisch M, Sliwinski C, Bylykbashi E et al. A 3D human neural cell culture system for modeling Alzheimer's disease. Nat Protoc 2015; 10: 985–1006.

16 Bardy C, van den Hurk M, Eames T, Marchand C, Hernandez R V., Kellogg M et al. Neuronal medium that supports basic synaptic functions and activity of human neurons in vitro. Proc Natl Acad Sci 2015; : 201504393.

17 Zhang SC. Defining glial cells during CNS development. Nat Rev Neurosci 2001; 2: 840–3.

18 Zuchero JB, Barres BA. Glia in mammalian development and disease. Development 2015; 142: 3805–9.

19 Johnson MA, Weick JP, Pearce RA, Zhang S-C. Functional neural development from human embryonic stem cells: accelerated synaptic activity via astrocyte coculture. J Neurosci 2007; 27: 3069–77.

20 Brennand KJ, Simone A, Jou J, Gelboin-Burkhart C, Tran N, Sangar S et al. Modelling schizophrenia using human induced pluripotent stem cells. Nature 2011; 473: 221–5.

21 Espuny-Camacho I, Michelsen K a., Gall D, Linaro D, Hasche A, Bonnefont J et al. Pyramidal Neurons Derived from Human Pluripotent Stem Cells Integrate Efficiently into Mouse Brain Circuits In Vivo. Neuron 2013; 77: 440–456.

22 Gaspard N, Bouschet T, Herpoel A, Naeije G, van den Ameele J, Vanderhaeghen P. Generation of cortical neurons from mouse embryonic stem cells. Nat Protoc 2009; 4: 1454–63.

23 Pasantes-Morales H. Volume regulation in brain cells: cellular and molecular mechanisms. Metab Brain Dis 1996; 11: 187–204.

24 Kasper EM, Lübke J, Larkman AU, Blakemore C. Pyramidal neurons in layer 5 of the rat visual cortex. III. Differential maturation of axon targeting, dendritic morphology, and electrophysiological properties. J Comp Neurol

1994; 339: 495–518.

25 Warren RA, Jones EG. Maturation of neuronal form and function in a mouse thalamo-cortical circuit. J Neurosci 1997; 17: 277–95.

26 Oswald A-MM, Reyes AD. Maturation of intrinsic and synaptic properties of layer 2/3 pyramidal neurons in mouse auditory cortex. J Neurophysiol 2008; 99: 2998–3008.

27 McCormick DA, Prince DA. Post-natal development of electrophysiological properties of rat cerebral cortical pyramidal neurones. J Physiol 1987; 393: 743–62.

28 Telias M, Segal M, Ben-Yosef D. Electrical maturation of neurons derived from human embryonic stem cells. F1000Research 2014; 3: 196.

29 Zhang Z. Maturation of layer V pyramidal neurons in the rat prefrontal cortex: intrinsic properties and synaptic function. J Neurophysiol 2004; 91: 1171–82.

30 Tripathy SJ, Savitskaya J, Burton SD, Urban NN, Gerkin RC. NeuroElectro: a window to the world's neuron electrophysiology data. Front Neuroinform 2014; 8: 40.

31 Song M, Mohamad O, Chen D, Yu SP. Coordinated development of voltage-gated Na+ and K+ currents regulates functional maturation of forebrain neurons derived from human induced pluripotent stem cells. Stem Cells Dev 2013; 22: 1551–63.

32 Prè D, Nestor MW, Sproul A a., Jacob S, Koppensteiner P, Chinchalongporn V et al. A time course analysis of the electrophysiological properties of neurons differentiated from human induced Pluripotent Stem Cells (iPSCs). PLoS One 2014; 9. doi:10.1371/journal.pone.0103418.

33 Pașca AM, Sloan S a, Clarke LE, Tian Y, Makinson CD, Huber N et al. Functional cortical neurons and astrocytes from human pluripotent stem cells in 3D culture. Nat Methods 2015. doi:10.1038/nmeth.3415.

34 Ivenshitz M, Segal M. Neuronal density determines network connectivity and spontaneous activity in cultured hippocampus. J Neurophysiol 2010; 104: 1052–60.

35 Warlich E, Kuehle J, Cantz T, Brugman MH, Maetzig T, Galla M et al. Lentiviral vector design and imaging approaches to visualize the early stages of cellular reprogramming. Mol Ther 2011; 19: 782–9.

36 de Esch CEF, Ghazvini M, Loos F, Schelling-Kazaryan N, Widagdo W, Munshi ST et al. Epigenetic characterization of the FMR1 promoter in induced pluripotent stem cells from human fibroblasts carrying an unmethylated full mutation. Stem cell reports 2014; 3: 548–55.

Chapter 3

Oligodendrocyte precursor cells generated from induced pluripotent stem cell derived neural progenitors

N. Gunhanlar, B. Lendemeijer, M. Baghdadi, G. Shpak, D.E. Slump, W.J.G. Hoogendijk, F.M.S. de Vrij and S.A. Kushner

Manuscript in preparation

Oligodendrocyte precursor cells generated from induced pluripotent stem cells derived neural progenitors

N. Gunhanlar[*], *B. Lendemeijer*[*], *M. Baghdadi, G. Shpak, D.E. Slump, W.J.G. Hoogendijk, F.M.S. de Vrij*[#] *and S.A. Kushner*[#]

[*] These authors contributed equally to this work
[#] These authors contributed equally to this work

[1] Department of Psychiatry, Erasmus University Medical Center, Rotterdam, The Netherlands.

ABSTRACT

Oligodendrocte precursor cells (OPCs) are one of the most obscure cell types in the central nervous system (CNS). OPCs form a highly proliferative, tightly regulated and abundant population of glial cells. Besides their well-established role in generating oligodendrocytes, they also receive synaptic inputs, can generate astrocytes and are involved in inflammatory responses. Multiple brain disorders, ranging from multiple sclerosis to schizophrenia, have been associated with white matter abnormalities. Studying the oligodendrocyte lineage might provide insight into the mechanisms underlying these disorders. In order to achieve this, we established a protocol that could reliably produce OPC enriched populations of neural cells derived from Induced Pluripotent Stem Cells (iPSCs). iPSC-derived OPCs express the canonical OPC markers, migrate towards chemoattractants and have the potential to produce myelinating oligodendrocytes. In the future, our protocol can be used to derive patient derived-OPCs for unraveling the etiology surrounding brain disorders associated with the oligodendrocyte lineage and possibly screen for therapeutic interventions.

INTRODUCTION

Oligodendrocyte precursor cells (OPCs), also known as NG2 cells or polydendrocytes are one of the most mysterious cell types in the central nervous system (CNS). Despite the major advances made by recent studies in our understanding of OPCs, much remains unknown about the intrinsic properties of OPCs and how to classify them. Their most well established role is to produce oligodendrocytes, the myelinating cells of the CNS. By selectively myelinating axons, oligodendrocytes regulate proper action potential signaling between neurons by creating the insulating effects of multilayered myelin ensheathment. It has become clear that oligodendrocytes and especially OPCs are responsible for multiple other processes in the brain besides myelination[1]. In addition to their myelinating function, oligodendrocytes provide metabolic support to surrounding neurons, for example enhancing the energy production of axonal mitochondria[2]. Even though myelination occurs at an early age, in the adult rodent brain OPCs remain a highly proliferative and abundant population of glial cells[3]. Recent studies found that they also receive synaptic inputs[4], have the ability to also differentiate into astrocytes in some brain regions[5] or simply remain OPCs. These diverse biological properties suggest that this seemingly homogenic population of cells, previously mostly known for their function as precursors to oligodendrocytes, might also be responsible for multiple supportive processes in the brain. Likewise, human OPCs (hOPCs) show similarity to the rodent brain such as the distribution and shape of hOPCs are identical[6]. hOPCs are present after 17 weeks gestation and form the 10-15% of non-neuronal cells of adult human cerebral cortex and white matter[7]. In the presence of pathology they show morphological changes such as reduced density of hOPC within

the lesion compared with hOPC density outside the lesion[6,7]. In addition, subpopulation of hOPCs exit and distributed unevenly in Multiple Sclerosis (MS) lesions[6].

Recently, an increasing number of studies suggest oligodendrocyte dysfunction as an underlying cause for schizophrenia[8–10]. Disturbances in oligodendrocyte function have been associated with other severe and lethal neurological disorders such as MS[11] and amyotrophic lateral sclerosis (ALS)[12]. However, a definitive etiology for all these disorders still remains elusive. In an attempt to reverse the loss of oligodendrocytes in MS patients, pioneering pilot studies are being proposed where patients receive transplantations of isolated fetal OPCs, which theoretically have the potential to repopulate the CNS and differentiate into mature oligodendrocytes[13]. A similar approach proved successful in a mouse model with congenital hypomyelination, in which human neural stem cells could rescue the myelination deficit when transplanted in neonatal mice[14,15].

Induced pluripotent stem cells (iPSCs) can provide patient specific cells to study disease mechanisms *in vitro*, or in transplantation experiments in animal models *in vivo*. There are different protocols to generate iPSC-derived OPCs by using different growth factors to direct different pathways[16–19]. One of the most extensive studies showed a protocol that had the ability to generate iPSC-derived OPCs capable of differentiating into myelinating oligodendrocytes *in vivo*[14]. In this study, human glial chimeric mouse brains were generated for modeling myelin disorders. The engrafted human progenitor cells differentiated into astrocytes and oligodendrocytes in a hypomyelinated environment and over time dominated the host brain. This chimeric mouse brain model allows studying the human specific contribution of glia in health and disease. Remarkably, in Douvaras et al.[18] OPCs from viral and integration free iPSCs from primary progressive MS patients were generated, which were able to differentiate into myelinating oligodendrocytes in the *shiverer* mouse brain. These results encourage the pursuit of potential autologous cell therapies using iPSCs for myelin disorders such as MS. For psychiatric diseases, these protocols can provide disease modeling tools to study the contribution of human and/or patient specific oligodendrocyte lineage cells.

RESULTS

Generation of OPCs from NPCs

iPSC-derived Neural Precursor Cells (NPCs) were generated using the neural differentiation protocol described in Chapter 2. These NPCs were differentiated to Oligodendrocyte Precursor Cells (OPCs) by devising a protocol adopted from Monaco et al.[20] **(Figure 1A)**. NPCs were cultured with basic Fibroblast Growth Factor (bFGF) and Epidermal Growth Factor (EGF) for a week before starting differentiation towards the oligodendrocyte lineage. bFGF is important for self-renewal and proliferation of neural precursors and known for its role in regulating oligodendrogenesis from the spinal cord, progenitor cell populations of the telencephalon and embryonic ventricular zone progenitors[21–26]. Moreover, bFGF facilitates the expression of PDGFRα in OPCs which makes them more sensitive to PDGF extracellular ligands[27]. EGF stimulates cell growth, proliferation and differentiation and induces Subventricular zone (SVZ) progenitors to migrate and differentiate into oligodendrocytes[28].

As was stated in Kerman et al.[29], we used a serum-free approach to minimize the variability due to the different batches of serum. Our OPC induction media was developed by supplementing growth factors required for oligodendrocyte lineage differentiation *in vivo* to HAMS DMEM/F12, these factors are Platelet derived growth factor AA (PDGF-AA), bFGF, Neurotrophic factor 3 (NT-3), Sonic Hedgehog (Shh) and triiodothyronine (T3). Factors are required for cell proliferation and differentiation by activating the Sonic Hedgehog (Shh) pathway and PDGFRα signaling. PDGF-AA is known to regulate cell proliferation via activating the PDGF receptor (PDGFR) intracellular Tyrosine

Kinase Domain through several pathways and is often used in CNS demyelination models to regulate the number of OPCs[30,31]. Also, PDGF signaling is a key pathway for neural stem cells to commit to the oligodendrocyte lineage[32]. The NT3 protein belongs to the Nerve Growth Factor (NGF) family, which is known to support the survival and differentiation of existing neurons and to stimulate and control neurogenesis. Also, NT3 induces oligodendrocyte proliferation and the myelination of regenerating axons[33]. Thyroid hormone (T3) controls the proliferation and differentiation of progenitors and maturation of oligodendrocytes[34,35]. By culturing iPSC-derived NPCs in OPC induction media for 3 weeks we were able to generate OPCs as confirmed by immunohistochemistry and western blot.

Variability in OPC differentiation potential

During development OPCs differentially express

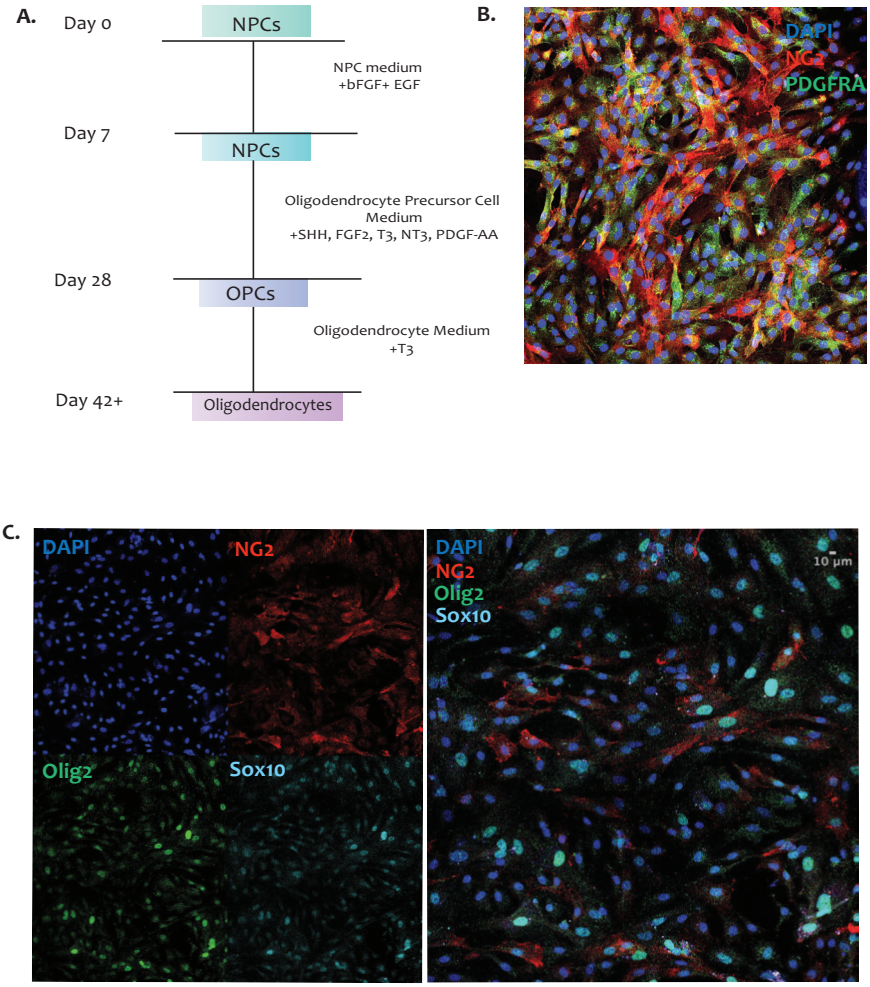

Figure 1. Generation and characterization of iPSC-derived OPCs. (A) Scheme illustrating the main developmental stages of the protocol for generating OPC from iPSCs derived NPCs. **(B, C)** Immunostaining for OPC markers CSPG4/NG2, PDGFRα, nuclear Olig2 and Sox10.

specific markers when differentiating to oligodendrocytes. We were able to generate OPCs that express the canonical membrane proteins late OPC marker NG2 and the earlier expressed receptor for PDGF-AA (PDGFRα) **(Figure 1B),** and nuclear markers OLIG2 and SOX10 which are considered both early and late OPC markers **(Figure 1C).** We performed a western blot analysis to confirm expression of NG2 **(Supplementary Figure 1A).** Remarkably, co-culturing iPSC-derived OPCs with primary mouse neurons changed their morphology, mimicking a more *in vivo*-like appearance. The characteristic complex cellular extensions could only be observed in the presence of neurons **(Supplementary Figure 1B)**.

After culturing NPCs in OPC-induction media for three weeks, we obtained a heterogeneous pool of OPC-enriched cells. The percentages of OPC markers showed variation between cell lines clones and experiments**.** This low efficiency is comparable to that reported in Kerman et al., ~25% PDGFRα and ~50% NG2 positive cells, where OPCs were generated from embryonic stem cells[29]. To achieve a more homogenous cell population we performed flow cytometry sorting the OPCs for CD140α (PDGFRα) using a BD FACSAria III. Before sorting we had a cell population in which 23.4% was positive for NG2 and 46.2% for PDGFRα. After using flow cytometry these numbers increased to 92.8% and 71.6% respectively **(Figure 2A and B)**. Even though the sorting was performed with an antibody for PDGFRα, immocytochemistry did not show the strongest increase for this marker. This can be explained by the different antibodies used for PDGFRα in flow cytometry and immunocytochemistry. This population of OPCs could be expanded and was stored in liquid nitrogen for future experiments.

Myelinating potential of human oligodendrocytes in murine organotypic cortex slice cultures

Further differentiation for an additional 2 weeks of OPCs yielded myelinating oligodendrocytes

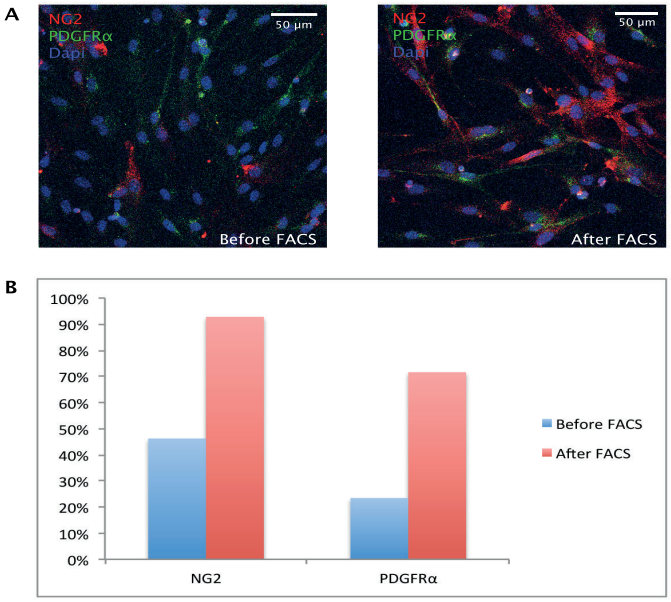

Figure 2. Flowcytometry of OPCs. Purified iPSC-derived OPCs. (A) Populations before (Left) and after (Right) FACS are shown in, PDGFRα is shown in green and NG2 in red. **(B)** Before FACS the cell population contains 46.2% cells positive for NG2 and 23.4% positive for PDGFRα. After sorting the percentage increased to 92.8% and 71.6% respectively.

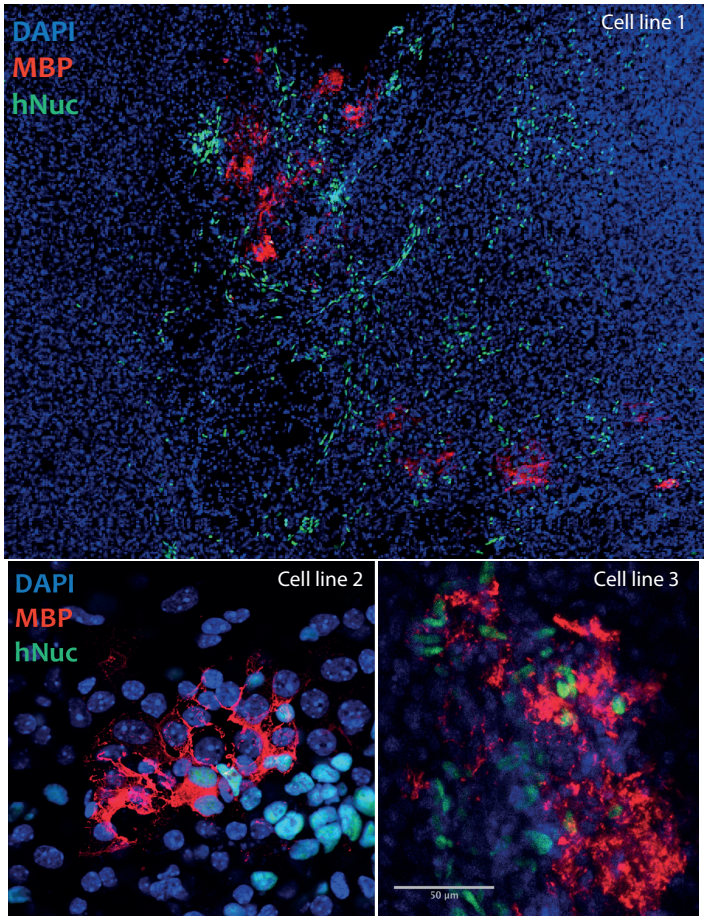

Figure 3. iPSC-derived OPCs can differentiate into myelinating oligodendrocytes. OPCs are injected into organotypic cortex slices from *shiverer* mouse brain. Slices are stained 10days after transplantation. iPSC-derived OPCs (green) are positive for hNuc. OPCs, generated from 3 different NPC lines, can differentiate into myelinating oligodendrocytes, producing MBP positive (red) myelin.

when grown on organotypic cortex slices. To investigate the differentiation and myelination ability of iPSCs-derived OPCs to mature into myelinating oligodendrocytes, we designed an experiment with *shiverer* mice. *Shiverer* mice have a premature stop mutation in the MBP gene, resulting in the absence of functional myelin. Studies show initiation of myelination requires signals from mature axons, which might affect the differentiation of OPCs into oligodendrocytes[36,37]. Organotypic cortex slice cultures create an *in vivo* like conditions thereby supply required factors for OPCs to differentiate into myelinating oligodendrocyte. We made frontal cortex slices of *shiverer* mice at postnatal days 3-5 and the iPSCs-derived OPCs are injected into the slices. At 10 days post-transplantation of OPCs, we observed MBP protein in organotypic cortex slices. To identify human specific cells, we used human nuclear antigen (hNuc)**(Figure 3)**.

Migration potential of iPSCs-derived OPCs

OPCs are known to be highly migratory. In particular, they are known to migrate towards demyelinated areas to initiate the remyelination process. It has been reported that insufficient OPC migration into demyelination lesions can

cause deprived remyelination in MS[38]. Growth factors like PDGF, FGF and chemokine CXCL1 are suggested to be involved in the migration of OPCS[39–41]. In addition, many different extracellular matrix proteins and cell surface molecules regulate OPC migration[42–44]. When modelling OPC function *in vitro*, the migration efficiency of OPCs is a critical characteristic to assess. In this study, we performed an in *vitro* migration assay to check the migration potential of human iPSC-derived OPCs in response to PDGF-AA. OPCs were grown on matrigel-coated coverslips and cultured without serum and other growth factors. The rate of migration towards medium containing PDGF-AA and without PDGF-AA was measured. iPSC-derived OPCs migrated faster towards PDGF-AA compared to medium without PDGF-AA **(Figure 4A)**. In addition, we checked the migration

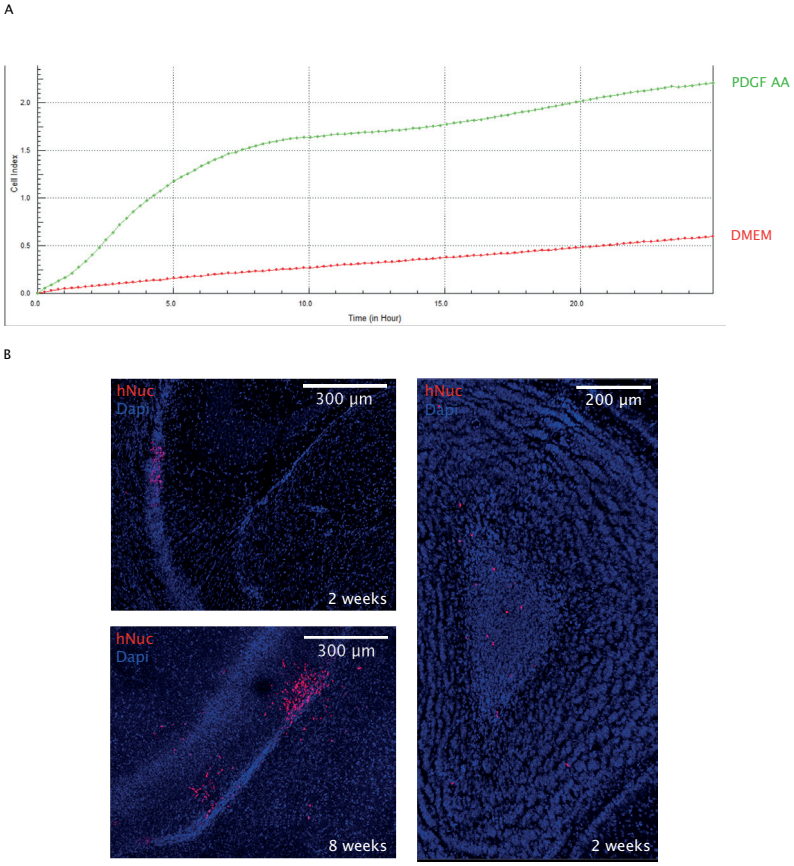

Figure 4. OPCs migrate both *in vitro* and *in vivo* conditions. (A) iPSC-derived OPCs can migrate *in vitro*. OPCs are incubated 24hrs in DMEM-only medium on matrigel-covered upper plate. Cell index shows the amount of OPCs migrating towards the lower plate, which is higher to OPC medium containing PDGF-AA (in green) than DMEM (in red) only medium. **(B)** iPSC-derived OPCs can migrate *in vivo*. iPSC-derived OPCs transplanted in a host mouse brain. Human cells are labeled using an antibody against human nuclei (red). (top-left) 2 weeks after neonatal transplantation cells seem to establish a niche in the subventricular zone (SVZ), a major neurogenic region. (bottom-left) 8 weeks after transplantation the population of human cells has expanded and cells migrate away from the SVZ towards the cortex, hippocampus and amygdala. (right) 2 weeks after transplantation human cells were found in the olfactory bulb of the mouse, suggesting that they have the ability to detect physiological cues from their host environment and migrate along the rostral migratory stream.

efficiency of iPSC-derived OPCs *in vivo*. OPCs were transplanted in neonatal immunodeficient *shiverer* mice, bilaterally in the anlagen of the corpus callosum. *Shiverer* mice provide a null background for any myelination that results from transplanted OPCs. Therefore, any myelin found after transplantation will have to originate from the human cells that differentiate to oligodendrocytes in the mouse brain. Two weeks after transplantation, the human OPCs had established a niche in the SVZ **(Figure 4B)**, a major neurogenic region, and had already migrated towards the olfactory bulb via the rostral migratory stream **(Figure 4B)**. Eight weeks post-transplantation the cells had expanded in the SVZ and migrated into the cortex, hippocampus and amygdala **(Figure 4B)**. No myelin was found in the brains of immunodeficient *shiverer* mice up to 12 weeks after transplantation. Therefore, we aim to optimize our protocol; by checking later time points and by injecting FACS sorted OPCs to increase the amount of bona fide oligodendroctyes progenitors injected.

DISCUSSION

OPCs are the main proliferative cell type of the CNS, composing about 5% of all brain cells in the adult brain. Impairments associated with this cell population can lead to decreased myelin integrity, which has been reported for several major mental and neurobiological disorders[45–47]. OPCs can be found both in gray and white matter, with different physiological properties[48]. White matter OPCs are more proliferative, whereas gray matter OPCs are generally in a quiescent and immature state[49]. OPCs that can differentiate into oligodendrocytes arise from multiple regions in the developing brain. Data from human fetal forebrain at midgestation suggest three different populations of OPCs[50–52]. One early subpopulation originates from the ganglionic eminence and expresses NKX2.1. Another population originates from the SVZ and expresses DLX2. The third population of oligodendrocyte lineage cells originates from neural stem cells in the forebrain. All populations express typical OPC markers such as CSPG4/NG2, PDGFRα and Olig1. However, it is not yet clear if these different OPC types have different efficiency to form myelinating oligodendrocytes or have basic cellular and molecular differences.

For the current OPC differentiation protocol, we used growth factors required for oligodendrogenesis. Several protocols in literature suggest different combinations of growth factors for the generation of OPCs. For instance, even though PDGF-AA has been commonly used in OPC cultures, some studies use the PDGF-AB heterodimer and PDGF-BB homodimer for the induction of PDGF signaling in OPC generation[26,53,54]. In addition, heparin and IGF-1 are other factors used for *in vitro* oligodendrogenesis[54]. However, most protocols are specific for rodents or for progenitors isolated from brain but not differentiated from iPSCs. Thus, it is important to consider the species and developmental differences.

The generation of myelinating oligodendrocytes *in vitro* is challenging. Previously published protocols yielded variable amounts of myelin *in vivo.* Also, these protocols took several months, not always produce myelin *in vitro*, therefore they are not consistently efficient[55–58]. Remarkably, a previous study did show recovery of the myelin deficit in *shiverer* mice 7 months after transplantation of FACS-purified human iPSC-derived OPCs[17]. In this study, Wang et al. established OPCs from multiple iPSC lines and were able to show myelination 13 weeks after transplantation and a full rescue after 7 months when using their most efficient cell line. The *Mbp* mutation in *shiverer* mice is normally lethal; however by performing these transplantations they were able to greatly increase the lifespan of these mice. In our study we were not able to replicate these results. When transplanting our iPSC-derived OPCs in *shiverer* mice we were not able to observe any myelin 12 weeks after transplantations. We observed a small amount of human cells were able to integrate and migrate into the mouse brain. Important to report that our preliminary transplantation studies were

performed with unsorted lines. To avoid issues of heterogeneity in the injected cell population, our future experiments aim to focus on using FACS-purified OPC-lines. Furthermore, allowing transplanted *shiverer* mice to survive longer might yield more myelinating oligodendrocytes.

In our differentiation protocol, we observed a small amount of MBP when OPCs were co-cultured with primary mouse neurons and the MBP amount in *in vitro* differentiation experiments was not always consistent. OPCs might require additional factors from the extracellular matrix and from other cell types to initiate processes required for myelination. For instance, neuronal signals can be required for the initiation of the myelination process[36,37] in which OPCs receive signals (growth factors, synaptic inputs or other factors) and initiate differentiation to oligodendrocytes leading to myelination. Consistently, the amount of MBP is much higher when iPSC-derived OPCs are cultured in organotypic cortex slices, which might suggest that OPCs indeed require more environmental cues to differentiate into myelinating oligodendrocytes.

To increase the differentiation efficiency of OPCs to form myelinating oligodendrocytes, we aim to inject FACS-purified OPCs in organotypic slices**.** Further characterization of OPCs, such as RNA sequencing and detailed electrophysiological recordings would give more insight into the properties and region specificity of the OPCs generated with this protocol.

In a pilot experiment, we performed electrophysiological recordings of iPSC-derived OPCs, which showed a typical OPC physiology **(Supplementary Figure 2)**. The physiology of OPCs has been described previously[59]. Although, far from the physiological features of neurons, OPCs had a negative membrane potential, sodium currents and action potentials (mostly single action potentials) and even synaptic connectivity. We measured 9 cells for their ability to fire an action potential upon current injection. Out of 9 cells, 5 exhibited a fast action potential, while 4 were completely inert. Our future aim is to have voltage clamp recordings from iPSC-derived OPCs and to further assess their properties upon pharmacological manipulation.

In summary, here we propose a relatively fast protocol in which iPSCs-derived NPCs can be differentiated into OPCs during a 3-week period after which OPCs express basic OPC markers; CSPG4/NG2, PDGFRα, Olig2 and Sox10. These iPSC-derived OPCs can differentiate into myelinating oligodendrocytes in organotypic slices (and when cultured with primary mouse neurons). Furthermore, our iPSC-derived OPCs can migrate towards PDGF-AA in conductance-based migration assays. The ability of the OPCs to integrate and migrate after transplantation into mouse brain, providing opportunities to study potential therapeutic interventions for disorders associated with the oligodendrocyte lineage.

Acknowledgements: We would like to thank the lab of Ype Elgersma for supplying the primary mouse neuron cultures.

MATERIALS AND METHODS

Cell culture

iPSC-derived NPCs were differentiated to enriched population of OPCs using a protocol adapted from Monaco *et al.*[20]. hES and iPSC-derived NPCs were plated on laminin coated 10cm plates in NPC medium (DMEM/F12, 1x N2, 1x B27-RA, 1µg/ml laminin, 1 %P/S 25ng/ml Fibroblast Growth Factor (bFGF) and 20ng/ml Epidermal growth factor (EGF)). When NPCs were 90% confluent, NPC medium was changed with OPC medium (DMEM/HAMS F12, 1x N2, 1% BSA, 1% L-Glutamine, 1% P/S, 20ng/ml basic fibroblast growth factor (bFGF), 10ng/ml platelet derived growth factor (PDGF-AA), 2ng/ml Sonic hedgehog (Shh), 2ng/ml Neurotrophic factor 3 (NT-3) and 3nM triiodothyronine (T3) for three weeks. OPC medium was changed every other day and growth factors were added freshly each time to

the medium. Resulting OPCs were passaged one in four every week using 100U/ml of Collagenase Type IV (ThermoFisher).

Immunocytochemistry

Cell cultures were fixed using 4% formaldehyde in PBS for 15 minutes at room temperature and rinsed three times with PBS. Primary antibodies were incubated overnight at 4°C in labelling buffer containing 0.05 M Tris, 0.9% NaCl, 0.25% gelatin, and 0.5% Triton-X-100 (pH 7.4). The following primary antibodies were used: Sox2, Nestin, MAP2, NeuN, GFAP, FoxG1 [ProSci], Vimentin, PDGFRα [Santa Cruz Biotechnology], AFP, SOX10 [R&D Systems], TRA-1-81, Nanog [Beckton Dickinson], Oct4, OLIG2, APC (CC1), MBP [Abcam]. NG2 [kindly provided by W Stallcup]. The following secondary antibodies were used: Alexa-488, Alexa-546, Alexa-555 and Cy3 antibodies [Jackson ImmunoResearch]. Samples were embedded in Mowiol 4-88 (Fluka) after which confocal imaging was performed with a Zeiss LSM700 confocal microscope (Apochromatic 40x objective, 1.3 NA, oil immersion) using ZEN software (Zeiss, Germany).

Flowcytometry

Following the three-week differentiation of NPCs to OPCs, the obtained cell population was purified using a BD FACSAria III. Cells were dissociated from a confluent 10 cm culture dish using collagenase, washed with PBS and put on ice in 100µl PBS containing CD140α antibody (1:150) conjugated to Cy5 (BD Biosciences) and Hoechst 33258 (1:200) (Invitrogen). Next, cells were washed twice with PBS before filtration through a cell strainer cap (Falcon) to obtain a single cell suspension. Finally, cells were run through a BD FACSAria III, from which cells positive for CD140α and negative for Hoechst 33258 were collected in culture plates. The purified population was expanded, analyzed and stored in liquid nitrogen. Purified OPCs were recovered from liquid nitrogen and expanded one week before each experiment.

Myelination assay

Organotypic cortex slices were established according to Stoppini *et al*,[60] with modifications. Briefly, *shiverer* mice (C3Fe.SWV-*Mbp*^{shi}, Jackson Laboratory) were sacrificed at P3-P5. The brain was rapidly removed and transferred to ice cold Gey's Balanced Salt Solution (Sigma) containing 5.4 mg/ml glucose and 1% P/S. After dividing the brain sagittally into two hemispheres, 300 µm fronto-parietal coronal slices were obtained using a tissue chopper (McIlwain). Slices were cultured on an air-fluid interface at 37°C with 5% CO, using culture plate inserts (Millipore: 0.4 µm pore size; 30 mm diameter; 3 cultures per insert) in 1.0 mL culture medium containing 50% MEMα, 25% HBSS, 25% horse serum, 6.5 mg/mL glucose, 2 mM glutamine, 1% N2 supplement and 1% P/S, supplemented with PDGF-AA. For each *Mbp*$^{shi/shi}$ mouse, adjacent slices were randomly assigned for transplantation with either patient or control OPCs, thereby providing comparative matched pairs. Each slice was transplanted with 1 x 10^4 iPSC-derived OPCs in 1.0 µL PBS containing 0.1% FastGreen (Gibco-Invitrogen) using a Picospritzer. OPCs were allowed to differentiate into myelinating oligodendrocytes for 10 days, following the procedure described in Najm *et al*.[19].

Transplantations

Heterozygous *shiverer* mice (*Mbp*$^{shi/shi}$) were crossed with homozygous Rag2 immunodeficient mice with normal myelin. The use of immunodeficient mice avoids issues of host rejection of foreign cells, thereby improving the success rare of transplantation. The resulting liters were used for transplantation studies. On the day of birth a total of 250.000 OPCs resuspended in 0,1% Fastgreen DPBS was delivered in 5 injection sites, bilateral into the posterior and anterior anlagen of the corpus callosum and into the cerebellar peduncle. Prior to the transplantation, pups were wrapped in a sheet of nitrile and immobilized in ice for cryoanesthesia, leaving the head exposed. Cell delivery was performed using pulled glass pipettes with a diameter of 0.1-1 mm. After penetrating the skull with a pipette containing the cell solution at one of the target sites the needle was lowered approximately 1 mm into the brain and a short burst of positive

pressure was applied to the pipette using a picospritzer to deliver a 1-µl drop. Following the transplantations the pups were placed on a 37°C heat mat to recover, after all pups had recovered they were placed back with their mothers.

Immunohistochemistry

Animals transplanted with iPSC-derived progenitors were sacrificed after 2 weeks by decapitation, or after 8 weeks by standard transcardiac perfusion with 4% paraformaldehyde under deep isoflurance anesthesia, prior to decapitation, brains were removed, left in 4% pFA overnight and embedded in gelatin. Next, 40 µm cryosections were made and stained with different fluorescent markers. Identification of transplanted human cells was achieved by co-labeling multiple combinations of anti-human nuclear antigen (MAB1281, 1:250, Millipore) with different cell lineage markers. Cell lineage identification was obtained with anti-NG2 (Stallcup, 1:1000), anti-hNG2 (MAB2029, 1:1000 Millipore), anti-NeuN (MAB377, 1:2000, Millipore), anti-Tuj1 (AB9354. 1:1000, Millipore), anti-GFAP (AB5804, 1:1000, Millipore) and anti-MBP (ab7349, 1:1000, Abcam). All secondary antibodies were used 1:200 (Invitrogen). Counterstaining was performed using 4,6-diamidino-2-phenylindole (DAPI, 1:10.000, Invitrogen). As a final step sections were mounted rostral to caudal on glass slides in Mowiol (Sigma-Aldrich).

Migration assay

In vitro migration assays were performed using an xCELLigence RTCA DP Biosciences instrument that allows flexible real-time cell monitoring, according to the manufacturers' protocol. Briefly, the plate has two separate compartments for experimental setup; OPCs are seeded and incubated 24hrs in serum free DMEM only on the upper plate coated with matrigel. OPC medium containing chemoattractant PDGF-AA was placed in lower chamber. Migration of OPCs through the microporous membrane was monitored over a 24-hour period. During the migration, OPCs passing the microelectrode sensors elicit a pulse, which is measured by the RTCA DP instrument. All serum-starved samples showed base-line Cell Index levels indicating the absence of migration, while those wells with chemoattractant did show migration.

Electrophysiology

OPCs were plated on laminin-plated coverslips and collected from 6/12 wells culture plates. Whole-cell patch clamp recordings were performed in 3-5 week old cultures of iPSCs-derived OPCs. The recording micropipettes (tip resistance 3–6 MΩ) were filled with internal solution composed of (mM): 130 K-gluconate, 0.1 EGTA, 1 MgCl2, 2 MgATP, 0.3 NaGTP, 10 HEPES, 5 NaCl, 11 KCl, 5 phosphocreatine (pH 7.4). Recordings were made using a MultiClamp 700B amplifier (Molecular Devices). Signals were sampled and filtered at 10 kHz and 3 kHz, respectively. The whole-cell capacitance was compensated and series resistance was monitored throughout the experiment. Voltage was corrected for liquid junction potential. The bath was constantly perfused with fresh saline composed of (mM): 110 NaCl, 2.5 KCl, 2 CaCl2, 10 glucose, 1 NaH2PO4, 25 NaHCO3, 0.2 ascorbic acid and 2 MgCl2 (pH 7.4). For current-clamp recordings cells were held at -70mV. Hyperpolarized and depolarized voltage responses were stimulated by 500 msec current steps varied from −20 to +150 pA in 3 pA increments. All recordings were performed at room temperature. Data analysis was performed by Clampfit 10.2 software (Molecular devices).

SUPPLEMENTARY FIGURES

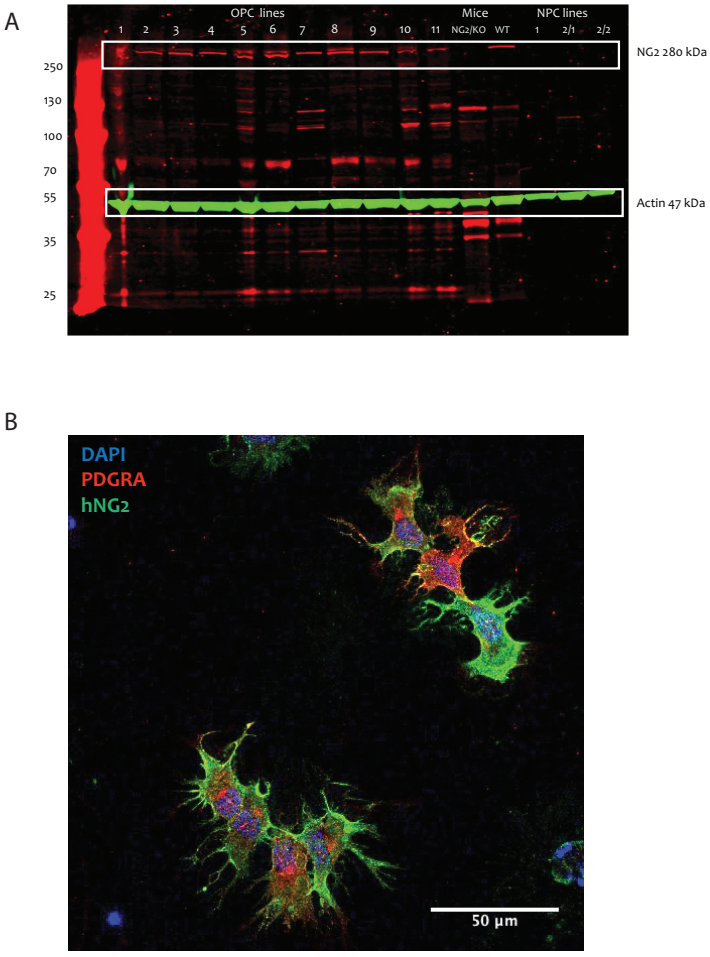

Supplementary Figure 1. OPC markers CSPG4/NG2 and PDGFRα (A) Western Blot showing OPC marker CSPG4/NG2 that is present in different OPC lines but not in NPCs. **(B)** OPCs have more processes after co-culturing with primary mouse neurons.

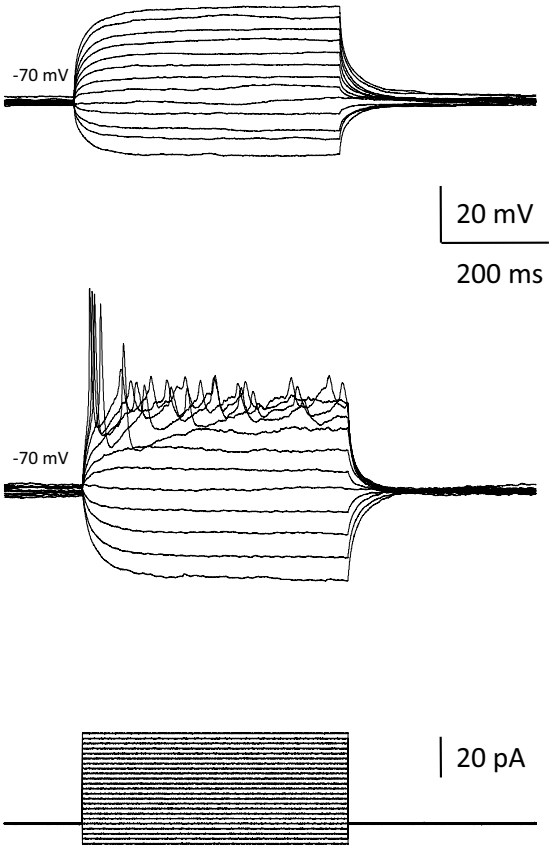

Supplementary Figure 2. Electrophysiological properties of iPSC-derived OPCs. Two traces are from two different cells, one inert and one spiking. Lower trace is the current injected (500 ms in 3 pA increments). Cells were held at -70 mV.

REFERENCES

1 Nishiyama A, Komitova M, Suzuki R, Zhu X. Polydendrocytes (NG2 cells): multifunctional cells with lineage plasticity. Nat Rev Neurosci 2009; 10: 9–22.

2 Nave K-A. Myelination and the trophic support of long axons. Nat Rev Neurosci 2010; 11: 275–83.

3 Hughes EG, Kang SH, Fukaya M, Bergles DE. Oligodendrocyte progenitors balance growth with self-repulsion to achieve homeostasis in the adult brain. Nat Neurosci 2013; 16: 668–76.

4 Bergles DE, Jabs R, Steinhäuser C. Neuron-glia synapses in the brain. Brain Res Rev 2010; 63: 130–7.

5 Zhu X, Hill RA, Nishiyama A. NG2 cells generate oligodendrocytes and gray matter astrocytes in the spinal cord. Neuron Glia Biol 2008; 4: 19–26.

6 Chang A, Nishiyama A, Peterson J, Prineas J, Trapp BD. NG2-Positive Oligodendrocyte Progenitor Cells in Adult Human Brain and Multiple Sclerosis Lesions. J Neurosci 2000; 20: 6404–6412.

7 Staugaitis SM, Trapp BD. NG2-positive glia in the human central nervous system. Neuron Glia Biol 2009; 5: 35–44.

8 Tkachev D, Mimmack ML, Ryan MM, Wayland M, Freeman T, Jones PB et al. Oligodendrocyte dysfunction in schizophrenia and bipolar disorder. Lancet (London, England) 2003; 362: 798–805.

9 Ren Y, Wang H, Xiao L. Improving myelin/oligodendrocyte-related dysfunction: a new mechanism of antipsychotics in the treatment of schizophrenia? Int J Neuropsychopharmacol 2013; 16: 691–700.

10 Roussos P, Haroutunian V. Schizophrenia: susceptibility genes and oligodendroglial and myelin related abnormalities. Front Cell Neurosci 2014; 8: 5.

11 Nave K-A, Trapp BD. Axon-Glial Signaling and the Glial Support of Axon Function. Annu Rev Neurosci 2008; 31: 535–561.

12 Philips T, Bento-Abreu A, Nonneman A, Haeck W, Staats K, Geelen V et al. Oligodendrocyte dysfunction in the pathogenesis of amyotrophic lateral sclerosis. Brain 2013; 136: 471–82.

13 Yang N, Wernig M. Harnessing the stem cell potential: a case for neural stem cell therapy. Nat Med 2013; 19: 1580–1.

14 Windrem MS, Schanz SJ, Guo M, Tian G-F, Washco V, Stanwood N et al. Neonatal chimerization with human glial progenitor cells can both remyelinate and rescue the otherwise lethally hypomyelinated shiverer mouse. Cell Stem Cell 2008; 2: 553–65.

15 Uchida N, Chen K, Dohse M, Hansen KD, Dean J, Buser JR et al. Human Neural Stem Cells Induce Functional Myelination in Mice with Severe Dysmyelination. Sci Transl Med 2012; 4: 155ra136–155ra136.

16 Douvaras P, Fossati V. Generation and isolation of oligodendrocyte progenitor cells from human pluripotent stem cells. Nat Protoc 2015; 10: 1143–54.

17 Wang S, Bates J, Li X, Schanz S, Chandler-Militello D, Levine C et al. Human iPSC-derived oligodendrocyte progenitor cells can myelinate and rescue a mouse model of congenital hypomyelination. Cell Stem Cell 2013; 12: 252–264.

18 Douvaras P, Wang J, Zimmer M, Hanchuk S, O'Bara MA, Sadiq S et al. Efficient generation of myelinating oligodendrocytes from primary progressive multiple sclerosis patients by induced pluripotent stem cells. Stem cell reports 2014; 3: 250–9.

19 Najm FJ, Zaremba A, Caprariello A V, Nayak S, Freundt EC, Scacheri PC et al. Rapid and robust generation of functional oligodendrocyte progenitor cells from epiblast stem cells. Nat Methods 2011; 8: 957–62.

20 Monaco MCG, Maric D, Bandeian A, Leibovitch E, Yang W, Major EO. Progenitor-derived oligodendrocyte culture system from human fetal brain. J Vis Exp 2012; : 1–8.

21 Kessaris N, Jamen F, Rubin LL, Richardson WD. Cooperation between sonic hedgehog and fibroblast growth factor/MAPK signalling pathways in neocortical precursors. Development 2004; 131: 1289–98.

22 Bilican B, Fiore-Heriche C, Compston A, Allen

ND, Chandran S. Induction of Olig2+ Precursors by FGF Involves BMP Signalling Blockade at the Smad Level. PLoS One 2008; 3: e2863.

23 Naruse M, Nakahira E, Miyata T, Hitoshi S, Ikenaka K, Bansal R. Induction of oligodendrocyte progenitors in dorsal forebrain by intraventricular microinjection of FGF-2. Dev Biol 2006; 297: 262–73.

24 Azim K, Raineteau O, Butt AM. Intraventricular injection of FGF-2 promotes generation of oligodendrocyte-lineage cells in the postnatal and adult forebrain. Glia 2012; 60: 1977–1990.

25 Mason JL, Goldman JE. A2B5+ and O4+ Cycling progenitors in the adult forebrain white matter respond differentially to PDGF-AA, FGF-2, and IGF-1. Mol Cell Neurosci 2002; 20: 30–42.

26 Gard AL, Pfeiffer SE. Glial cell mitogens bFGF and PDGF differentially regulate development of O4+GalC- oligodendrocyte progenitors. Dev Biol 1993; 159: 618–630.

27 McKinnon RD, Matsui T, Dubois-Dalcq M, Aaronsont SA. FGF modulates the PDGF-driven pathway of oligodendrocyte development. Neuron 1990; 5: 603–614.

28 Gonzalez-Perez O, Romero-Rodriguez R, Soriano-Navarro M, Garcia-Verdugo JM, Alvarez-Buylla A. Epidermal growth factor induces the progeny of subventricular zone type B cells to migrate and differentiate into oligodendrocytes. Stem Cells 2009; 27: 2032–43.

29 Kerman BE, Kim HJ, Padmanabhan K, Mei A, Georges S, Joens MS et al. In vitro myelin formation using embryonic stem cells. Development 2015; 142: 2213–25.

30 Demoulin J-B, Essaghir A. PDGF receptor signaling networks in normal and cancer cells. Cytokine Growth Factor Rev 2014; 25: 273–83.

31 Woodruff RH, Fruttiger M, Richardson WD, Franklin RJM. Platelet-derived growth factor regulates oligodendrocyte progenitor numbers in adult CNS and their response following CNS demyelination. Mol Cell Neurosci 2004; 25: 252–262.

32 Hu B-Y, Du Z-W, Zhang S-C. Differentiation of human oligodendrocytes from pluripotent stem cells. Nat Protoc 2009; 4: 1614–22.

33 Neurotrophin-3 and brain-derived neurotrophic factor induce oligodendrocyte proliferation and myelination of regenerating axons in the contused adu... - PubMed - NCBI. http://www.ncbi.nlm.nih.gov/pubmed/9651218 (accessed 14 Jan2016).

34 Baas D, Bourbeau D, Sarlième LL, Ittel ME, Dussault JH, Puymirat J. Oligodendrocyte maturation and progenitor cell proliferation are independently regulated by thyroid hormone. Glia 1997; 19: 324–32.

35 Baas D, Legrand C, Samarut J, Flamant F. Persistence of oligodendrocyte precursor cells and altered myelination in optic nerve associated to retina degeneration in mice devoid of all thyroid hormone receptors. Proc Natl Acad Sci U S A 2002; 99: 2907–11.

36 Colello RJ, Pott U. Signals that initiate myelination in the developing mammalian nervous system. Mol Neurobiol 1997; 15: 83–100.

37 Taveggia C, Feltri ML, Wrabetz L. Signals to promote myelin formation and repair. Nat Rev Neurol 2010; 6: 276–87.

38 Boyd A, Zhang H, Williams A. Insufficient OPC migration into demyelinated lesions is a cause of poor remyelination in MS and mouse models. Acta Neuropathol 2013; 125: 841–59.

39 de Castro F, Bribián A. The molecular orchestra of the migration of oligodendrocyte precursors during development. Brain Res Brain Res Rev 2005; 49: 227–41.

40 Redwine JM, Blinder KL, Armstrong RC. In situ expression of fibroblast growth factor receptors by oligodendrocyte progenitors and oligodendrocytes in adult mouse central nervous system. J Neurosci Res 1997; 50: 229–37.

41 Spassky N, Heydon K, Mangatal A, Jankovski A, Olivier C, Queraud-Lesaux F et al. Sonic hedgehog-dependent emergence of oligodendrocytes in the telencephalon: evidence for a source of oligodendrocytes in the olfactory bulb that is independent of PDGFRalpha signaling. Development 2001; 128: 4993–5004.

42 Wang C, Rougon G, Kiss JZ. Requirement of polysialic acid for the migration of the O-2A glial progenitor cell from neurohypophyseal explants. J Neurosci 1994; 14: 4446–57.

43 Kiernan BW, Götz B, Faissner A, ffrench-Constant C. Tenascin-C inhibits oligodendrocyte precursor cell migration by both adhesion-dependent and adhesion-independent mechanisms. Mol Cell Neurosci 1996; 7: 322–35.

44 Frost E, Kiernan BW, Faissner A, ffrench-Constant C. Regulation of oligodendrocyte precursor migration by extracellular matrix: evidence for substrate-specific inhibition of migration by tenascin-C. Dev Neurosci 1996; 18: 266–73.

45 Edgar N, Sibille E. A putative functional role for oligodendrocytes in mood regulation. Transl Psychiatry 2012; 2: e109.

46 Levine JM, Reynolds R, Fawcett JW. The oligodendrocyte precursor cell in health and disease. Trends Neurosci 2001; 24: 39–47.

47 Bradl M, Lassmann H. Oligodendrocytes: Biology and pathology. Acta Neuropathol 2010; 119: 37–53.

48 Káradóttir R, Hamilton NB, Bakiri Y, Attwell D. Spiking and nonspiking classes of oligodendrocyte precursor glia in CNS white matter. Nat Neurosci 2008; 11: 450–6.

49 Dimou L, Simon C, Kirchhoff F, Takebayashi H, Götz M. Progeny of Olig2-expressing progenitors in the gray and white matter of the adult mouse cerebral cortex. J Neurosci 2008; 28: 10434–42.

50 Jakovcevski I, Zecevic N. Olig transcription factors are expressed in oligodendrocyte and neuronal cells in human fetal CNS. J Neurosci 2005; 25: 10064–73.

51 Jakovcevski I, Zecevic N. Sequence of oligodendrocyte development in the human fetal telencephalon. Glia 2005; 49: 480–91.

52 Rakic S, Zecevic N. Early oligodendrocyte progenitor cells in the human fetal telencephalon. Glia 2003; 41: 117–27.

53 Chojnacki A, Weiss S. Isolation of a novel platelet-derived growth factor-responsive precursor from the embryonic ventral forebrain. J Neurosci 2004; 24: 10888–99.

54 Franco PG, Pasquini JM, Silvestroff L. Optimizing Culture Medium Composition to Improve Oligodendrocyte Progenitor Cell Yields In Vitro from Subventricular Zone-Derived Neural Progenitor Cell Neurospheres. PLoS One 2015; 10: e0121774.

55 Brüstle O, Jones KN, Learish RD, Karram K, Choudhary K, Wiestler OD et al. Embryonic stem cell-derived glial precursors: a source of myelinating transplants. Science 1999; 285: 754–6.

56 Jiang P, Selvaraj V, Deng W. Differentiation of embryonic stem cells into oligodendrocyte precursors. J Vis Exp 2010. doi:10.3791/1960.

57 Liu S, Qu Y, Stewart TJ, Howard MJ, Chakrabortty S, Holekamp TF et al. Embryonic stem cells differentiate into oligodendrocytes and myelinate in culture and after spinal cord transplantation. Proc Natl Acad Sci U S A 2000; 97: 6126–31.

58 Numasawa-Kuroiwa Y, Okada Y, Shibata S, Kishi N, Akamatsu W, Shoji M et al. Involvement of ER stress in dysmyelination of Pelizaeus-Merzbacher Disease with PLP1 missense mutations shown by iPSC-derived oligodendrocytes. Stem cell reports 2014; 2: 648–61.

59 Livesey MR, Magnani D, Cleary EM, Vasistha NA, James OT, Selvaraj BT et al. Maturation and electrophysiological properties of human pluripotent stem cell-derived oligodendrocytes. Stem Cells 2016. doi:10.1002/stem.2273.

60 Stoppini L, Buchs P -a., Muller D. A simple method for organotypic cultures of nervous tissue. J Neurosci Methods 1991; 37: 173–182.

Chapter 4

CSPG4 mutations implicate oligodendrocyte precursor cell dysfuntion as a pathophysiological mechanism of schizophrenia

F.M. de Vrij, C.G. Bouwkamp, N. Gunhanlar,

G. Shpak, B. Lendemeijer, M. Baghdadi, M. Ghazvini, T.M. Li, M. Quadri, S. Olgiati, G.J. Breedveld, M. Coesmans, E. Mientjes, T. de Wit, F.W. Verheijen, H.B. Beverloo, D. Cohen, R.M. Kok, P.R. Bakker, A. Nijburg, A.T. Spijker, P.J. Haffmans, E. Hoencamp, V. Bergink, GROUP Study Consortium, J.A. Vorstman, N. Amin, C.D. Langen, A. Hofman, C.M. van Duijn, W.J. Hoogendijk, M.A. Ikram, M.W. Vernooij, H. Tiemeier, A.G. Uitterlinden, Y. Elgersma, B. Distel, J. Gribnau, R.A. Ophoff, T. White, V. Bonifati,

S.A. Kushner

Manuscript in preparation

CSPG4 Mutations implicate Oligodendrocyte Precursor Cell Dysfunction as a Pathophysiological Mechanism of Schizophrenia

F.M. de Vrij[†], C.G. Bouwkamp[1,2†], N. Gunhanlar[1†], G. Shpak[1], B. Lendemeijer[1], M. Baghdadi[1], M. Ghazvini[3], T.M. Li[3], M. Quadri[2], S. Olgiati[2], G.J. Breedveld[2], M. Coesmans[1,11], E. Mientjes[8,9], T. de Wit[2], F.W. Verheijen[2], H.B. Beverloo[2], D. Cohen[12], R.M. Kok[13], P.R. Bakker[14,15], A. Nijburg[13], A.T. Spijker[13], P.J. Haffmans[13], E. Hoencamp[13], V. Bergink[1], GROUP Study Consortium, J.A. Vorstman[16], N. Amin[4], C.D. Langen[7], A. Hofman[4], C.M. van Duijn[4], W.J. Hoogendijk[1], M.A. Ikram[4,5,6], M.W. Vernooij[4,6], H. Tiemeier[1,4,7], A.G. Uitterlinden[4,10], Y. Elgersma[8,9], B. Distel[8,9,17], J. Gribnau[3], R.A. Ophoff[18], T. White[7], V. Bonifati[2], S.A. Kushner[1]

[†] *These authors contributed equally*

[1] Department of Psychiatry,
[2] Department of Clinical Genetics,
[3] Department of Developmental Biology, and Erasmus MC iPS Facility,
[4] Department of Epidemiology,
[5] Department of Neurology,
[6] Department of Radiology,
[7] Department of Child and Adolescent Psychiatry,
[8] Department of Neuroscience,
[9] ENCORE Expertise Centre For Neurodevelopmental Disorders,
[10] Department of Internal Medicine, Erasmus Medical Center, Rotterdam, The Netherlands
[11] Delta Psychiatric Centre, Poortugaal, The Netherlands
[12] Mental Health Care Organization North-Holland North, Heerhugowaard, The Netherlands
[13] Parnassia Psychiatric Institute, The Hague, The Netherlands
[14] Department of Psychiatry and Psychology, School of Mental Health and Neuroscience, Maastricht University Medical Centre, Maastricht, The Netherlands
[15] Psychiatric Centre GGZ Centraal, Amersfoort, The Netherlands
[16] Department of Psychiatry, Rudolf Magnus Institute of Neuroscience, University Medical Center Utrecht, The Netherlands
[17] Medical Biochemistry, Academic Medical Centre, Amsterdam, The Netherlands
[18] Center for Neurobehavioral Genetics, Semel Institute for Neuroscience and Human Behavior, University of California, Los Angeles, CA, USA

ABSTRACT

Family history is the strongest known risk factor for schizophrenia. Although the majority of schizophrenia cases appear to be sporadic, many families have been described with a Mendelian pattern of disease inheritance, suggestive of highly penetrant genetic determinants. Here, we report multiple rare missense mutations in *Chondroitin Sulfate Proteoglycan 4 (CSPG4)* demonstrating familial segregation with schizophrenia. CSPG4/NG2 is abundantly expressed in oligodendrocyte progenitor cells (OPCs), the exclusive precursor of myelinating oligodendrocytes. Induced pluripotent stem cell-derived OPCs from *CSPG4*^{A1731T} mutation carriers exhibited abnormal posttranslational processing and subcellular localization of mutant NG2, and aberrant cellular morphology. Moreover, and highly consistent with clinically-relevant OPC dysfunction, *in vivo* diffusion tensor imaging demonstrated a significant reduction of brain white matter integrity in *CSPG4*^{A1731T} mutation carriers. Taken together, our findings identify *CSPG4* as a novel candidate gene for schizophrenia. Moreover, these data provide evidence to implicate OPC dysfunction as a pathophysiological mechanism of schizophrenia.

INTRODUCTION

Schizophrenia is a severely debilitating psychiatric disorder affecting ~1% of the population worldwide. The strongest known risk factor for developing schizophrenia is family history. A recent meta-analysis which included five decades of twin studies found a monozygotic twin correlation for schizophrenia of 0.76 ± 0.018 and a heritability estimate of 0.77 ± 0.051 but with a relatively limited contribution of shared environmental influences (0.013 ± 0.025) [1].

With the advent of the microarray-based genotyping arrays, genome-wide association studies (GWAS) became the standard method of genetic study into disease etiology in many fields of medicine, with some notable successes. The latest iteration of the Psychiatric Genomics Consortium investigating 36,989 cases and 113,075 controls, identified 128 genome-wide significant single-nucleotide variants in 108 independent genomic loci, suggesting an important contribution of common genetic variation to schizophrenia risk[10].

The development of next-generation sequencing methods has opened up another possibility to examine whether rare single nucleotide variants or small insertions-deletions might contribute to schizophrenia risk. In the largest case-control study to date using whole exome sequencing, a Swedish cohort including 2,536 cases and 2,543 controls yielded no single mutation or single gene reaching genome-wide significance for association with schizophrenia[2]. Nevertheless, the authors identified functional gene sets containing rare coding variants enriched in cases, suggesting that schizophrenia is a polygenic disorder with shared pathophysiological mechanisms.

Among classical neurological diseases with a complex genetic architecture, rare familial monogenic causes of Alzheimer's disease and Parkinson's disease have been identified, in addition to idiopathic non-familial forms. Notably, in most cases, patients carrying familial variants are clinically indistinguishable from those with sporadic forms of the disease[3–8]. We reasoned that severe psychiatric illness, such as schizophrenia, has shared characteristics with these neurological diseases, as their primary pathology resides in the brain, with normal progression of childhood developmental milestones, of moderate-to-high heritability, and currently diagnosed using primarily clinical criteria. Therefore, we implemented a family-based genetic discovery approach using linkage-based next generation sequencing[3, 9].

Recent genetic and induced pluripotent stem cell (iPSC)-based studies have converged on a model by which neuronal function and in particular synaptic transmission, is a major pathophysiological mechanism of schizophrenia[2,10.11,12]. However, functional neuronal alterations may arise either by a cell-type autonomous effect of risk factors on neurons themselves, or indirectly through a primary pathophysiological influence on other cell types which regulate neuronal function. Numerous studies have reported the involvement of glial cell biology in the pathophysiology of schizophrenia, including alterations in oligodendrocytes, myelination, and white matter integrity[13–16,17–19,20], which directly regulate neuronal function. The late adolescent critical period for cerebral cortex myelination has long been recognized as overlapping closely with the typical age of onset for schizophrenia[21,22].

We now report the discovery of multiple rare missense variants in the *CSPG4* gene that segregate with schizophrenia. CSPG4, widely known by the alias NG2 (neural/glial antigen 2), is a single-pass transmembrane proteoglycan with abundant expression in oligodendroctye precursor cells (OPCs)[23,24]. Using iPSCs reprogrammed from affected $CSPG4^{A131T}$ mutation carriers and their unaffected non-carrier siblings, we demonstrate that patient-derived OPCs exhibit aberrant subcellular localization of NG2 and abnormal cellular morphology. Moreover, and highly confirmatory of clinically-relevant OPC dysfunction, diffusion tensor imaging of $CSPG4^{A131T}$ mutation carriers demonstrated a global impairment in white matter microstructure.

RESULTS

Genetic findings in the discovery family

A non-consanguineous Dutch family was ascertained with an autosomal-dominant pattern of inheritance for schizophrenia. The core sibship consisted of nine children (5 males, 4 females) of whom 4 males suffered from non-syndromic schizophrenia (**Figure 1a** and **Supplementary Table 1**).

Genome-wide parametric linkage analysis was performed on peripheral blood DNA using an autosomal-dominant model of inheritance with full penetrance, in order to identify genomic regions shared among all affected family members (**Supplementary Table 2**). Whole exome sequencing was performed on three individuals of the family (pedigree IDs: II-2, III-5 and III-9; **Figure 1a**). An initial list of heterozygous variants was compiled based on the following criteria: a) present within the genomic regions shared among all affected family members, b) predicted to affect protein coding (missense, nonsense, frameshift, splice site), c) called in at least one of the affected individuals [III-5 and III-9], d) absent from the unaffected mother [II-2], e) absent from dbSNP129, and f) with a minor allele frequency (MAF) < 0.003 in the Exome Variant Server (EVS6500 European Americans, NHLBI Exome Sequencing Project)[25], 1000 Genomes[26], and Genome of the Netherlands[27] cohorts. Genotyping of these variants in all participating family members was performed by Sanger sequencing. Variants present in all affected family members and absent from all unaffected family members were considered candidates.

This procedure yielded a single

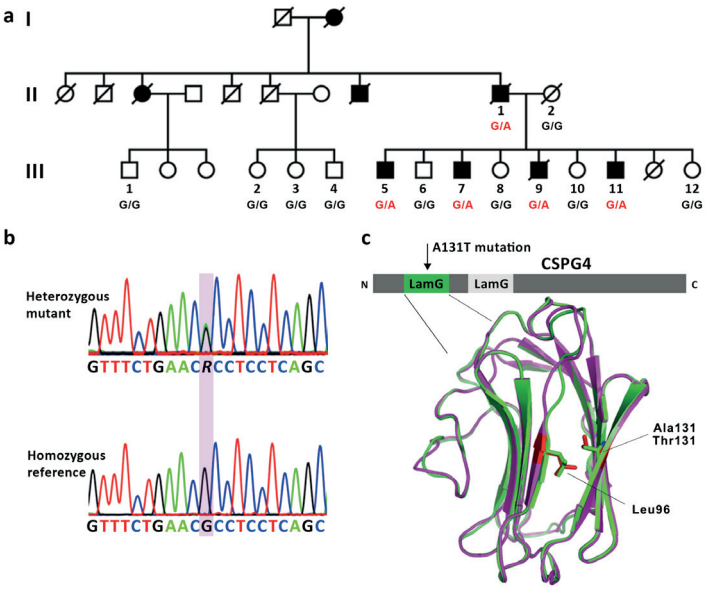

Figure 1. ***CSPG4*^{A131T} mutation in a multiplex family with schizophrenia.** **(a)** Family pedigree. Symbols: filled, schizophrenia; open, unaffected; G/A, heterozygous carrier of the *CSPG4* c.391G>A mutation; G/G, homozygous reference. **(b)** Representative sequencing results for heterozygous carriers of the *CSPG4* c.391G>A mutation. The lower panel reflects homozygous reference sequence. **(c)** Homology model of the first Laminin G domain of CSPG4. Structural alignment of the reference (green) and mutant model (magenta) reveals a difference in the predicted interaction between amino acid positions 131 and 96 (Leu) in the opposing β-strand inside the hydrophobic core of the β-sandwich (predicted change in side-chains in red).

candidate variant, *CSPG4* c.391G>A (p.A131T). *CSPG4* c.391G>A (p.A131T) is present in the Exome Aggregation Consortium Browser (Total: A=6/G=118,148 alleles [MAF 5.08 x 10^{-5}], including European (Non-Finnish): A=5/G=64,215 alleles [MAF 7.79 x 10^{-5}])[25], and absent from the Swedish Schizophrenia Population-Based Case-control Exome Sequencing Study (2536 cases, 2543 controls)[2], 1000 Genomes[26], and Genome of the Netherlands[27]. No region of genome-wide significant association overlapping *CSPG4* was reported in the recent schizophrenia GWAS analysis[10].

We performed TaqMan genotyping and Sanger sequencing validation of *CSPG4* c.391G>A (p.A131T) in an independent Dutch cohort of 1219 schizophrenia cases, 429 bipolar disorder cases, and 12,381 subjects from a population-based study (Rotterdam Study). One carrier was identified among the schizophrenia cases and none in the group with bipolar disorder. Remarkably, of the four carriers identified in the Rotterdam Study cohort, two had a clinically significant history of psychiatric illness. One subject had a history of inpatient psychiatric hospitalization for depression, and the other required chronic antidepressant and anxiolytic pharmacotherapy. In contrast, the overall Rotterdam Study cohort had a low lifetime risk of inpatient psychiatric hospitalization ~1%) or antidepressant treatment ~10%.

Identification of additional rare *CSPG4* variants that segregate with schizophrenia

A previous study identified suggestive linkage at 15q22-24 overlapping *CSPG4* in a cohort of 175 families with schizophrenia or schizoaffective disorder of Central American/Hispanic origin[28,29]. We therefore sequenced the full open reading frame of *CSPG4* in one proband from each of the 73 families that positively contributed to the linkage signal at this locus (markers D15S131 and D15S655, **Supplementary Table 3**). We identified four missense mutations with a MAF < 0.003 (ExAC Browser, Latino) involving five families: c.1921C>T p.R641W, c.2702T>G p.V901G, c. 3535 C>T p.R1179W, and c.5939 G>A p.R1980H (**Figure 2, Supplementary Figure 1**). The c.2702T>G p.V901G variant was particularly notable for segregation in two independent Hispanic families (**Figure 2**). Moreover, the association of the c.2702T>G p.V901G variant with schizophrenia was further confirmed by the Swedish Schizophrenia Population-Based Case-control Exome Sequencing Study[2] (MAF_{cases} 0.0022; $MAF_{controls}$ 5.82 x 10^{-4}, P = 0.033, OR 3.77). In contrast, the R641W and R1980H variants demonstrated no evidence of a significant association (R641W: MAF_{cases} 3.98 x 10^{-4}, $MAF_{controls}$ 1.94 x 10^{-4}, P = 1, OR 2.05 and R1980H: MAF_{cases} 0.0032, $MAF_{controls}$ 0.0031, P = 1, OR 0.97), and the R1179W variant was absent from the dataset. Together, these

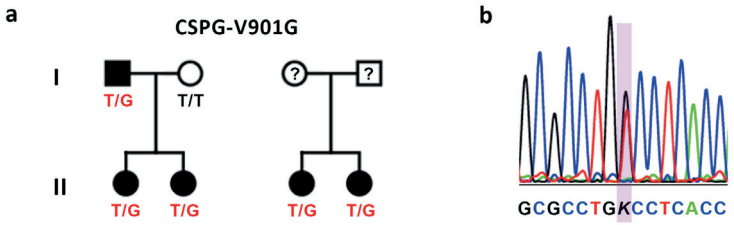

Figure 2. *CSPG4*^{V901G} variant in independent cohort. (a) Family pedigrees carrying the V901G mutation that replicates in the Sweden Schizophrenia Exome study. Symbols: filled, schizophrenia; open, unaffected; T/G, heterozygous carrier of the *CSPG4* c.2702T>G mutation; T/T, homozygous reference. **(b)** Representative Sanger sequencing trace.

data suggest that rare coding variation of *CSPG4* contributes to schizophrenia risk.

Structural modeling of *CSPG4* mutations

The *CSPG4*^{A131T} mutation is located within the first Laminin G domain of the protein (**Figure 1c**). Laminin G (LamG) domains are highly conserved and present in a diverse group of extracellular matrix proteins[30]. Intriguingly, several schizophrenia-associated genes such as *NRXN1* and *LAMA2* also contain LamG domains[31–34]. The presence of several crystal structures of LamG domains in the Protein Data Bank allowed homology modelling of the first LamG domain of NG2. Models implemented using Phyre2[35] and I-TASSER[36] both suggested that in the reference sequence, Ala^{131} and Leu^{96} interact across opposing β-strands inside the hydrophobic core of the β-sandwich. The mutation of Ala^{131}, which has a small hydrophobic side chain, to Thr^{131}, containing a larger polar side-chain, suggested a conformational change impairing the proper folding of the β-sandwich (**Figure 1c**).

Interestingly, R641W and V901G are located in a putative 3rd LamG domain predicated by I-TASSER[36] (**Supplementary Figure 1c**). This region has not previously been annotated as a LamG domain, despite the striking resemblance to other LamG domains with available crystal structures, most notably that of NRXN1. In contrast to the A131T mutation that is located on the inside of the globular structure of the first LamG domain of NG2, the V901G and R641W mutations are predicted to be located on the outside of the putative third LamG domain (DALI-server modelling[37])(**Supplementary Figure 1c**), therefore perhaps affecting protein-protein interactions. Intriguingly, the same protein region has been found to bind to collagen V and VI, implicated in cell adhesion and migration [38,39].

Family-based iPSC modelling of the *CSPG4*^{A131T} mutation

No evidence for a cell-type autonomous neuronal phenotype

Recent genetic and iPSC-based studies of schizophrenia have converged on a model by which neuronal function, and in particular synaptic transmission, is a major pathophysiological mechanism[2,10-11,12]. In order to examine the influence of the *CSPG4*^{A131T} mutation on neuronal function, we obtained skin biopsies for iPSC reprogramming from three affected *CSPG4*^{A131T} carriers and three unaffected non-carriers within the core sibship of the discovery family (**Supplementary Figure 2, a-d**). Directed differentiation of iPSCs yielded forebrain-specified neural progenitor cells (NPCs) uniformly positive for Nestin, Sox2, Vimentin, and FoxG1 (**Supplementary Figure 2e**).

NPCs were differentiated to neural cultures for 8-10 weeks. Both control and patient-derived neurons developed robust synaptic network connectivity, confirmed by confocal immunofluorescence and whole-cell patch-clamp electrophysiological recordings (**Figure 3**). No significant differences were observed between neurons derived from patient carriers and their unaffected siblings regarding passive membrane properties, action potential characteristics, or synaptic physiology (**Figure 3, d-r**). Accordingly, the lack of any discernible neuronal phenotype is highly consistent with the cell-type selective expression of NG2, the protein encoded by *CSPG4*, for which OPC expression is highly abundant while neuronal expression is absent.

Abnormal posttranslational processing and subcellular localization of CSPG4^{A131T} *in OPCs*

Given the highly abundant expression of NG2 in OPCs, widely referred to as NG2 cells, we next sought to investigate the influence of the *CSPG4*^{A131T} mutation on iPSC-derived OPCs. Directed differentiation of iPSCs to OPCs resulted in robust expression of the cell-type selective markers CSPG4/NG2, PDGFR, Olig2, and SOX10 (**Supplementary Figure 3**). We first examined the

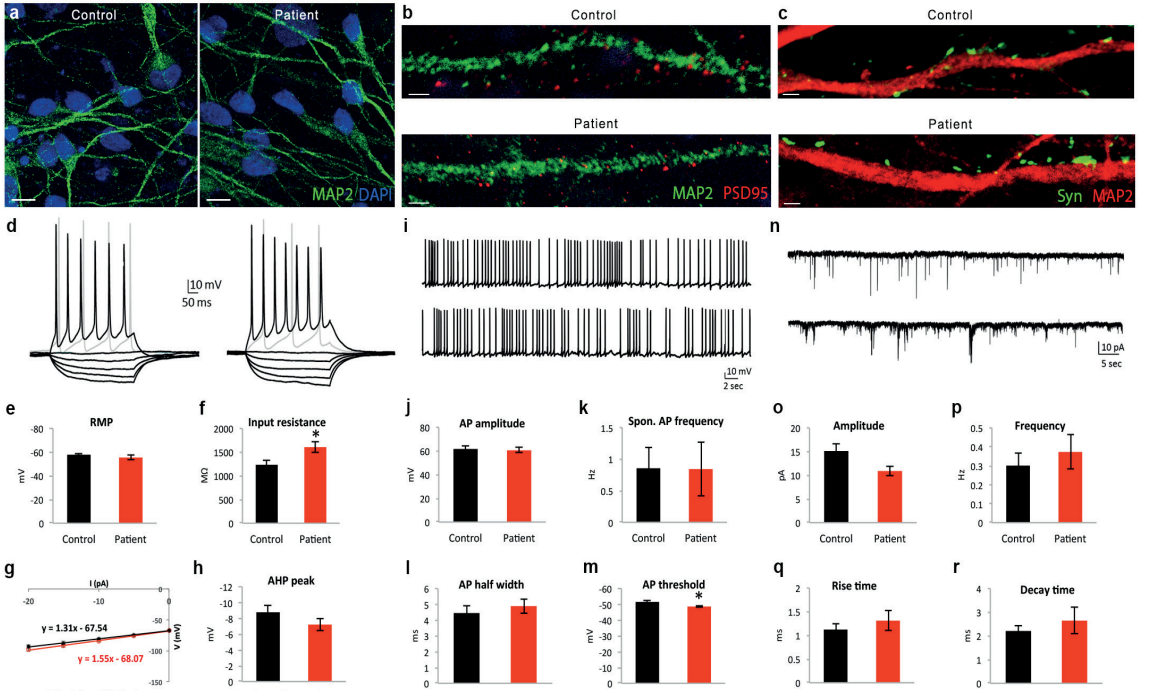

Figure 3. Normal passive, active, and synaptic function in *CSPG4*^{A1311T} patient iPSC-derived neurons. (**a**) Immunostaining of iPS-derived neural cultures after 8 weeks of differentiation (scale bar = 10 μm). (**b, c**) Immunostaining with MAP2, PSD95 and synapsin antibodies revealed the presence of synaptic proteins on dendrites of iPS-derived neurons 8weeks post-differentiation (scale bar = 2 μm). (**d-r**) Electrophysiological measurements of iPSC-derived neurons. (**d**) Representative voltage responses to hyperpolarizing (-20 – 0 pA, 5 pA increments) and depolarizing (10 and 20 pA) current steps (left: control, right: patient). (**e**) Resting membrane potential (t_{44}=1.04, *P*=0.3). (**f**) Input resistance (t_{51}=2.54, *P*=0.01). (**g**) Current-voltage (I-V) relationship of patient and control cells. (**h**) AHP peak (t_{50}=1.35, *P*=0.18). (**i**) Representative traces of spontaneous action potential (AP) firing (50 sec at RMP; top: control, bottom: patient). (**j**) AP amplitude (t_{50}=0.31, *P*=0.76). (**k**) Spontaneous firing rate (t_{19}=0.03, *P*=0.98). **l**: AP half width (t_{50}=0.65, *P*=0.52). (**m**) AP voltage threshold (t_{50}=2.84, *P*<0.01). (**n**) Representative traces of spontaneous postsynaptic currents (100 sec at -90 mV; top: control, bottom: patient). (**o**) sPSC amplitude (t_{27}=2.84, *P*=0.01). (**p**) sPSC frequency (t_{27}=0.75,*P*=0.46). (**q**) sPSC rise time (t_{27}=2.29, *P*=0.03). (**r**) sPSC decay time (t_{27}=1.48, *P*=0.15). (**d-r**) Unpaired two-tailed Student's t test. Passive properties and evoked APs (*N*=24 control, *N*=28 patient). Spontaneous APs (*N*=11 control, *N*=9 patient). Spontaneous postsynaptic currents (*N*=17 control, *N*=10 patient). All error bars are +/- standard errors of the mean (SEM).

subcellular distribution of NG2, given that the structural homology modeling of the *CSPG4*^{A131T} mutation suggested aberrant protein folding (**Figure 1c**). Since NG2 is a transmembrane protein, it requires processing by the secretory pathway. Consistent with an impairment of protein processing, *CSPG4*^{A131T} patient-derived OPCs showed a highly abnormal subcellular localization of NG2 exemplified by an increase of co-localization with the endoplasmic reticulum marker calreticulin (**Figure 4a and b**).

In order to further characterize the altered subcellular localization, we performed biochemical analysis of NG2 from *CSPG4*^{A131T} patient and non-carrier sibling control OPCs. NG2 is known to undergo substantial posttranslational modification through the addition of chondroitin sulphate moieties throughout the protein[40,41]. Consequently, NG2 appears as multiple bands by western blotting: a sharp band at 300 kDa corresponding to chondroitin sulfate-unmodified NG2 and a large polydisperse smear at >300 kDa corresponding to chondroitin sulfate-modified NG2 (**Figure 4c**). Addition of chondroitinase ABC to the protein lysate confirmed the identity of the >300 kDa polydisperse smear as chondroitin sulfate-modified NG2 and the 300 kDa band as chondroitin sulfate-unmodified NG2 (**Figure 4c**).

In whole cell lysates of *CSPG4*^{A131T} patient OPCs, there was a significant decrease in the ratio of modified versus unmodified NG2 compared to OPCs from their unaffected non-carrier siblings (P=0.04) (**Figure 4d and e**). Importantly, the total level of NG2 was unchanged between patient and control OPCs (**Figure 4d, Supplementary Figure 4**). Surface biotinylation followed by immunoprecipitation revealed a significant reduction of both intracellular (P=0.02) and transmembrane localized (P=0.03) chondroitin sulfate-modified NG2 in *CSPG4*^{A131T} patient OPCs (**Figure 4d and e**). Taken together, these results demonstrate that the *CSPG4*^{A131T} mutation results in abnormal processing of NG2.

Abnormal morphology of OPCs derived from CSPG4^{A131T} *mutation carriers*

We showed morphological differences between OPCs derived from patients and controls **(Figure 5)**. Firstly, we observed OPCs derived from patients tend to localize close to each other in culture conditions whereas control OPCs are more evenly distributed on the culture plate **(Figure 5a)**. To identify the morphological differences, we measured the size of OPCs both derived from patients and controls by using Image J software. We found significantly higher number of patient OPCs with smaller area than control OPCs **(Figure 5b)**. Overall, these results suggest that abnormal processing of NG2 might influence the morphology of OPCs derived from *CSPG4*^{A131T} mutation carriers.

Impaired white matter microstructure in CSPG4^{A131T} *mutation carriers*

Given the observed abnormalities of patient-derived OPCs, we reasoned that affected *CSPG4*^{A131T} mutation carriers might exhibit impairments of white matter integrity since OPCs are the exclusive precursor of myelinating oligodendrocytes. Therefore, we performed brain magnetic resonance imaging (MRI)-based diffusion tensor imaging (DTI) in affected carrier and unaffected non-carrier siblings with 294 matched population controls (**Figure 6a**). DTI images were analysed for global and focal reductions in fractional anisotropy (FA), the latter referred to as white matter potholes[13]. Consistent with the hypothesis that the *CSPG4*^{A131T} mutation compromises the integrity of myelination, patient carriers exhibited both a significant reduction in global FA and a markedly increased number of potholes, compared to unaffected sibling and matched population controls (**Figure 6b and c**).

DISCUSSION

Our findings implicate a causal link between the *CSPG4*^{A131T} mutation causing impaired protein

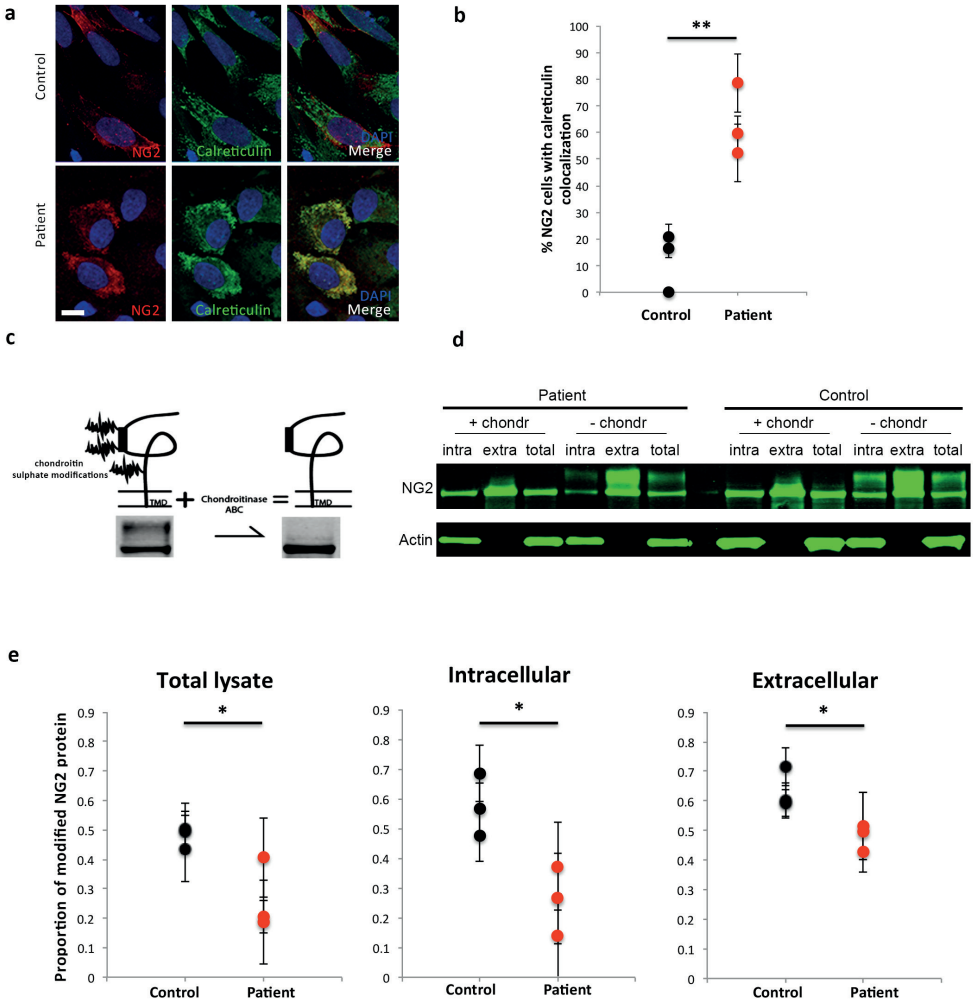

Figure 4. Aberrant subcellular localization and posttranslational chondroitin sulphate modification of NG2 in *CSPG4*$^{A_{131T}}$ patient-derived OPCs. (a, b) Immunostaining for NG2 and Calreticulin reveals increased ER colocalization of NG2 in patient OPCs (scale bar = 10 µm). Quantification was performed in two independent experiments with three control and three patient OPC lines each. **(c)** Schematic of specific removal of chondroitin sulphate side chains by chondroitinase treatment, reveiling the upper NG2 western blot band to be highly specific for chondroitin sulphate-modified NG2. **(d)** Representative western blot of biotinylation assay samples of control and patient OPCs +/- chondroitinase treatment, showing the upper band to be highly specific for chondroitin sulphate-modified NG2. **(e)** Quantification of the proportion of NG2 protein that is modified with chondroitin sulphate side chains. The proportion of modified to unmodified NG2 in OPC extracts was determined by normalizing the integrated density of modified NG2 (>300 kDa) to the sum integrated density of the modified and unmodified NG2 bands. Multiple blots of different control OPC lines (n=9) and patient OPC lines (n=8), shown as aggregated data per individual (3 control and 3 patient siblings). Error bars in all panels reflect standard errors of the mean.

processing in oligodendrocyte precursor cells and the susceptibility to schizophrenia. In addition, we have identified five families in an independent cohort with overlapping linkage in the same genomic region, that demonstrate 4 different rare missense mutations in *CSPG4*, segregating with schizophrenia. One of these mutations was found to segregate in two families and significantly

replicated in the Sweden schizophrenia exome study[2]. Taken together, *CSPG4* represents a novel candidate gene for schizophrenia, harbouring multiple rare exome variants that show familial segregation with high penetrance.

Notably, the protein sequence surrounding the $CSPG4^{A131T}$ mutation is conserved only among higher-order primates, suggesting recent evolutionary pressure. The $CSPG4^{R641W}$, $CSPG4^{V901G}$ and $CSPG4^{R1179W}$ variants are predicted

a.

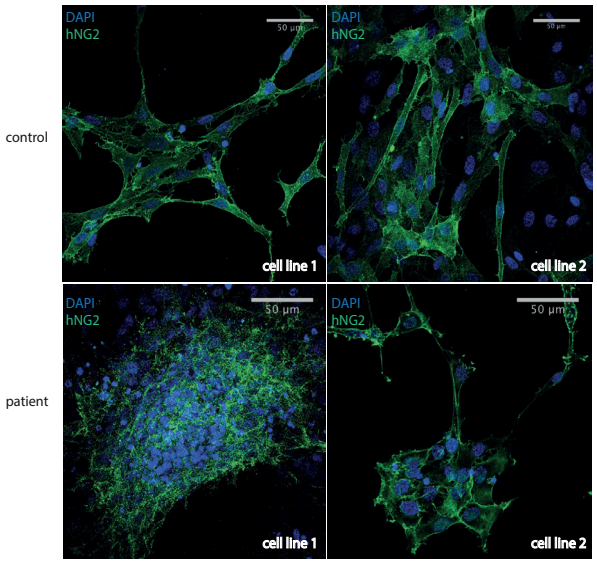

b.

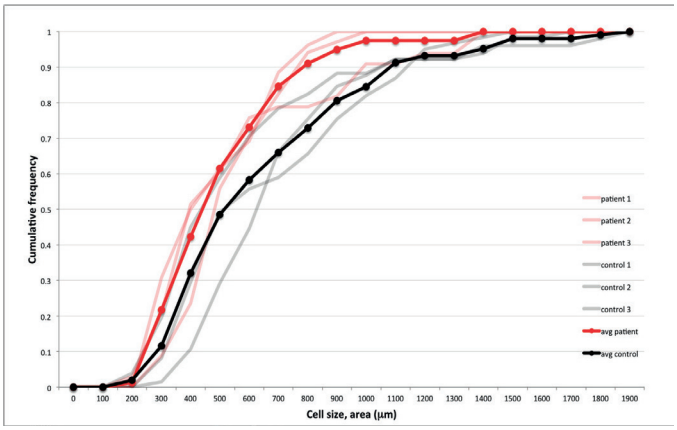

Figure 5. Abnormal morphology of OPCs derived from $CSPG4^{A131T}$ mutation carriers. (a) Patient cells are more clustered on the cell culture plate than control cells that are more evenly distributed. **(b)** Cumulative frequency showing the size distribution of 3 control and 3 patient OPC lines (n= 61,65,15 control cells and n=26+33+34 patient cells). Size was measured as the projected area of z-stack images covering the depth of the cells, calculated from the manually drawn surface contour of NG2-positive cells using ImageJ

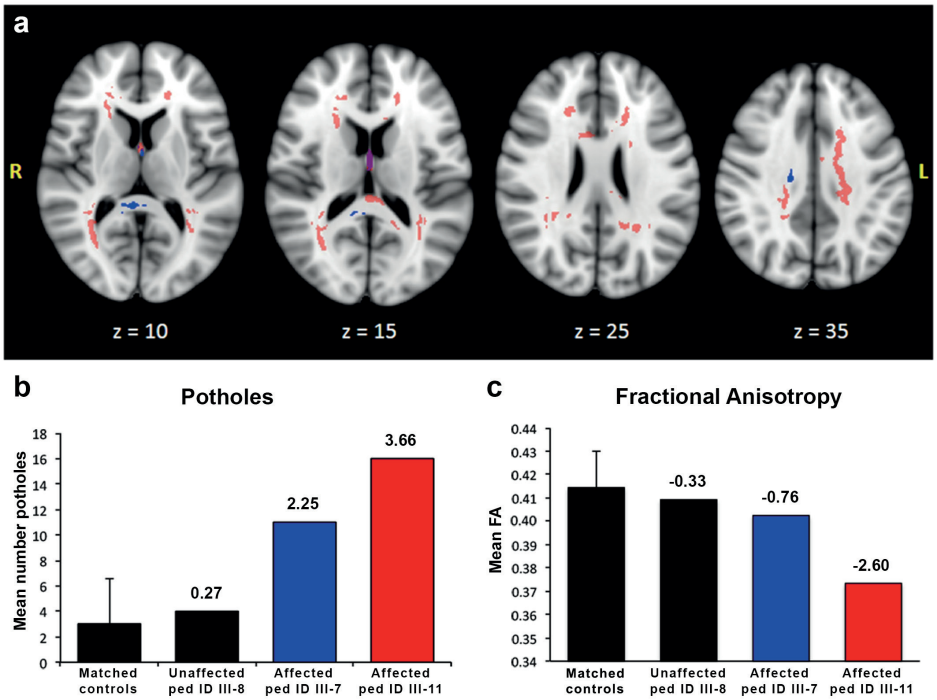

Figure 6. White matter abnormalities in *CSPG4*^{A131T} patients. (**a**) White matter potholes found in the two affected family members are shown in red and blue, respectively. Purple regions define a spatial overlap of potholes in both patients. The z-measures provide coordinates of the axial plane in MNI-space. (**b**) Mean number of potholes comparing the matched control population to the unaffected and two affected family members. (**c**) Whole-brain white matter fractional anisotropy (FA) comparing the matched control population to unaffected and affected family members. Error bars in (**b**) and (**c**) reflect the standard deviation of the matched control population. The number above each bar reflects the individual z-score compared to the matched control population.

to be disease-causing mutations by PolyPhen2[42]. In non-primate vertebrates, the reference amino acid at position 131 is threonine, corresponding to the patient mutation *CSPG4*^{A131T}, contributing to a benign PolyPhen score. Interestingly, this is analogous to the human *SNCA*^{A53T} mutation, one of the most well established mutations for autosomal dominant Parkinson's disease[43]. In rodents, the reference amino acid at SCNA position 53 is a threonine. However, although transgenic expression of the reference human sequence in mice is benign, introduction of the mutant human sequence is highly pathogenic.

To study the cellular impact of mutations in *CSPG4*, detailed iPSC modelling was performed of the discovery family carrying the *CSPG4*^{A131T} mutation. Remarkably, detailed electrophysiological analysis of patient-derived neurons did not reveal any apparent phenotype. Regarding the lack of expression of *CSPG4* in neurons, this may not be surprising, although ultimately diverse pathological mechanisms are bound to converge in a neuronal phenotype within the brains of schizophrenic patients. Taken together with previous studies implicating direct neuronal mechanisms[2,10,11,12,44], our findings suggest that the underlying pathophysiology of schizophrenia can become manifest through primary deficits in either neurons or glia. In vivo transplantation studies in mice or co-culture

experiments might shed more light on the developmental impact of these *CSPG4* mutations on brain functioning.

Our results show abnormal subcellular localization of NG2 in patient-derived OPCs. Notably, cells of the oligodendrocyte lineage are known to be particularly susceptible to disruptions in the secretory pathway, as their maturation requires a substantial upregulation of membrane protein expression[45]. Therefore, it is tempting to speculate that this may cause a delay in oligodendrocyte maturation, with a consequent functional impairment of myelination that is highly consistent with the deficits of white matter integrity observed in the patients. These hypotheses are under current investigation.

In summary, our findings support the validity of family-based genome-wide genetic analyses and integrative functional genomics to unravel the underlying mechanisms of heterogeneous psychiatric diseases. In addition, the identification of specific defects in patient-derived cells shows the potency of functional iPSC-modelling for rare variants that lack statistical power in genomics. In analogy to neurodegenerative disease research, the study of rare familial variants may reveal underlying neuropathological mechanisms that translate to the general patient population. The identified *CSPG4* mutations implicate oligodendrocyte precursor cell function as an important mechanism of susceptibility for schizophrenia, thereby pointing to new pathways to be explored in the search for the underlying biological mechanisms of severe mental illness.

METHODS SUMMARY

Genetic analysis

Linkage and Copy Number Analysis was performed with Illumina HumanCytoSNP-12v2 chip arrays using an all-affected model with an assumption of 99.9% penetrance. Analysis revealed a total of 294.34 Mb of genomic regions, with suggestive linkage on chromosomes 2, 11, 14, 15, and 16. Whole-genome exome sequencing was performed twice: initially at 40x, and again at 90x coverage. Exonic coding variants were only considered for additional validation if they were rare (MAF < 0.003), occurred within the defined regions of suggestive linkage, and showed disease segregation with full penetrance.

Cellular studies

Human iPSCs were differentiated to NPCs and neurons according to Brennand *et al*[12], with modifications. Electrophysiology was performed in whole cell patch-clamp configuration after 8-10 weeks of differentiation. iPSC-derived OPCs were differentiated according to Monaco *et al.*[46] with modifications. Biotinylation of cell surface proteins was adapted from Huang *et al.*[47].

Magnetic Resonance Imaging (MRI)

Two patients and one control sibling of the family were subjected to MRI scanning. Population controls (n=294) matched on age, gender, and pack-years of cigarette smoking were selected from the Rotterdam Study. MRI images were obtained using a 1.5 Tesla General Electric (GE Healthcare, Milwaukee, Wisconsin, USA) MR system using a bilateral phased-array head coil. A full description of the imaging protocol and Rotterdam Study design has been described elsewhere[48]. An in-house MATLAB (Mathworks, Natick, MA) program was used to quantify the number and spatial characteristics of white matter 'potholes' along the major white matter tracts[49].

MATERIALS AND METHODS

Recruitment of family with schizophrenia and obtaining patient material

A Dutch white Caucasian non-consanguineous family with a high incidence of schizophrenia was ascertained. Written informed consent was obtained from all participating subjects. This study was approved by the medical ethical committee of the Erasmus University Medical Centre (Rotterdam, The Netherlands). Participating family members were screened for current or past psychiatric symptoms using the

Structural Clinical Interview for DSM-IV (SCID-1)[50]. Medical screening revealed no evidence of multiply occurring somatic comorbidities, dysmorphologies, or neurological symptoms. All individuals with schizophrenia were documented to be of average intelligence at the time of their initial diagnosis. DNA isolation from venous blood samples and skin biopsies were performed using standard procedures. Two family members (II-2 and III-9) passed away since the start of the study. For skin biopsies, a small area of skin of the inner side of the upper arm was anesthetised with an EMLA patch (AstraZeneca) for one hour, after which the skin was disinfected with ethanol and the biopsy was obtained through all skin layers with a standard 3mm biopsy punch. The tissue was collected in Dulbecco's Modified Eagle Medium (DMEM) (Gibco-Invitrogen) without additives and transferred to culture within 24 hours. Primary human fibroblasts were cultured in DMEM containing 10% fetal calf serum and 1% penicillin/streptomycin (P/S).

Genetic analysis

Genomic DNA was isolated using standard methodology from 14 family members, including 13 by whole blood samples and one subject (pedigree ID II-1) using paraffin-embedded tissue (**Figure 1a**). Linkage and Copy Number Analysis was performed with Illumina HumanCytoSNP-12v2 chip arrays (294,975 markers). Linkage analysis was conducted exclusively for the purpose of identifying the genome-wide set of chromosomal regions shared by all affected family members (defined as those regions for which the observed LOD score approached the theoretical maximum). Linkage was performed using Allegro and implemented in the EasyLinkage version 5.08 interface[51] with one marker every 0.5 cM using a co-dominant allele frequency algorithm and dominant scoring function, assuming 99.9% penetrance among the affected individuals. Unaffected family members were not included in the linkage model, providing no *a priori* constraints on the rate of incomplete penetrance. Copy number analysis was performed using NEXUS discovery edition, version 6 (BioDiscovery, El Segundo, CA), which did not indicate the presence of copy number variants segregating with the phenotype.

Whole exome sequencing was performed on three individuals of the discovery family (pedigree IDs: II-2, III-5 and III-9). Sequencing was performed twice for all three samples: initially at 40x, and subsequently at 90x coverage. Exome sequencing was performed using in-solution capturing (Agilent SureSelect V2 and V4 Human 50 Mb kit respectively, Agilent Technologies) and paired-end sequencing with Illumina Hi-Seq 2000 sequencers. Reads were aligned to the human reference genome version 19 using Burrows-Wheeler Aligner. SNPs and indels were called using the Genome Analysis Toolkit (GATK).

The heterozygous variants were filtered based on the following criteria: a) present within the genomic regions shared among all affected family members, b) predicted to affect protein coding (missense, nonsense, frameshift, splice site), c) called in at least one of the affected individuals [III-5 and III-9], d) absent from the unaffected mother [II-2], e) absent from dbSNP129, and f) with a minor allele frequency (MAF) of < 0.01 in Exome Variant Server (EVS6500, NHLBI Exome Sequencing Project)[25], 1000 Genomes[26], and Genome of the Netherlands[27] cohorts. These variants were genotyped by Sanger sequencing of all participating family members, for which only variants present in all affected family members and not in unaffected family members were considered candidates.

Genotyping of *CSPG4* c.391G>A was performed in a cohort of Dutch subjects with 1219 schizophrenia cases, 429 bipolar disorder cases, and 12.381 population-based controls. Genotyping of 763 schizophrenia and 386 control samples were performed using a custom Illumina Infinum Human Exome Beadchip array. TaqMan genotyping was performed on 456 schizophrenia cases, 429 bipolar disorder cases, and 11,995 controls. All samples with ALT calls genotyped by exome array or TaqMan were additionally confirmed by Sanger sequencing.

Taqman genotyping of *CSPG4* c.391G>A

was performed with the following primers and probes:
F_GGCTGGTTCCCCTCAGGTA, R_GTGGTGCTGACTGTCGTAGAG
VIC_TTTCTGAACGCCTCCTC, FAM_TTTCTGAACACCTCCTC.

The following primer sets were used for Sanger sequencing of *CSPG4* c.391G>A: F_5'-TCTGGGGCCCCAAGTGTGG-3' and R_5'-AGAGTGGGGCCCAGAGAAGC-3', with an internal forward primer for sequencing: Fseq_5'-GGGCCAGGAGGAGCTGAGG-3'. A second primer set was used for confirmation: F2_5'-CCACTCCCCATCTCTCTTCAGG-3' and R2_5'-CAGGGCCACATCATCACTGG-3'.

Structural homology modelling

Homology modelling of the first Laminin G domain (amino acids 29-176) was performed independently using both the Protein Homology/analogY Recognition Engine – Version 2.0 (Phyre2)[35] and Iterative Threading ASSEmbly Refinement (I-TASSER)[36] protein structure prediction servers. All 148 residues (100%) of the reference and mutant sequences were modelled at >99% confidence by Phyre2 using intensive mode. For I-TASSER, the confidence (C-score) was 0.81 and topological similarity (TM-score) was 0.82+/- 0.08, for both models. Reference and mutant models were structurally aligned with PyMol (http://www.pymol.org).

Generation and characterization of iPSCs

Reprogramming of human primary skin fibroblasts was performed as previously described[52]. Briefly, fibroblasts were infected with a multicistronic SIN lentiviral vector containing an SFFV promoter, encoding OCT4, SOX2, KLF4 and MYC, as well as dTomato to visualize reprogramming. Emerging iPSC colonies were cultured on γ-irradiated mouse embryonic feeder (MEF) cells.

Characterization of iPSC clones was performed by RT-PCR (**Supplementary Figure 2a**), immunostaining for undifferentiated human ES markers (**Supplementary Figure 2b**) and markers of three embryonal germ layers on embryoid bodies (EBs) differentiated *in vitro* (**Supplementary Figure 2c**). Total RNA of iPSCs was isolated for RT-PCR using standard protocols (primers listed in **Supplementary Table 4**). For EB differentiation, iPSC colonies were dissociated by collagenase IV treatment and transferred to ultra-low attachment 6-well plates (Corning). Floating EBs were cultured in iPSC medium without bFGF for a minimum of 6 days with supplemented SB431542 (Tocris Bioscience) for ectoderm conditions only. EBs designated for endoderm differentiation were transferred to gelatin-coated 12-well plates containing the following medium: RPMI 1640 (Gibco-Invitrogen), supplemented with 20% FBS, 1% P/S, 1% glutamine and 0.4mM alpha-thioglycerol. Mesoderm differentiation from the EBs was induced in gelatin-coated 12-well-plates with DMEM medium (low glucose) supplemented with 15% fetal bovine serum, 1% P/S, 1% glutamine and 1% MEM-non-essential amino acids. Ectoderm differentiation was induced in Matrigel (BD)-coated plates with the following medium: neurobasal medium (Gibco-Invitrogen) and DMEM/F12 (v/v 50/50) supplemented with 1% P/S, 1% glutamine, 1% MEM-non-essential amino acids, 0.02% BSA (Gibco-Invitrogen), 0,5% N2 (Gibco-Invitrogen) and 1% B27 (Gibco-Invitrogen). After two weeks in culture, cells were fixed with 4% formalin for immunolabelling.

iPSCs were cultured in standard ES cell culture medium containing DMEM/F12 (Gibco-Invitrogen) supplemented with 20% knock-out serum replacement (Gibco-Invitrogen), 2mM L-glutamine (Gibco-Invitrogen), 1% P/S (Gibco-Invitrogen), 1% MEM-non-essential amino acids (PAA Laboratories GmbH), 0.1mM β-mercapto-ethanol, and 10 ng/ml bFGF (Gibco-Invitrogen). Medium was replenished daily and colonies were passaged weekly using collagenase IV (1 mg/ml, Gibco-Invitrogen) with 10μM ROCK inhibitor (Y-27632, Sigma).

Karyotype analysis

iPSCs were dissociated to single-cell suspension using TrypLE Express (Gibco-Invitrogen) and plated feeder-free in mTeSR1 medium on three Matrigel-coated wells of a 6-well plate in the presence of 10μM ROCK inhibitor. The next

day, cells were harvested using TrypLE Express, treated with colcemid (200 ng/ml) and hypotonic solution, and fixed using Carnoy's Fixative. At least 20 metaphases were analysed for each clone, for which the chromosome count was considered normal if more than 70% of cells analysed had 46 chromosomes. More detailed karyotypic analysis with RBA and QFQ band analysis was performed for one individual patient clone (individual III-11) to further exclude segregating cytogenetic abnormalities (**Supplementary Figure 2d**).

Neuronal differentiation

iPSCs were differentiated to NPCs and neurons according to Brennand *et al*[12], with modifications. Briefly, iPSC colonies were dissociated from MEFs with collagenase and transferred to non-adherent plates in hES cell medium on a shaker in an incubator at 37°C/5% CO_2. After two days, EBs were changed to neural induction medium [DMEM/F12, 1% N2-supplement (Gibco-Invitrogen), 2 µg/ml heparin (Sigma), 1% P/S] and cultured for another four days in suspension. EBs were gently dissociated and plated onto laminin-coated dishes in neural induction medium. Cells were dissociated with collagenase after 8 days and plated onto laminin-coated dishes in NPC medium [DMEM/F12, 1% N2, 2% B27-RA, 1 µg/ml laminin (Sigma) and 20 ng/ml FGF-2 (Millipore), 1% P/S]. After one week, NPCs were dissociated with collagenase, re-plated, and passaged 1:4 weekly. For neural differentiation, passage 5 NPCs were plated on coverslips coated with 100 µg/ml PDL (Sigma) and 50 µg/ml laminin in neural differentiation medium consisting of Neurobasal medium supplemented with 1% MEM-non-essential amino acids, 1% N2 supplement, 2% B27-RA supplement, 20 ng/ml BDNF (ProSpecBio), 20 ng/ml GDNF (ProSpecBio), 1 µM db-cAMP (Gibco-Invitrogen), 200 µM ascorbic acid (Gibco-Invitrogen), 2 µg/ml laminin and 1% P/S.

Electrophysiological recordings

After 8-10 weeks of neuronal differentiation, culture slides were transferred to the recording chamber following a thirty-minute serial partial exchange of cell culture medium with artificial cerebrospinal fluid (aCSF) containing the following (in mM): 110 NaCl, 2.5 KCl, 2 $CaCl_2$, 2 $MgCl_2$, 1 NaH_2PO_4, 25 $NaHCO_3$, 10 glucose, 0.2 ascorbate (pH 7.4). In the recording chamber, slides were continuously perfused with ACSF at 1.5-2 mL/min, saturated with 95% O_2/5% CO_2 and maintained at 20-22°C.

Whole-cell patch-clamp recordings were performed under infrared differential interference contrast visual guidance using an upright microscope (Zeiss) with borosilicate glass recording micropipettes (3-6 MΩ) filled with the following medium (in mM): 130 K-gluconate, 11 KCl, 10 HEPES, 5 NaCl, 0.1 EGTA, 1 $MgCl_2$, 2 Mg-ATP, 0.3 Na-GTP, 5 phosphocreatine (pH 7.4). Data were acquired at 10 kHz using an Axon Multiclamp 700B amplifier (Molecular Devices), filtered at 3 kHz, and analyzed using pClamp 10.1 (Molecular Devices). Whole-cell capacitance and series resistance were compensated, and voltage was adjusted for liquid junction potential.

Current-clamp recordings were performed at a holding potential of -60 mV. Passive membrane properties were analysed using a series of hyperpolarizing and depolarizing square wave currents (500 msec duration, 1 sec interstimulus interval) in 5 pA steps, ranging from -20 to +30 pA. AP amplitude, rise time, decay time and half width were measured for the first evoked AP resulted by a depolarizing step, from the threshold to the peak, for which the threshold was defined by the moment at which the second derivative of the voltage exceeded the baseline. Spontaneous APs were recorded at resting membrane potential. Voltage-clamp recordings were performed at a holding potential of -90 mV.

Oligodendrocyte lineage differentiation

iPSC-derived NPCs were differentiated to OPCs according to Monaco *et al*[46], with modifications. NPCs were plated on laminin-coated 10 cm plates in NPC medium consisting of DMEM/F12, 1% N2, 2% B27-RA, 1µg/ml laminin, 1% P/S, 25 ng/ml basic Fibroblast Growth Factor (bFGF) and 20 ng/ml Epidermal Growth Factor (EGF).

When NPCs reached 90% confluence, NPC medium was changed to OPC differentiation medium for three weeks: DMEM/HAMS F12, 1%

N2, 1% BSA, 1% L-Glutamine, 1% P/S, 20 ng/ml bFGF, 10 ng/ml platelet derived growth factor (PDGF-AA, ProspecBio), 2ng/ml Sonic hedgehog (Shh), 2 ng/ml neurotrophic factor 3 (NT-3) and 3 nM triiodothyronine (T3). OPC medium was changed every other day, and cells were passaged weekly at 1:4.

Surface Biotinylation

Biotinylation of cell surface proteins was adapted from Huang *et al*.[47], with modifications. First, the OPCs were washed twice in cold PBS/CaCL2/MgCl2 (2.5 mM CaCl2, 1 mM MgCl2, pH 7.4). Then, the OPCs were incubated for 15 minutes on ice with or without 0.3mg/ml of freshly dissolved Sulfo-NHS-SS-Biotin (Thermo Scientific) in PBS/CaCL2/MgCl2. Next, the OPCs were washed three times on ice in cold biotin quenching solution consisting of 50 mM glycine in PBS/CaCl2/MgCl2. Subsequently, the OPCs were lysed by incubation for 10 minutes on ice with lysis buffer, pH7.4, consisting of 5mM EDTA, 5mM EGTA, 1% Phosphatase inhibitor cocktail 2 and 3 (Sigma), 1% PIC (Sigma), and 1% Triton X in PBS. At least 3 wells were pooled from each cell line at each experimental condition, to minimize any plating or growing variability in the cell culture. A portion of the lysate was removed and labelled as the total fraction. The remaining lysate was then spun down at 13200rpm at 4°C for 15 minutes. The supernatants were incubated overnight at 4°C with PBS-washed and lysis buffer-equilibrated Pierce™ NeutrAvidin™ Agarose beads (Life Technologies). Next, the mixture was spun down at 2000 rpm, separating the supernatant termed the intracellular fraction from the extracellular fraction attached to the beads. Subsequently, the beads were washed four times by rotating with lysis buffer and after the final wash the beads were dried completely and taken up in 20µl of lysis buffer, labelled as the extracellular fraction.

Sodium dodecyl sulfate (SDS)-PAGE and Western Blotting

First, 25% XT Sample Buffer (Biorad) and 10% 100mM dithiothreitol (DTT) were added to equal volumes of cell extract followed by heating to 65°C for 15 minutes. Then, the samples were electrophoresed through 4%-12% Criterion™ XT Bis-Tris gradient gels (Biorad) in XT-Mops buffer (Biorad). Proteins were transferred overnight at 4°C on 0.45µm pore nitrocellulose membrane (Biorad) in a Tris-Glycine buffer consisting of 10% Tris/Glycine buffer (Biorad) and 20% anhydrous methanol in distilled water. Membranes were blocked for 2 hours while shaking at room temperature in TBST buffer containing 4% blotting grade blocker (Biorad). Then, the membranes were incubated with a monoclonal antibody generated from hybridoma B5 cells raised against purified intact NG2 protein from melanoma cells (generous gift from W.B. Stallcup) and mouse anti-actin (Sigma) in TBST buffer containing 2% blotting grade blocker for 48 hours at 4°C followed by washing with TBST buffer. Finally, the blots were incubated with IRDye® secondary antibodies (LI-COR) against the primary antibody species for two hours at room temperature. The blots were washed twice in TBST and TBS followed by one wash in water, subsequently the antibody fluorescence was visualized using an ODYSSEY® CLx scanner (LI-COR). Quantification of NG2 western blot bands was performed using Image J software (http://imagej.nih.gov/ij/).

Immunocytochemistry and imaging

Cell cultures were fixed using 4% formalin in PBS. Primary antibodies were incubated overnight at 4°C in labelling buffer containing 0.05 M Tris, 0.9% NaCl, 0.25% gelatin, and 0.5% Triton-X-100 (pH 7.4). The following primary antibodies were used: Sox2, Nestin, MAP2, NeuN, GFAP, FoxG1 [ProSci], NG2-EC [kindly provided by W.B. Stallcup], Olig2 [Abcam], Vimentin [Santa Cruz Biotechnology], AFP [R&D Systems], TRA-1-81, Nanog [Beckton Dickinson], Oct4 [Abcam], Calreticulin [Fisher Scientific], SOX10 [R&D Systems]. The following secondary antibodies were used: Alexa-488, Alexa-546, Alexa-555 and Cy3 antibodies [Jackson ImmunoResearch]. Samples were imbedded in Mowiol 4-88 (Fluka) after which confocal imaging was performed with a Zeiss LSM510 confocal microscope (Apochromatic 40x objective, 1.3 NA, oil immersion) using ZEN software (Zeiss,

Germany).

Magnetic Resonance Imaging (MRI)

Two patients and two control siblings of the discovery family provided additional written informed consent for MRI scanning. One of the unaffected siblings was excluded due to a history of systemic chemotherapy known to influence white matter integrity[53]. Population controls (n=294) were selected from the Rotterdam Study based on matching for age, gender, smoking behaviour, and alcohol use. All subjects, including population controls and family members, were imaged using the identical MRI scanner and acquisition protocol.

MRI images were obtained using a 1.5 Tesla General Electric scanner (GE Healthcare, Milwaukee, Wisconsin, USA, software version 11X), with a bilateral phased-array head coil. A full description of the imaging protocol has been described previously[48]. Diffusion-weighted imaging was performed using echo planar imaging (EPI) sequences collected in 25 directions with a b value of 1,000 s/mm^2 and three b = 0 images. Additional sequence parameters were TR = 8,000 ms, TE = 74.6 ms, bandwidth 14.71 kHz, flip angle = 13, acceleration of 2, and a voxel resolution of 3.3 x 2.2 x 3.5 mm^3.

Pre-processing of the diffusion-weighted images was performed using FSL[54]. After conversion from dicom to nifti format, individual images were eddy-current corrected using FMRIB's eddy_correct[54] followed by skull stripping using BET[55]. Fractional anisotropy (FA) images were created by fitting a tensor model to the diffusion data using FMRIB's Diffusion Toolbox (FDT)[54]. All subjects' FA data were then aligned into common space using the nonlinear registration tool FNIRT[56], which employs a b-spline representation of the registration warp field[57]. Whole brain mean FA was calculated by masking each image using the Johns Hopkins University White Matter Atlas (JHU WMA)[58] and determining the mean intensity of FA within the mask.

An in-house MATLAB (Mathworks, Natick, MA) algorithm was used to quantify the number and spatial characteristics of white matter 'potholes' along the major white matter tracts[49]. The input to the algorithm was the set of FA images that had undergone non-linear registration into MNI space using TBSS[59]. No spatial filtering was applied to the images. The first step was to generate a voxel-by-voxel mean and standard deviation (SD) image of the 294 matched population controls. These group and SD images were then used to individually create a voxel-wide z-image for all of the subjects, including the three family members. This resulted in individual z-images with each voxel based on the mean and SD of the matched population controls. To ensure the search involved only white matter regions, each image was masked with the cortical areas defined by the Johns Hopkins University white matter atlas[58].

The individual z-FA images were then used to search for contiguous voxels of white matter below a threshold of $z < -2$[13,49]. Clusters were determined by thresholding each image and labelling contiguous voxels in three-dimensional space that fell below the defined threshold. Only clusters greater than 250 voxels were used in the analyses.

Statistical Analysis

Significance of observations was established for genetic case-control analyses using the Fisher's exact test. Brain imaging results in family members were evaluated using z-scores based on the matched population control cohort distribution. For cell biological experiments, statistical comparisons were performed using a two-tailed Student's t-test or Kolmogorov Smirnov (for cell shape distribution). Data points in cell shape distribution data were defined as outliers if more than 1.5* the interquartile range above the third quartile or below the first quartile. Data are expressed as mean ± S.E.M, unless otherwise specified. The threshold for significance was set at $P<0.05$ for all statistical comparisons.

Acknowledgements: We wish to thank Gerard Borst for helpful discussions regarding the electrophysiological analyses, Justine Kent and Linda Brustowicz for advice regarding the RUCDR repository, and Siska Verploegh for

her assistance in sample collection. This project was partially funded by the Erasmus MC – University Medical Centre Rotterdam, the Netherlands Organization for Scientific Research (NWO) and Netherlands Organisation for Health Research and Development (ZonMW) to S.A.K, V.B., Y.E. and J.G., the NeuroBasic-PharmaPhenomics consortium to S.A.K. and Y.E., Stichting Parkinson Fonds (The Netherlands) to V.B., Netherlands Institute for Regenerative Medicine (NIRM) and European Research Council (Consolidator Grant) to J.G., National Institute of Mental Health (NIMH) to R.A.O.

The authors would like to thank the NHLBI GO Exome Sequencing Project and its ongoing studies which produced and provided exome variant calls for comparison: the Lung GO Sequencing Project (HL-102923), the WHI Sequencing Project (HL-102924), the Broad GO Sequencing Project (HL-102925), the Seattle GO Sequencing Project (HL-102926) and the Heart GO Sequencing Project (HL-103010).

This study makes use of data generated by the Genome of the Netherlands Project. A full list of the investigators is available from www.nlgenome.nl. Funding for the project was provided by the Netherlands Organization for Scientific Research under award number 184021007, dated July 9, 2009 and made available as a Rainbow Project of the Biobanking and Biomolecular Research Infrastructure Netherlands (BBMRI-NL). The sequencing was carried out in collaboration with the Beijing Institute for Genomics (BGI).

The generation and management of genomics data for the Rotterdam Study were supported by the Netherlands Organisation of Scientific Research Investments (nr. 175.010.2005.011, 911-03-012) and the Netherlands Genomics Initiative (NGI) project nr. 050-060-810 (Netherlands Consortium for Healthy Ageing; NCHA). We thank the members of the Genomics Lab and the ERGO support team for their help in sampling the data and in creating the database. The Rotterdam Study is funded by Erasmus Medical Centre and Erasmus University, Rotterdam, Netherlands Organisation for Health Research and Development (ZonMw), the Research Institute for Diseases in the Elderly (RIDE), the Ministry of Education, Culture and Science, the Ministry for Health, Welfare and Sports, the European Commission (DG XII), and the Municipality of Rotterdam. The authors are grateful to the study participants, the staff from the Rotterdam Study and the participating general practitioners and pharmacists.

NIMH Study 13 -- Data used in this research report were collected by the International Neuro-Genetics Association of Spanish America and the United States (INGASU), and funded by a collaborative NIMH grant (Genetics of Schizophrenia in Latino Populations) to Dr. Michael Escamilla (University of Texas Health Science Center at San Antonio) (MH60881) and to Dr. Ricardo Mendoza (University of California at Los Angeles-Harbor) (MH60875). Additional principal investigators who participated in these grants were Dr. Henriette Raventos (University of Costa Rica, San Jose, Costa Rica), Dr. Alfonso Ontiveros (Instituto de Informacion de Investigacion en Salud Mental, Monterrey, Mexico), Dr. Humberto Nicolini (Medical and Family Research Group, Carracci S.C., Mexico City, Mexico), Dr. Rodrigo Munoz (Family Health Centers of San Diego, California), and Dr. Alvaro Jerez (Centro Internacional de Trastornos Afectivos y de la Conducta Adictiva-CITACA, Guatemala). Additional investigators from the University of Texas Health Science Center at San Antonio included Dr. Albana Dassori and Dr. Rolando Medina.

Swedish Schizophrenia Exome Sequencing project

Author contributions: F.M.dV., C.G.B., N.G., V.B. and S.A.K. designed the experiments. C.G.B. and S.A.K. established the family-based ascertainment program. C.G.B., F.M.dV. and M.C. conducted the family recruitment. C.G.B. and F.M.dV. performed the genetic analysis, with assistance from M.Q., S.O. and G.J.B. B.D. conceived the protein misfolding hypothesis and implemented the structural modelling. D.C., R.M.K., P.R.B., A.N., A.T.S., J.H., E.H., V.Bergink, N.A., A.H., C.M.vD., H.T., A.U., J.A.V. and R.A.O. provided case-control cohort samples. C.G.B., M.A.I. and M.W.V. coordinated the brain imaging studies. C.D.L. and T.W. performed the brain imaging data analyses. T.dW., F.W.V. and H.B.B. established the fibroblast lines. M.G., T.L. and J.G. performed the iPSC reprogramming. F.M.dV. and N.G. conducted the neuronal and oligodendrocyte progenitor cell experiments. G.S. performed the electrophysiological recordings. B.L. and M.B. assisted with the oligodendrocyte progenitor cell studies. Genetic analyses were supervised by V.B. and S.A.K. iPSC and brain imaging studies were supervised by S.A.K. F.M.dV., C.G.B., N.G. and S.A.K wrote the manuscript. The manuscript was reviewed, edited and approved by all authors.

Author Information: The authors declare no competing financial interests. Correspondence should be addressed to s.kushner@erasmusmc.nl.

SUPPLEMENTARY FIGURES

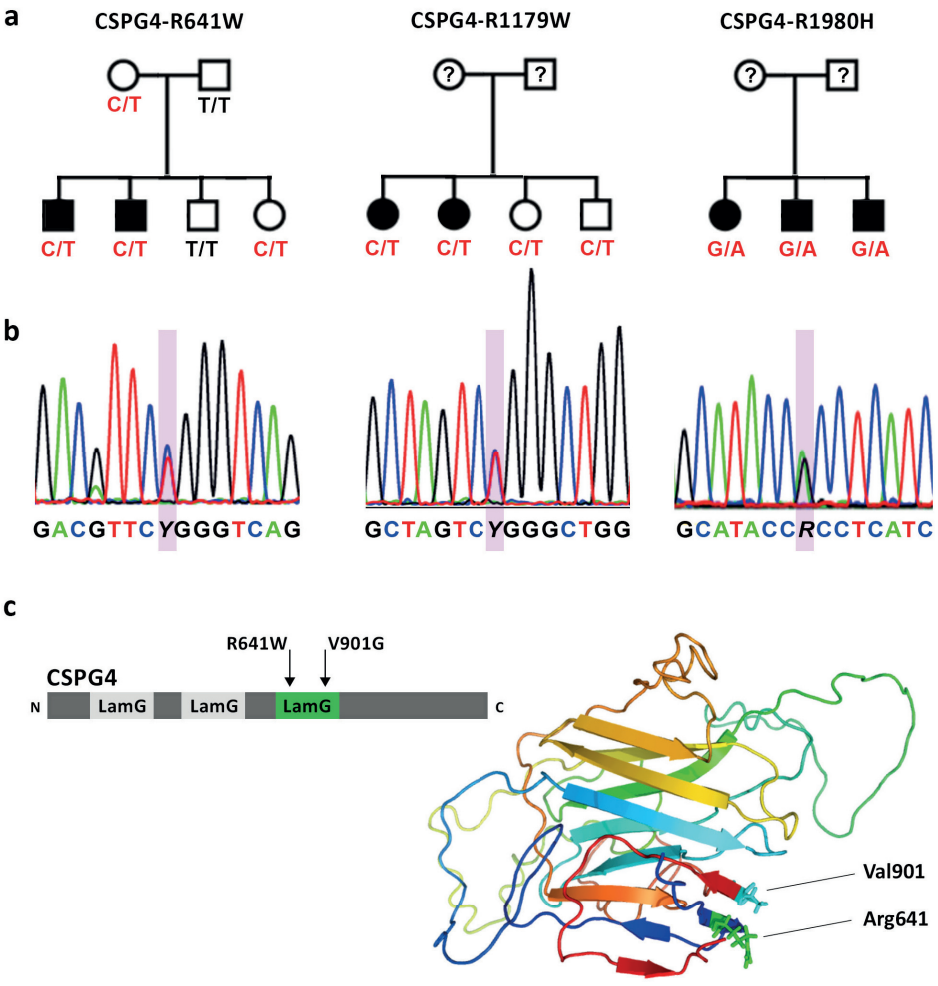

Supplementary Figure 1. Familial segregation rare coding variants in *CSPG4* with schizophrenia. (a) Pedigrees carrying variants *CSPG4*^{R641W}, *CSPG4*^{R1179W}, and *CSPG4*^{R1980H}. Symbols: filled, schizophrenia; open, unaffected; heterozygous carriers of the CSPG4 c.1921C>T p.R641W, c.3535C>T p.R1179W, and c.5939G>A p.R1980H. **(b)** Representative sequencing results for heterozygous carriers of the corresponding CSPG4 mutations mentioned in panel A. **(c)** Three-dimensional structural homology modelling of the putative 3rd LamG domain of CSPG4, demonstrating the close proximity of Arg^{641} and Val^{901}.

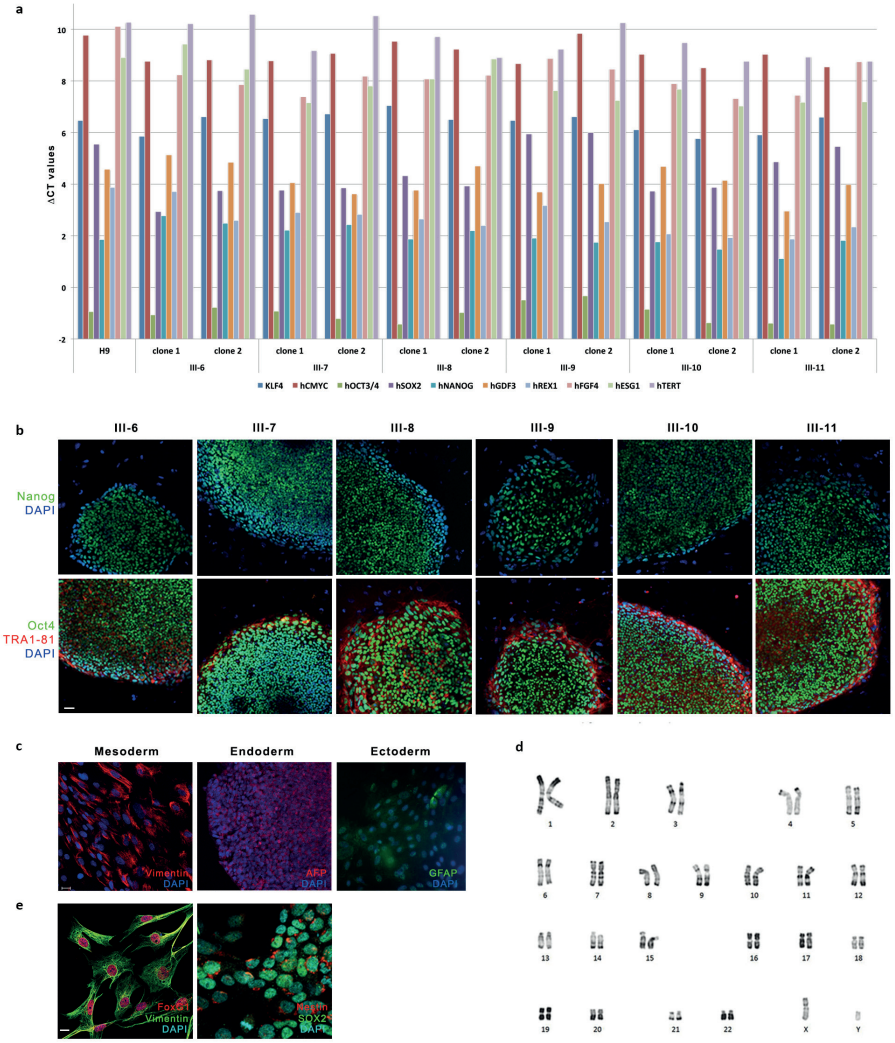

Supplementary Figure 2. Characterization of iPSC clones and NPCs. (a) RT-PCR of pluripotency genes normalised to GAPDH expression levels confirmed down-regulation of exogenous reprogramming genes and up-regulation of endogenous stem cell genes, similar to H9 human embryonic stem cells. **(b)** iPSC colonies showed uniform staining for pluripotency markers Nanog, Oct4 and TRA-1-81. **(c)** EB differentiation confirmed that iPSCs were capable of generating cell types representative of all 3 embryonal layers: endoderm (AFP), mesoderm (Vimentin) and ectoderm (GFAP) (scale bar = 20 µm). **(d)** Karyotyping was performed on all iPSC clones to confirm genomic integrity following iPSC reprogramming, shown is a representative karyogram from an iPSC line (subject III-11). **(e)** NPCs were positive for SOX2, Nestin, Vimentin and FoxG1, confirming their forebrain specification (scale bar = 10 µm).

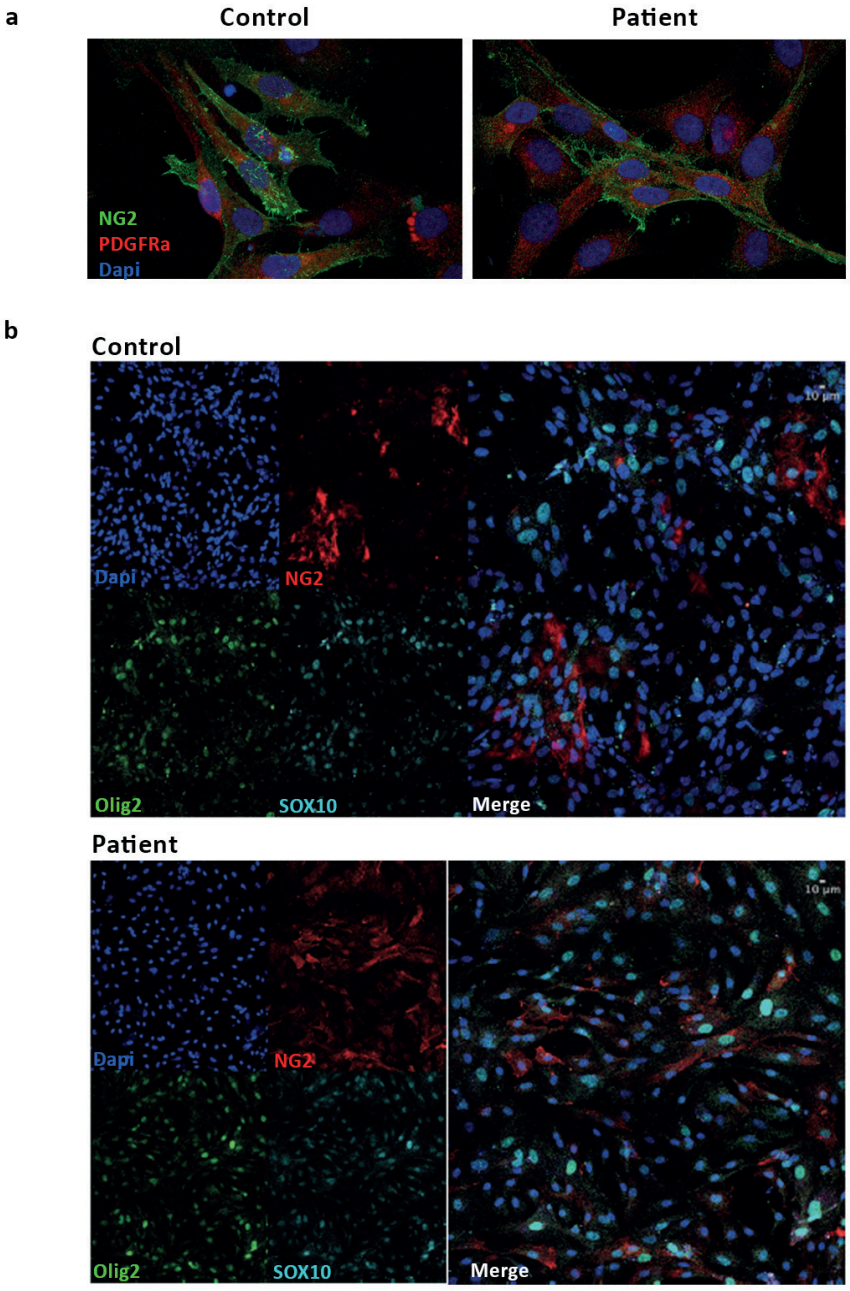

Supplementary Figure 3. Characterization of OPCs. The vast majority of NG2+ cells co-expressed the OPC marker **(a)** PDGFRα and **(b)** Olig2 and SOX10 (scale bars = 10 µm).

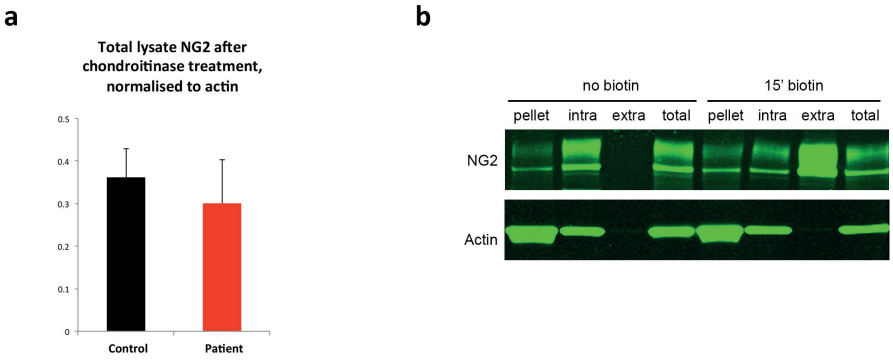

Supplementary Figure 4. Biotinylation assay controls. (a) Upon chondroitinase treatment no significant difference is found in the amount of 300 kDa NG2 in the total lysate fraction. **(b)** Without biotinylation (left panel), no NG2 protein is found in the immunoprecipitated extracellular fraction. In addition, the lack of actin signal in the extracellular samples indicates high specificity of the biotin pulldown.

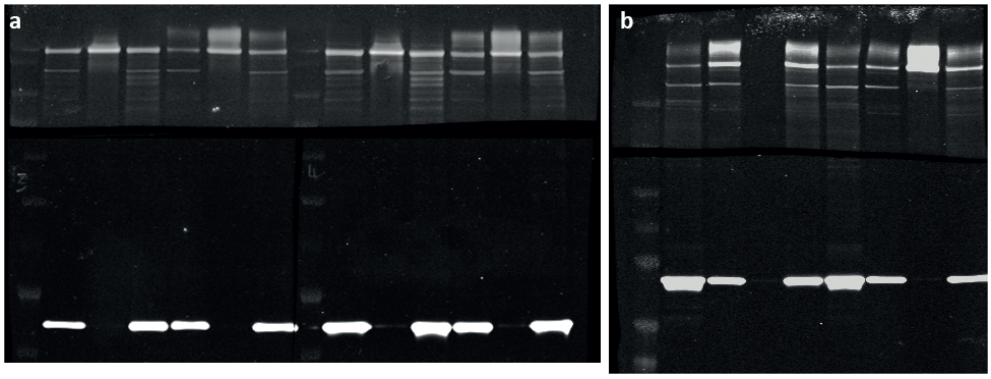

Supplementary Figure 5. Raw LI-COR western blot images. Full western blot showing upper half stained for NG2 protein and corresponding lower half stained for actin **(a)** Full blot corresponding to Figure 4d (lower half cut vertically for processing). **(b)** Full blot corresponding to Supplementary Figure 4b.

Supplementary Table 1. Discovery Family – Patient characteristics

Patient	II-1	III-5	III-7	III-9	III-11
Diagnosis (DSM)	SZ	SZ	SZ	SZ	SZ
Age of onset first psychosis	46	18	36	18	15
Medication	n/a	Clozapine Biperidene Lithium Oxazepam	Quetiapine Paroxetine Lorazepam	Zuclopenthixol	Zuclopenthixol Trihexyphenidyl Lithium Lorazepam

Supplementary Table 2. Linkage analysis – Affected only model

Chr	Start position	End position	Start SNP	End SNP	Mb	Max LOD score
2	2686579	17262830	rs11694900	rs17476649	14.576251	0.8809
4	14744996	20524715	rs4464561	rs16869706	5.779719	0.8808
6	164665485	End	rs942731	rs9459964	5.675712	0.8809
7	Start	2739017	rs6583338	rs809547	2.692778	0.8852
7	69935641	97595184	rs4717530	rs9692345	27.659543	0.8852
7	148239179	End	rs6957883	rs1125769	10.809432	0.8852
10	1147045	9247586	rs4880763	rs1469993	8.100541	0.8808
11	Start	4905155	rs1045454	rs11603903	4.700927	0.8852
11	68289796	129160763	rs11228269	rs4644651	60.870967	0.8852
14	89036519	End	rs2116445	rs2583292	18.068524	0.8852
15	39135102	101779863	rs7167406	rs11858464	62.644761	0.8852
16	10480846	76592633	rs7195621	rs12599021	66.111787	0.8826
19	52447068	End	rs8105910	rs7910	6.646396	0.8851

Supplementary Table 3. Sanger sequencing primers for *CSPG4* open reading frame

PCR amplification primers

Name	Sequence
CSPG4_ex01_F	ctgccccagagaggaacagc
CSPG4_ex01_R	cccctaactggacagccttgg
CSPG4_ex02_F	gggctggacacaaggtgagc
CSPG4_ex02_R	caagagcctggcagcaagc
CSPG4_ex03a_F	tgccacagcctccaaagtagc
CSPG4_ex03a_R	gcagagtccgggtcataggc
CSPG4_ex03b_F	gctggaggtgtcggtgacg
CSPG4_ex03b_R	ggcacgtgcacacatgtaacc
CSPG4_ex04_F	accagctgcatgtctggctgc
CSPG4_ex04_R	ctggctccgaggagttgtgagg
CSPG4_ex05_F	cagtctgggggttatacacagagagg
CSPG4_ex05_R	gctctgagccgcgaagtagg
CSPG4_ex06-07_F	agctggggccttcctgggta
CSPG4_ex06-07_R	gccaggtccaggcctgtgttt
CSPG4_ex08_F	ggtcacgctgcctctttgc
CSPG4_ex08_R	acgtctgctgccagtgatgc
CSPG4_ex09_F	cccagagtggggcctgag
CSPG4_ex09_R	cccaaccatcaagccaggtc
CSPG4_ex10a_F	gggagggacaatgggagagg
CSPG4_ex10a_R	ccagctcgccagcatctagg
CSPG4_ex10b_F	ctccgggtggtttcagatcg
CSPG4_ex10b_R	tctccaggctcggagtgagc

Internal Sanger sequencing primers

Name	Sequence
CSPG4_ex3a_int_f1	atgcagccaccctcaatgg
CSPG4_ex3a_int_r1	tcctcctccagcctgcagc
CSPG4_ex3a_int_f2	cgtcacctccaggaacaccg
CSPG4_ex3a_int_r2	ggcagccagagagtgggg
CSPG4_ex3b_int_f1	ctggcccaaggctctgccat
CSPG4_ex3b_int_r1	ggtgccctggcctccttgag
CSPG4_ex3b_int_f2	acaaggctgtcagatggccagg
CSPG4_ex3b_int_f3	ggaggtacggggtgtcttccg
CSPG4_ex3b_int_f4	ccaacctcgacatccgcagtg
CSPG4_ex3b_int_r2	gccggccacgcaacagg
CSPG4_ex3b_int_r3	tgggtgttctgagtgtgcagtgg
CSPG4_ex3b_int_r4	cggcaggagaactcggtcg
CSPG4_ex10a_int_f1	cccagctggctgcagggc
CSPG4_ex10a_int_f2	catcgaggtgcagctgcggg
CSPG4_ex10a_int_r1	ctgccacgctgctcccgttg
CSPG4_ex10a_int_r2	ccggctggggaactgtgtgac
CSPG4_ex10b_int_f1	gaccttgaggacgggaggct
CSPG4_ex10b_int_f2	ctgactgccaagccccgcaa
CSPG4_ex10b_int_r1	gtaaggctcagtggcaaagtcca
CSPG4_ex10b_int_r2	atctaggacggtggggtccagg

Supplementary Table 4. qPCR primers for iPSC pluripotency genes

hOCT3/4-F	GAC AGG GGG AGG GGA GGA GCT AGG
hOCT3/4-R	CTT CCC TCC AAC CAG TTG CCC CAA AC
hSOX2-F	GGG AAA TGG GAG GGG TGC AAA AGA GG
hSOX2-R	TTG CGT GAG TGT GGA TGG GAT TGG TG
hNANOG-F	CAG CCC CGA TTC TTC CAC CAG TCC C
hNANOG-R	CGG AAG ATT CCC AGT CGG GTT CAC C
hGDF3-F	CTT ATG CTA CGT AAA GGA GCT GGG
hGDF3-R	GTG CCA ACC CAG GTC CCG GAA GTT
hREX1-F	CAG ATC CTA AAC AGC TCG CAG AAT
hREX1-R	GCG TAC GCA AAT TAA AGT CCA GA
hFGF4-F	CTA CAA CGC CTA CGA GTC CTA CA
hFGF4-R	GTT GCA CCA GAA AAG TCA GAG TTG
hESG1-F	ATA TCC CGC CGT GGG TGA AAG TTC
hESG1-R	ACT CAG CCA TGG ACT GGA GCA TCC
hTERT-F	CCT GCT CAA GCT GAC TCG ACA CCG TG
hTERT-R	GGA AAA GCT GGC CCT GGG GTG GAG C
hKLF4-F	TGA TTG TAG TGC TTT CTG GCT GGG CTC C
hKLF4-R	ACG ATC GTG GCC CCG GAA AAG GAC C
h-cMYC-F	GCG TCC TGG GAA GGG AGT TCC GGA GC
h-cMYC-R	TTG AGG GGC ATC GTC GCG GGA GGC TG

REFERENCES

1 Polderman TJC, Benyamin B, de Leeuw CA, Sullivan PF, van Bochoven A, Visscher PM et al. Meta-analysis of the heritability of human traits based on fifty years of twin studies. Nat Genet 2015; 47: 702–709.

2 Purcell SM, Moran JL, Fromer M, Ruderfer D, Solovieff N, Roussos P et al. A polygenic burden of rare disruptive mutations in schizophrenia. Nature 2014. doi:10.1038/nature12975.

3 Bonifati V. Genetics of Parkinson's disease--state of the art, 2013. Parkinsonism Relat Disord 2014; 20 Suppl 1: S23–8.

4 Lesage S, Brice A. Parkinson's disease: from monogenic forms to genetic susceptibility factors. Hum Mol Genet 2009; 18: R48–59.

5 Papapetropoulos S, Adi N, Ellul J, Argyriou AA, Chroni E. A prospective study of familial versus sporadic Parkinson's disease. Neurodegener Dis 2007; 4: 424–7.

6 Klein C, Westenberger A. Genetics of Parkinson's disease. Cold Spring Harb Perspect Med 2012; 2: a008888.

7 Loy CT, Schofield PR, Turner AM, Kwok JBJ. Genetics of dementia. Lancet 2014; 383: 828–40.

8 Ryan NS, Rossor MN. Correlating familial Alzheimer's disease gene mutations with clinical phenotype. Biomark Med 2010; 4: 99–112.

9 Ott J, Wang J, Leal SM. Genetic linkage analysis in the age of whole-genome sequencing. Nat Rev Genet 2015; 16: 275–284.

10 Ripke S, Neale BM, Corvin A, Walters JTR, Farh K-H, Holmans P a. et al. Biological insights from 108 schizophrenia-associated genetic loci. Nature 2014. doi:10.1038/nature13595.

11 Fromer M, Pocklington AJ, Kavanagh DH, Williams HJ, Dwyer S, Gormley P et al. De novo mutations in schizophrenia implicate synaptic networks. Nature 2014. doi:10.1038/nature12929.

12 Brennand KJ, Simone A, Jou J, Gelboin-Burkhart C, Tran N, Sangar S et al. Modelling schizophrenia using human induced pluripotent stem cells. Nature 2011; 473: 221–5.

13 White T, Ehrlich S, Ho B-C, Manoach DS, Caprihan A, Schulz SC et al. Spatial characteristics of white matter abnormalities in schizophrenia. Schizophr Bull 2013; 39: 1077–86.

14 Zalesky A, Fornito A, Seal ML, Cocchi L, Westin CF, Bullmore ET et al. Disrupted axonal fiber connectivity in schizophrenia. Biol Psychiatry 2011; 69: 80–89.

15 Davis KL, Stewart DG, Friedman JI, Buchsbaum M, Harvey PD, Hof PR et al. White matter changes in schizophrenia: evidence for myelin-

16 Andreasen NC, Nopoulos P, Magnotta V, Pierson R, Ziebell S, Ho BC. Progressive brain change in schizophrenia: A prospective longitudinal study of first-episode schizophrenia. Biol Psychiatry 2011; 70: 672–679.

17 Terwisscha Van Scheltinga AF, Bakker SC, Van Haren NEM, Derks EM, Buizer-Voskamp JE, Boos HBM et al. Genetic schizophrenia risk variants jointly modulate total brain and white matter volume. Biol Psychiatry 2013; 73: 525–531.

18 van den Heuvel MP, Sporns O, Collin G, Scheewe T, Mandl RCW, Cahn W et al. Abnormal rich club organization and functional brain dynamics in schizophrenia. JAMA psychiatry 2013; 70: 783–92.

19 Nave K-A, Ehrenreich H. Myelination and oligodendrocyte functions in psychiatric diseases. JAMA psychiatry 2014; 71: 582–4.

20 Goudriaan A, de Leeuw C, Ripke S, Hultman CM, Sklar P, Sullivan PF et al. Specific Glial Functions Contribute to Schizophrenia Susceptibility. Schizophr Bull 2013; : 1–11.

21 Fields RD. White matter in learning, cognition and psychiatric disorders. Trends Neurosci. 2008; 31: 361–370.

22 Paus T, Keshavan M, Giedd JN. Why do many psychiatric disorders emerge during adolescence? Nat Rev Neurosci 2008; 9: 947–57.

23 Nishiyama A, Dahlin KJ, Prince JT, Johnstone SR, Stallcup WB. The primary structure of NG2, a novel membrane-spanning proteoglycan. J Cell Biol 1991; 114: 359–71.

24 Kang SH, Fukaya M, Yang JK, Rothstein JD, Bergles DE. NG2+ CNS glial progenitors remain committed to the oligodendrocyte lineage in postnatal life and following neurodegeneration.

Neuron 2010; 68: 668–681.

25 Exome Variant Server, NHLBI GO Exome Sequencing Project (ESP), Seattle, WA. 2013; : http://evs.gs.washington.edu/EVS/.

26 Abecasis GR, Altshuler D, Auton A, Brooks LD, Durbin RM, Gibbs RA et al. A map of human genome variation from population-scale sequencing. Nature 2010; 467: 1061–73.

27 Consortium TG of the N. Whole-genome sequence variation, population structure and demographic history of the Dutch population. Nat Genet 2014; 46: 818–825.

28 Escamilla M, Hare E, Dassori AM, Peralta JM, Ontiveros A, Nicolini H et al. A schizophrenia gene locus on chromosome 17q21 in a new set of families of Mexican and central american ancestry: evidence from the NIMH Genetics of schizophrenia in latino populations study. Am J Psychiatry 2009; 166: 442–9.

29 Vieland VJ, Walters KA, Azaro M, Brzustowicz LM, Lehner T. The value of regenotyping older linkage data sets with denser marker panels. Hum Hered 2014; 78: 9–16.

30 Timpl R, Tisi D, Talts JF, Andac Z, Sasaki T, Hohenester E. Structure and function of laminin LG modules. Matrix Biol. 2000; 19: 309–317.

31 Xu B, Ionita-Laza I, Roos JL, Boone B, Woodrick S, Sun Y et al. De novo gene mutations highlight patterns of genetic and neural complexity in schizophrenia. Nat Genet 2012. doi:10.1038/ng.2446.

32 Xu B, Roos JL, Dexheimer P, Boone B, Plummer B, Levy S et al. Exome sequencing supports a de novo mutational paradigm for schizophrenia. Nat Genet 2011; 43: 864–868.

33 Rujescu D, Ingason A, Cichon S, Pietiläinen OPH, Barnes MR, Toulopoulou T et al. Disruption of the neurexin 1 gene is associated with schizophrenia. Hum Mol Genet 2009; 18: 988–96.

34 Kirov G, Gumus D, Chen W, Norton N, Georgieva L, Sari M et al. Comparative genome hybridization suggests a role for NRXN1 and APBA2 in schizophrenia. Hum Mol Genet 2008; 17: 458–465.

35 Kelley LA, Sternberg MJE. Protein structure prediction on the Web: a case study using the Phyre server. Nat Protoc 2009; 4: 363–71.

36 Zhang Y. I-TASSER server for protein 3D structure prediction. BMC Bioinformatics 2008; 9: 40.

37 Holm L, Rosenström P. Dali server: conservation mapping in 3D. Nucleic Acids Res 2010; 38: W545–9.

38 Burg MA, Nishiyama A, Stallcup WB. A central segment of the NG2 proteoglycan is critical for the ability of glioma cells to bind and migrate toward type VI collagen. Exp Cell Res 1997; 235: 254–64.

39 Tillet E, Gential B, Garrone R, Stallcup WB. NG2 proteoglycan mediates beta1 integrin-independent cell adhesion and spreading on collagen VI. J Cell Biochem 2002; 86: 726–36.

40 Nishiyama A, Lin X, Stallcupt WB. Generation of Truncated Forms of the NG2 Proteoglycan by Cell Surface Proteolysis. 1995; 6: 1819–1832.

41 Sakry D, Neitz A, Singh J, Frischknecht R, Marongiu D, Binamé F et al. Oligodendrocyte precursor cells modulate the neuronal network by activity-dependent ectodomain cleavage of glial NG2. PLoS Biol 2014; 12: e1001993.

42 Adzhubei IA, Schmidt S, Peshkin L, Ramensky VE, Gerasimova A, Bork P et al. A method and server for predicting damaging missense mutations. Nat Methods 2010; 7: 248–9.

43 Lee MK, Stirling W, Xu Y, Xu X, Qui D, Mandir AS et al. Human alpha-synuclein-harboring familial Parkinson's disease-linked Ala-53 --> Thr mutation causes neurodegenerative disease with alpha-synuclein aggregation in transgenic mice. Proc Natl Acad Sci U S A 2002; 99: 8968–73.

44 Wen Z, Nguyen HN, Guo Z, Lalli MA, Wang X, Su Y et al. Synaptic dysregulation in a human iPS cell model of mental disorders. Nature 2014; 515: 414–418.

45 Lin W, Popko B. Endoplasmic reticulum stress in disorders of myelinating cells. Nat Neurosci 2009; 12: 379–85.

46 Monaco MCG, Maric D, Bandeian A, Leibovitch E, Yang W, Major EO. Progenitor-derived oligodendrocyte culture system from human fetal brain. J Vis Exp 2012; : 1–8.

47 Huang GN, Zeng W, Kim JY, Yuan JP, Han L, Muallem S et al. STIM1 carboxyl-terminus activates native SOC, I(crac) and TRPC1 channels.

Nat Cell Biol 2006; 8: 1003–1010.

48 Ikram MA, van der Lugt A, Niessen WJ, Krestin GP, Koudstaal PJ, Hofman A et al. The Rotterdam Scan Study: design and update up to 2012. Eur J Epidemiol 2011; 26: 811–24.

49 White T, Schmidt M, Karatekin C. White matter 'potholes' in early-onset schizophrenia: A new approach to evaluate white matter microstructure using diffusion tensor imaging. Psychiatry Res - Neuroimaging 2009; 174: 110–115.

50 First M, Gibbon M, Spitzer R. Structured Clinical Interview for DSM-IV Axis II Personality Disorders (SCID-II). Am Psychiatr Press Inc 1997.

51 Hoffmann K, Lindner TH. easyLINKAGE-Plus - Automated linkage analyses using large-scale SNP data. Bioinformatics 2005; 21: 3565–3567.

52 Warlich E, Kuehle J, Cantz T, Brugman MH, Maetzig T, Galla M et al. Lentiviral vector design and imaging approaches to visualize the early stages of cellular reprogramming. Mol Ther 2011; 19: 782–9.

53 Koppelmans V, de Groot M, de Ruiter MB, Boogerd W, Seynaeve C, Vernooij MW et al. Global and focal white matter integrity in breast cancer survivors 20 years after adjuvant chemotherapy. Hum Brain Mapp 2014; 35: 889–99.

54 Smith SM, Jenkinson M, Woolrich MW, Beckmann CF, Behrens TEJ, Johansen-Berg H et al. Advances in functional and structural MR image analysis and implementation as FSL. In: NeuroImage. 2004 doi:10.1016/j.neuroimage.2004.07.051.

55 Smith SM. Fast robust automated brain extraction. Hum Brain Mapp 2002; 17: 143–155.

56 Andersson JLR, Jenkinson M, Smith S. Non-linear registration aka Spatial normalisation FMRIB Technial Report TR07JA2. 2007.

57 Rueckert D, Sonoda LI, Hayes C, Hill DL, Leach MO, Hawkes DJ. Nonrigid registration using free-form deformations: application to breast MR images. IEEE Trans Med Imaging 1999; 18: 712–721.

58 Mori S, Oishi K, Jiang H, Jiang L, Li X, Akhter K et al. Stereotaxic white matter atlas based on diffusion tensor imaging in an ICBM template. Neuroimage 2008; 40: 570–582.

59 Smith SM, Jenkinson M, Johansen-Berg H, Rueckert D, Nichols TE, Mackay CE et al. Tract-based spatial statistics: Voxelwise analysis of multi-subject diffusion data. Neuroimage 2006; 31: 1487–1505.

Chapter 5

Discussion

GENERAL DISCUSSION AND FUTURE DIRECTIONS

The landmark discovery of Induced Pluripotent Stem Cells (iPSCs) has allowed for the first time the study of living neural cells derived directly from patients with brain diseases, including psychiatric disorders. iPSC technology provides the opportunity to investigate the molecular biology and neurophysiology of brain disorders, and thereby holds promise for the development of patient-specific treatments. Nevertheless, iPSC reprogramming introduces significant technical challenges, such as genome contamination, epigenetic changes, and low reprogramming efficiency. These are the main processes thought to underlie the large variability that is hampering most current neural differentiation protocols for human iPSCs. The following paragraphs discuss the future directions of iPSC technology to model psychiatric disorders and the potential pathological mechanisms for the *CSPG4*^{A131T} mutation in schizophrenia.

THE IMPORTANCE OF GOOD CONTROLS IN iPSC MODELLING

Variability in iPSC clones is one of the major challenges in disease modeling[1]. Reprogramming of somatic cells to iPSCs was first described using viral vectors that mediate integration of pluripotency genes into the host genome (e.g. fibroblasts)[2]. A disadvantage of this method is that it can introduce mutations or disruption of genes at the site of integration. In that sense, the integration site of viral vectors is critical; firstly integration sites might affect the basic cellular mechanisms in the cell after which assessing the effect of the mutations on disease phenotype might be challenging. Secondly, the integration sites are different for every clone from any particular cell line, causing variability between clones. Therefore, there is growing consensus that generation of several iPSC clones per individual and comparison of cellular characteristics of all clones are necessary for bona fide phenotype discovery. To circumvent issues of integration, there are also reprogramming methods using nonviral/non-integrating vectors. Especially in the fields of regenerative medicine, non-integrative methods are preferred for clinical reasons, avoiding risks of tumor formation in the patient. For disease modeling however, viral reprogramming is often still the method of choice.

Determining a control group for patient-derived iPSC is important for the design of experiments. hES and iPSCs from unrelated healthy individuals can be used as controls[3]. However, the genetic backgrounds of unrelated people are obviously different, with the risk that the variability between the cases and controls might mask any disease-specific phenotype. Thus, healthy family members (preferably first degree relatives, e.g. parents and siblings) are considered as better control groups than unrelated individuals, due to their genetic similarity.

As was shown in the chapter 4, we attempted to implement a methodology consisting of a family-based approach to model schizophrenia; first to perform genetic analysis for finding mutations in the family that segregate with schizophrenia[4] and further to generate iPSC-derived neural cells from patients and their healthy siblings. We identified the *CSPG4*^{A131T} mutation in all patients and not in the healthy siblings. In addition, other mutations in the *CSPG4* gene were identified, segregating in multiple families with a high incidence of schizophrenia. Overall, these findings support the validity of family-based genetic analyses to understand the mechanisms of such a heterogeneous psychiatric disease.

Recent advances in gene editing technologies have further progressed iPSC disease modeling, allowing the production of isogenic cell lines that differ only at the genetic position of the mutation. The last few years have seen *in vitro* techniques such as genome editing with zinc-finger (ZFN)-mediated gene targeting strategy, TALEN transcription activator-like effector nucleases and clustered regularly interspaced short palindromic repeat (CRISPR)/Cas9 techniques that allow to generate isogenic cell lines[5]. The generation of isogenic cell lines is

an effective way to prevent genome variations by either correcting the mutation in patient-derived iPSCs or creating the mutation in control iPSCs. Having the exact same genetic background with a single mutation difference can isolate the effect of a specific mutation. Isogenic cell lines have been used in different studies as a control to compare the effect of a specific mutation, for instance by correcting a mutation in the *SOD1* gene from an ALS patient by ZFN-mediated gene targeting[6] and a mutation in the *DISC1* gene from a patient with schizophrenia by TALEN[7]. *CSPG4* has many pseudogenes which complicate genome editing both using TALEN or CRISPR/Cas9 methods due to the homology between the pseudogenes and the protein-coding gene. Nevertheless, generation of isogenic lines is the future aim for comparing the effect of a single mutation.

IMPROVEMENT OF NEURAL DIFFERENTIATION PROTOCOLS

In Chapter 2, we described a two dimensional (2D) culture system to generate neural lineage cells from iPSCs. First, we generated embryoid bodies from iPSCs and then differentiated them into neural precursor cells (NPCs). With several optimization steps, after 8 weeks neurons exhibited all the functional traits of mature neurons, including repetitive firing of action potentials, sodium and potassium currents, spontaneous spiking activity and synaptic communication which was also described in Bardy et al.[8] in a 2D culture system.

Recent approaches involve developing three dimensional (3D) cultures by creating cerebral organoids in which iPSCs are embedded in Matrigel and are grown in a spinning bioreactor[9]. Another method generates cortical spheroids in floating conditions on low-attachment plates[10] to study brain disorders in an organ-like environment. These 3D cultures allow formation of nervous system tissue similar to the complexity and functionality of *in vivo* neural circuits. In a recent study, such a 3D culture system was used to model Alzheimer pathogenesis[11]. After 6 weeks of differentiation, aggregation of amyloid-β was observed followed by robust tau pathology after 10–14 weeks in culture, whereas the tau pathology in 2D culture conditions was never identified. In our hands, the protocol in which we create 3D culture shows comparable electrophysiological results with the 2D protocol for most parameters such as spike kinetics (rise and decay time, half width), spike amplitude, and membrane properties (input resistance and resting membrane potential), however better connectivity in 3D than 2D culture conditions was observed in preliminary experiments.

The onset of the modelled disorders is another point of consideration that might play a critical role for designing a culture system and to dissect the disease phenotype. For instance, late-onset disorders might require more complex culture conditions as further aging might be required to create late-onset pathogenesis. In an elegant study on Parkinson's disease (PD)[12], iPSC-derived dopaminergic neurons were aged by using induced expression of a protein called progerin. Progerin induces dopamine-specific phenotypes in PD-iPSC-derived dopamine neurons such as dendrite degeneration, loss of tyrosine-hydroxylase (TH) expression and enlarged mitochondria or Lewy body-precursor inclusions. Schizophrenia on the other hand is considered to have more neurodevelopmental aspects to its pathogenesis than neurodegenerative diseases. In Chapter 2, together with the data shown in other studies[8,10], we could define the iPSC-derived neurons in our cultures as "mature". On the other hand, studies comparing transcriptional profiles of human iPSC-derived neurons to brain tissue levels show that iPSC-derived neurons are at a human fetal stage[13]. Therefore, still it is a controversial topic whether or not the maturity of the neurons is enough to reveal neuronal pathogenesis.

Mimicking *in vivo* conditions, we have successfully generated neural populations such as neurons, astrocytes, oligodendrocytes and their precursors (NPCs and OPCs). Having multiple cell populations improves the physiological conditions for iPSC-derived neurons to become more mature and provides understanding of the interaction of different cell types in complex developmental

psychiatric disorders. On the other hand, neuron-glia protocols impose some limitations on those who wish to perform RNA and proteomics analysis in specific cell types. However, FACS sorting in NPC, OPC and neural cultures allows focusing on specific neural subtypes.

In Chapter 4, we describe the discovery of *CSPG4* as a candidate gene for schizophrenia. CSPG4, chondroitin sulfate proteoglycan 4, is also known as NG2 (neural/glial antigen 2). NG2 is a single-pass transmembrane proteoglycan with CNS cell-type specific expression in oligodendrocyte precursor cells (OPCs) and pericytes[14,15]. As was shown in chapter 4, the effect of the *CSPG4*^{A1311T} mutation is cell type specific for OPCs, while no difference was observed in NG2 ER retention or protein modification in fibroblasts from the same cases and controls. Nevertheless, our studies did not include investigations of the other NG2-expressing cell type of the brain, namely pericytes. Thus, it is interesting to dissect the effect of the *CSPG4*^{A1311T} mutation on pericytes. Another cell type that we cannot study in our neural cultures is microglia. Even though microglia are not an NG2-expressing cell, they are an interesting cell line in which changes have been reported in many schizophrenia studies. A recent paper showed overexpression of C4A protein in the brains of patients with schizophrenia[16]. C4A is expressed from the *C4* gene, which is located in the MHC locus. Overexpression of C4A might overstimulate microglia and lead to elimination of synapses during adolescence that results in schizophrenia pathogenesis[16]. Up to date, no iPSC-derived microglia protocol has been reported that might provide information about the interaction between the immune system and OPCs in co-culturing experiments with OPCs.

To conclude, iPSC-based studies of neuropsychiatric disorders provide a feasible and tractable approach for studying the neurobiological mechanisms of psychiatric disorders. There is great potential for modeling human neuropsychiatric phenotypes with iPSC technology.

POSSIBLE MECHANISMS FOR *CSPG4*^{A1311T} MUTATION IN SCHIZOPHRENIA

NG2 regulates diverse functions in OPCs including proliferation, migration, and regulation of oligodendrocyte maturation[17–19]. The *CSPG4*^{A1311T} mutation is located within the first Laminin G domain of the NG2 protein. Laminin G domains are highly conserved and present in many extracellular matrix proteins[20] that have multiple functions including protein-protein interactions, axon path finding, migration, adhesion and differentiation. The *CSPG4*^{A1311T} mutation in patient OPCs might cause defects in oligodendrocytes lineage cells (OPCs and oligodendrocytes), and indirectly in neurons or in both cell lineages. The next paragraphs speculate about the possible mechanisms by which the *CSPG4*^{A1311T} mutation might lead to a disease phenotype in patients with schizophrenia.

A. The effect of CSPG4^{A1311T} *mutation on OPCs*

CSPG4 is highly expressed in OPCs and correspondingly we found an OPC-specific phenotype in cells carrying the *CSPG4*^{A1311T} mutation. Firstly, morphological differences were observed between case and control OPCs. OPCs derived from patients carrying the *CSPG4*^{A1311T} mutation were smaller than control cells. Moreover, we observed that OPCs with the *CSPG4*^{A1311T} mutation tend to localize close to each other whereas control OPCs spread more evenly over the culture dish. This effect might be caused by the role of NG2 protein in contact inhibition[21].

In addition, differences were observed in NG2 modification. The ratio of modified to unmodified NG2 protein, meaning modified with chondroitin sulphate side chains or treated with chondroitinase, is significantly lower in patient OPCs. These results were consistent in membrane-bound and intracellular fractions of NG2 protein, reflecting an altered distribution pattern of modified NG2 isoforms in patient-derived OPCs suggestive of retention of NG2 in the ER. Based on the protein modeling that was described in chapter 4, the *CSPG4* ^{A1311T} mutation was predicted

to lead to structural changes in the NG2 protein that affect protein folding and thereby perhaps the transport of the protein. Importantly, since the *CSPG4*^{A1131T} mutation is heterozygous, patient OPCs have both WT and mutant NG2 protein, which will partly mask the effect on membrane localization. Less modified NG2 protein on the OPC membrane might influence the interaction with neurons or with other cell types of CNS. Also, we observed more cell death in patient iPSC-derived OPCs compared to control OPCs.

OPCs are known for their role in migration in response to extracellular responses, for instance to inflammation and demyelinating lesions[22]. Importantly, it has been known that the NG2 protein regulates directional migration of OPCs via Rho GTPases and polarity complex proteins[23]. The *CSPG4*^{A1131T} mutation is in the Laminin G domain, which is located in the ectodomain of the NG2 protein, and might therefore lead to differences in migration. In addition, OPCs with the *CSPG4*^{A1131T} mutation might be less sensitive to extracellular stimuli such as glutamate known to influence OPC migration[24].

Other *CSPG4* mutations were identified in a cohort of Mexican-American families with a high incidence of schizophrenia. Specifically, the following rare mutations were found: R641W, V901L, R1179W and R1980H. R641W and V901L are predicted to be in a putative third Laminin G domain in the ectodomain of NG2. Interestingly, R641W and V901L mutations are located close together in the 3D protein model, although they are more than 200 amino acids apart in sequence. Having a mutation in a Laminin G like domain might lead to structural changes on the cell membrane, which might affect the binding partners, interaction with extracellular matrix, or migration efficiency of the NG2 protein. Interestingly, the same protein region was shown to bind to collagen V and VI, suggesting a role in cell adhesion and migration[25,26]. Showing the cellular effect of other *CSPG4* mutations on OPCs would be of great value for schizophrenia research.

B. The effect of CSPG4^{A1131T} *mutation on neuronal activity and myelination*

Remarkably, various studies imply synapse formation between OPCs and different neuronal subtypes. Glutamatergic and GABAergic synapses have been shown on OPCs in the hippocampus[24,27–29], cerebellum, corpus callosum and the cortex[25O,252]. These synapses allow OPCs to respond to neuronal activity and regulate differentiation[33], Myelin Basic Protein (MBP) synthesis to initiate myelination[34] and for positioning and migration of OPCs during development[31]. In addition, synapse formation is also required to modulate neuronal glutamatergic signaling by the OPC protein NG2[35]. In Sakry et al., it has been shown how NG2 protein can modulate AMPA and NMDA receptors of neuronal synapses[36]. In another study it was shown that γ-secretase cleaves the intracellular domain of NG2 and ADAM10 protease (α-secretase) cleaves the two N-terminal Laminin G domains of the NG2 ectodomain and modulates the glutamatergic system in the cortex. In addition, OPCs express neuromodulatory factors, Prostaglandin D2 synthase (PTGDS) and neuronal Pentraxin 2 (Nptx2/Narp) that signal to the neural networks[37]. Interestingly, in the same study PTGDS is shown as a downstream target of NG2 signaling where PTGDS mRNA level is reduced in NG2 KO mouse brain compared to WT brain. OPCs having the *CSPG4*^{A1131T} mutation might lead to OPC dysfunctioning and directly affect neuronal activity via pathways described above. Another interesting study has shown, as extracellular matrix molecules, CSPGs in astrocytes are highly upregulated in the amygdala and entorhinal cortex of subjects diagnosed with schizophrenia[38]. Likewise, CSPGs from patient OPCs might also have an effect on the extracellular matrix and neurons.

Myelin is lipid-rich membrane, which forms an insulating sheath around axons. Myelin is produced by oligodendrocytes in the central nervous system (CNS) and this process is called myelination. Myelination occurs during postnatal development and is modulated by electrical activity and axon-derived molecular signals[39]. For

instance, the neurotransmitter glutamate and neuregulin are important factors for the regulation of myelination[40]. Oligodendrocytes are the myelin-producing cells of the CNS and are generated from OPCs that are also connected to neurons as explained above. Thus, neuron-to-OPC signalling might be an intermediary process for initiation of myelination. Neurons might initiate myelination through regulation of neuroregulatory molecules from OPCs. This provides a control between OPCs and neurons before myelination occurs. In this scenario, patient OPCs having the *CSPG4*^{A131T} mutation might not modulate neurons properly which might lead to a delay or change in timing in the initiation of myelination.

Interestingly, Kucharova et al., showed lower number of OPCs, oligodendrocytes and myelination in NG2KO mouse spinal cord after induction of demyelinating lesions[41]. This implies the importance of the NG2 protein in OPCs with respect to differentiation into myelinating oligodendrocytes. Thus, OPCs with the *CSPG4*^{A131T} mutation might not be able to differentiate into oligodendrocytes efficiently, which might result in delayed myelination. Interestingly, it is known that chondroitin sulfate glycosaminoglycan (CS-GAG) side chains regulate the differentiation of OPCs[42]. CS-GAGs become down-regulated upon oligodendrocyte differentiation and removal of CS-GAGs promotes oligodendrocyte differentiation. Less modified NG2 protein on the cell membrane of patient OPCs might therefore alter the differentiation efficiency of OPCs into myelinating oligodendrocytes. Any delay in OPC differentiation and the process of myelination might affect neuronal connectivity. Interestingly, the onset of schizophrenia correlates with the timing of the myelination process during development. In addition patients might have less myelination or unstructured MBP, which can lead to reduced axonal size or slower axonal transfer. Remarkably, MRI data shown in Chapter 4 demonstrate substantial white matter abnormalities in patients carrying the *CSPG4*^{A131T} mutation, which is likely the result of reduced myelination.

As reviewed in Nave et al.,[43] the hypothetical model for defects in myelination resulting in schizophrenia might be the consequence of reduced myelination, altered axonal diameter and fast axonal transport caused by dysfunction of oligodendrocytes. Transcallosal cortical projections are myelinated and maintain long-range oscillations between cortical subfields[43]. Myelin dependent spike-timing-dependent plasticity disturbed axonal transport thereby affecting the protein composition of presynaptic terminals. Abnormal axonal development, which might cause cognitive impairment, was shown in more severe oligodendrocyte perturbations resulting from inflammations and demyelination. Electron microscopy can be used for further understanding the structure and the amount of myelin both *in vitro* differentiation of OPCs into myelinating oligodendrocytes and *in vivo* human OPCs transplanted mouse brains. Nevertheless, the *in vitro* differentiation efficiency of OPCs into myelinating oligodendrocytes is not as efficient as *in vivo* transplanted OPCs.

FUTURE DIRECTIONS

Co-culture experiments

Studying the interaction between neurons and OPCs is important to shed light on the effect of the *CSPG4*^{A131T} mutation on neurons. Future experiments for dissecting the potential pathogenic mechanisms of the different *CSPG4* mutations include co-culturing of neurons with mutant OPCs. In Chapter 3, we designed a protocol to generate OPC cultures to study the effect of the A131T mutation on the NG2 protein and in Chapter 4, we showed differences in modifications of the NG2 protein between OPCs from cases and controls. In Chapter 2, we described an improved differentiation protocol for the generation of mixed cultures of neurons and glia from human iPSCs. Even though we observed a low amount of NG2-positive cells in our mixed neural cultures, the electrophysiological characteristics of iPSCsderived neurons from

patient and control groups did not show obvious differences. From this result, we cannot definitely conclude whether the patient's neurons are affected by the *CSPG4*^{A131T} mutation or not. To answer these questions, co-culturing OPCs from cases and controls with neurons might show the effect of mutant OPCs on neurons. In addition, differentiating OPCs into oligodendrocytes in co-culture might emphasize myelination differences in *in vitro* conditions and help understanding the myelination abnormalities of patient versus control OPC-derived oligodendrocytes. Possible *in vitro* myelination differences between patient and control cells might explain the difference that we observed in the MRI data in chapter 4.

Another important cell type in our mixed iPSC-derived neural cultures is astrocytes, which are present in a ratio of 60% neurons and 40% astrocytes. Several studies have shown that OPCs can differentiate into protoplasmic astrocytes in gray matter[44,45]. However, these results were not reproduced in other studies[46,47]. Likewise, in our OPC cultures, we did not observe astrocytes and NG2 protein was not expressed in GFAP positive cells. Remarkably, astrocytes have a dual role both in pathogenesis and in repair of the inflammatory demyelination process in MS[48]. Fibrous astrocytes dominate areas close to axon bundles in white matter[49]. Upregulation of GFAP, gliosis, has been used as a marker for pathology such in MS and Alzheimer's disease[50]. It was also shown that astrocytes induce OPC proliferation and prevent OPC migration and maturation[51]. It would therefore be interesting to co-culture iPSC-derived astrocytes and OPCs from patients and controls to check the morphology, GFAP expression level of astrocytes and proliferation and differentiation efficiency of OPCs.

Sakry et al., showed that the NG2 ectodomain can be cleaved by α-secretase which regulates neuronal activity[35]. The production of the extracellular part of the protein containing the α-secretase cleavage region and adding it to the medium of neurons might provide information about the effect of the mutation-containing region on electrophysiological properties of neurons.

Generation of humanized mouse brains

The disorders of myelin have become compelling targets for cell-based therapy. Firstly, isolation of human glial progenitor cells (hGPCs)[52,53] from human brains was an important step to be able to study the development of hGPCs *in vitro*. Then, the generation of hGPCs from patient-derived iPSCs has made it possible to study patient-specific causes of myelination disorders. *In vivo* experiments using transplantation of hGPCs in mice was shown in Wang et al.[54]. In this study, human glial chimeric mouse brains were generated for disease modeling of myelin disorders, in which transplanted hGPCs expanded within the murine hosts, and over time dominated the host brain. Specifically, the engrafted human progenitor cells differentiated into astrocytes and oligodendrocytes in a hypomyelinated environment. The generation of this chimeric mouse brain model allows for further dissection of the human specific contribution/role of glia in health and disease such as human specific glial infections and inflammatory disorders. Fascinatingly, using patient-derived hGPCs from iPSCs we can now establish mice with a fully humanized disease-specific astroglial brain composition, which is an important advance to study the pathogenesis of human neurological and neuropsychiatric disease[55].

Transplantation of iPSC-derived OPCs from patients with schizophrenia and healthy controls into myelin-deficient mice and subsequent assessment of the effect of the *CSPG4*^{A131T} mutation on OPC morphology, myelination and migration would shed light on the effect of the mutation *in vivo*. In addition, we generated a bacterial artificial chromosome (BAC) transgenic mouse model, carrying the human gene with the *CSPG4*^{A131T} mutation aiming to have a mouse expressing the mutant human NG2 protein. Mouse chimeric transplantation models should allow us to study the effect of the mutation in early brain development, which might not be as feasible under *in vitro* conditions. Importantly, in mouse, the reference amino acid at position 131 is threonine, corresponding to

the patient mutation *CSPG4*^{A131T} that is therefore predicted to have a benign effect of the mutation in mouse. Interestingly, a similar situation was described for the human *SNCA*^{A53T} mutation, causative for autosomal dominant Parkinson's disease, in which the reference amino acid at mouse SCNA position 53 is a threonine[56]. Even though the expression of the reference human sequence in mouse is benign, the mutant human *SNCA* sequence is highly pathogenic. Together with the cellular and molecular experiments we also aim to perform behavioral tests in the human BAC transgenic *CSPG4*^{A131T} mice compared to human wild type BAC transgenic *CSPG4* mice for further understanding the effect of the *CSPG4*^{A131T} mutation. Nevertheless, it is important to recall that mice and human have different genetic backgrounds; therefore there is a need for human specific studies together with mouse models.

Drug screening

Animal models for drug screening have some limitations such as obvious genetic background differences. For instance, some drugs have been developed that showed therapeutic effects in rodent models of ALS and Alzheimer's disease but which proved to be ineffective in the treatment of human patients[57,58]. Therefore, the development of screening tools with patient-derived iPSCs can have important contributions to disease modeling in a human genetic background.

Accordingly, many patient-specific iPSC lines of neurodegenerative disorders have been established and used for drug screening. For instance, the first drug validation was successfully reported for Rett syndrome and in familial dysautonomia[57] which holds promise for the potential application of iPSCs in drug screenings. Nevertheless, drug screening for psychiatric disorders is more difficult as there are multiple rare candidate genes for psychiatric disorders. Focusing on personalized medicine would support effective drug screening. In Brennand et al., iPSC-derived neurons show reduced neuronal connectivity, which was improved with Loxapine treatment, although this effect could not be replicated with other antipsychotic drugs[3]. Also, in a recent paper, iPSC-derived neurons from bipolar patients were found to respond differently to lithium[59]. Overall, iPSCs are a promising model to test therapeutic candidates, which can be further translated into clinical trials.

CONCLUDING REMARKS

Schizophrenia is a destructive psychiatric illness. With iPSC technology it is now possible to generate live patient-derived cells *in vitro*. However, there are still limitations such as the challenge to capture the complex environmental contribution to schizophrenia pathogenesis. Nevertheless, with the increasing number of techniques and strategies, iPSC research will continue to enlighten how molecular and cellular mechanisms are disrupted not only in schizophrenia, but also in other psychiatric and neurodegenerative illnesses.

REFERENCES

1 Miura K, Okada Y, Aoi T, Okada A, Takahashi K, Okita K et al. Variation in the safety of induced pluripotent stem cell lines. Nat Biotechnol 2009; 27: 743–5.

2 Takahashi K, Yamanaka S. Induction of pluripotent stem cells from mouse embryonic and adult fibroblast cultures by defined factors. Cell 2006; 126: 663–76.

3 Brennand KJ, Simone A, Jou J, Gelboin-Burkhart C, Tran N, Sangar S et al. Modelling schizophrenia using human induced pluripotent stem cells. Nature 2011; 473: 221–5.

4 Bonifati V. Genetics of Parkinson's disease--state of the art, 2013. Parkinsonism Relat Disord 2014; 20 Suppl 1: S23–8.

5 Gaj T, Gersbach CA, Barbas CF. ZFN, TALEN, and CRISPR/Cas-based methods for genome engineering. Trends Biotechnol 2013; 31: 397–405.

6 Kiskinis E, Sandoe J, Williams LA, Boulting GL, Moccia R, Wainger BJ et al. Pathways disrupted in human ALS motor neurons identified through genetic correction of mutant SOD1. Cell Stem Cell 2014; 14: 781–95.

7 Wen Z, Nguyen HN, Guo Z, Lalli MA, Wang X, Su Y et al. Synaptic dysregulation in a human iPS cell model of mental disorders. Nature 2014; 515: 414–418.

8 Bardy C, van den Hurk M, Eames T, Marchand C, Hernandez R V., Kellogg M et al. Neuronal medium that supports basic synaptic functions and activity of human neurons in vitro. Proc Natl Acad Sci 2015; : 201504393.

9 Lancaster MA, Renner M, Martin C-A, Wenzel D, Bicknell LS, Hurles ME et al. Cerebral organoids model human brain development and microcephaly. Nature 2013; 501: 373–9.

10 Paşca AM, Sloan S a, Clarke LE, Tian Y, Makinson CD, Huber N et al. Functional cortical neurons and astrocytes from human pluripotent stem cells in 3D culture. Nat Methods 2015; 12. doi:10.1038/nmeth.3415.

11 Kim YH, Choi SH, D'Avanzo C, Hebisch M, Sliwinski C, Bylykbashi E et al. A 3D human neural cell culture system for modeling Alzheimer's disease. Nat Protoc 2015; 10: 985–1006.

12 Miller JD, Ganat YM, Kishinevsky S, Bowman RL, Liu B, Tu EY et al. Human iPSC-based modeling of late-onset disease via progerin-induced aging. Cell Stem Cell 2013; 13: 691–705.

13 Espuny-Camacho I, Michelsen K a., Gall D, Linaro D, Hasche A, Bonnefont J et al. Pyramidal Neurons Derived from Human Pluripotent Stem Cells Integrate Efficiently into Mouse Brain Circuits In Vivo. Neuron 2013; 77: 440–456.

14 Nishiyama A, Dahlin KJ, Prince JT, Johnstone SR, Stallcup WB. The primary structure of NG2, a novel membrane-spanning proteoglycan. J Cell Biol 1991; 114: 359–71.

15 Kang SH, Fukaya M, Yang JK, Rothstein JD, Bergles DE. NG2+ CNS glial progenitors remain committed to the oligodendrocyte lineage in postnatal life and following neurodegeneration. Neuron 2010; 68: 668–681.

16 Sekar A, Bialas AR, de Rivera H, Davis A, Hammond TR, Kamitaki N et al. Schizophrenia risk from complex variation of complement component 4. Nature 2016; advance on. doi:10.1038/nature16549.

17 Niehaus a, Stegmüller J, Diers-Fenger M, Trotter J. Cell-surface glycoprotein of oligodendrocyte progenitors involved in migration. J Neurosci 1999; 19: 4948–4961.

18 Fang X, Burg MA, Barritt D, Dahlin-Huppe K, Nishiyama A, Stallcup WB. Cytoskeletal reorganization induced by engagement of the NG2 proteoglycan leads to cell spreading and migration. Mol Biol Cell 1999; 10: 3373–87.

19 Kucharova K, Stallcup WB. The NG2 proteoglycan promotes oligodendrocyte progenitor proliferation and developmental myelination. Neuroscience 2010; 166: 185–94.

20 Timpl R, Tisi D, Talts JF, Andac Z, Sasaki T, Hohenester E. Structure and function of laminin LG modules. Matrix Biol 2000; 19: 309–17.

21 Biname F, Sakry D, Dimou L, Jolivel V, Trotter J. NG2 regulates directional migration of oligodendrocyte precursor cells via Rho GTPases and polarity complex proteins. J Neurosci 2013; 33: 10858–10874.

22 Hughes EG, Kang SH, Fukaya M, Bergles DE. Oligodendrocyte progenitors balance growth with self-repulsion to achieve homeostasis in the adult brain. Nat Neurosci 2013; 16: 668–76.

23 Binamé F, Sakry D, Dimou L, Jolivel V, Trotter J. NG2 regulates directional migration of oligodendrocyte precursor cells via Rho GTPases and polarity complex proteins. J Neurosci 2013; 33: 10858–74.

24 Bergles DE, Roberts JD, Somogyi P, Jahr CE. Glutamatergic synapses on oligodendrocyte precursor cells in the hippocampus. Nature 2000; 405: 187–91.

25 Burg MA, Nishiyama A, Stallcup WB. A central segment of the NG2 proteoglycan is critical for the ability of glioma cells to bind and migrate toward type VI collagen. Exp Cell Res 1997; 235: 254–64.

26 Tillet E, Gential B, Garrone R, Stallcup WB. NG2 proteoglycan mediates beta1 integrin-independent cell adhesion and spreading on collagen VI. J Cell Biochem 2002; 86: 726–36.

27 Lin S, Bergles DE. Synaptic signaling between GABAergic interneurons and oligodendrocyte precursor cells in the hippocampus. Nat Neurosci 2004; 7: 24–32.

28 Bergles DE, Jabs R, Steinhäuser C. Neuron-glia synapses in the brain. Brain Res Rev 2010; 63: 130–7.

29 Vélez-Fort M, Maldonado PP, Butt AM, Audinat E, Angulo MC. Postnatal switch from synaptic to extrasynaptic transmission between interneurons and NG2 cells. J Neurosci 2010; 30: 6921–9.

30 Lin S-C, Huck JHJ, Roberts JDB, Macklin WB, Somogyi P, Bergles DE. Climbing fiber innervation of NG2-expressing glia in the mammalian cerebellum. Neuron 2005; 46: 773–85.

31 Mangin J-M, Li P, Scafidi J, Gallo V. Experience-dependent regulation of NG2 progenitors in the developing barrel cortex. Nat Neurosci 2012; 15: 1192–4.

32 Kukley M, Kiladze M, Tognatta R, Hans M, Swandulla D, Schramm J et al. Glial cells are born with synapses. FASEB J 2008; 22: 2957–69.

33 Simon C, Götz M, Dimou L. Progenitors in the adult cerebral cortex: cell cycle properties and regulation by physiological stimuli and injury. Glia 2011; 59: 869–81.

34 Wake H, Lee PR, Fields RD. Control of local protein synthesis and initial events in myelination by action potentials. Science 2011; 333: 1647–51.

35 Sakry D, Neitz A, Singh J, Frischknecht R, Marongiu D, Binamé F et al. Oligodendrocyte precursor cells modulate the neuronal network by activity-dependent ectodomain cleavage of glial NG2. PLoS Biol 2014; 12: e1001993.

36 Sakry D, Neitz A, Singh J, Frischknecht R, Marongiu D, Binamé F et al. Oligodendrocyte precursor cells modulate the neuronal network by activity-dependent ectodomain cleavage of glial NG2. PLoS Biol 2014; 12: e1001993.

37 Sakry D, Yigit H, Dimou L, Trotter J. Oligodendrocyte precursor cells synthesize neuromodulatory factors. PLoS One 2015; 10: e0127222.

38 Pantazopoulos H, Woo T-UW, Lim MP, Lange N, Berretta S. Extracellular matrix-glial abnormalities in the amygdala and entorhinal cortex of subjects diagnosed with schizophrenia. Arch Gen Psychiatry 2010; 67: 155–66.

39 Ahrendsen JT, Macklin W. Signaling mechanisms regulating myelination in the central nervous system. Neurosci Bull 2013; 29: 199–215.

40 Yates D. Myelination: Switching modes of myelination. Nat Rev Neurosci 2014; 15: 66–67.

41 Kucharova K, Stallcup WB. NG2-proteoglycan-dependent contributions of oligodendrocyte progenitors and myeloid cells to myelin damage and repair. J Neuroinflammation 2015; 12: 161.

42 Karus M, Ulc A, Ehrlich M, Czopka T, Hennen E, Fischer J et al. Regulation of oligodendrocyte precursor maintenance by chondroitin sulphate glycosaminoglycans. Glia 2015. doi:10.1002/glia.22928.

43 Nave K-A. Myelination and support of axonal integrity by glia. Nature 2010; 468: 244–252.

44 Zhu X, Hill RA, Nishiyama A. NG2 cells generate oligodendrocytes and gray matter astrocytes in the spinal cord. Neuron Glia Biol 2008; 4: 19–26.

45 Huang W, Zhao N, Bai X, Karram K, Trotter J, Goebbels S et al. Novel NG2-CreERT2 knock-in mice demonstrate heterogeneous differentiation potential of NG2 glia during development. Glia 2014; 62: 896–913.

46 Rivers LE, Young KM, Rizzi M, Jamen F, Psachoulia K, Wade A et al. PDGFRA/NG2 glia generate myelinating oligodendrocytes and piriform projection neurons in adult mice. Nat Neurosci 2008; 11: 1392–401.

47 Komitova M, Serwanski DR, Lu QR, Nishiyama A. NG2 cells are not a major source of reactive astrocytes after neocortical stab wound injury. Glia 2011; 59: 800–9.

48 Nair A, Frederick TJ, Miller SD. Astrocytes in multiple sclerosis: a product of their environment. Cell Mol Life Sci 2008; 65: 2702–20.

49 Butt AM, Duncan A, Berry M. Astrocyte associations with nodes of Ranvier: ultrastructural analysis of HRP-filled astrocytes in the mouse optic nerve. J Neurocytol 1994; 23: 486–99.

50 Eng LF. Glial fibrillary acidic protein (GFAP): the major protein of glial intermediate filaments in differentiated astrocytes. J Neuroimmunol 1985; 8: 203–14.

51 Fok-Seang J, Mathews GA, ffrench-Constant C, Trotter J, Fawcett JW. Migration of oligodendrocyte precursors on astrocytes and meningeal cells. Dev Biol 1995; 171: 1–15.

52 Roy NS, Wang S, Harrison-Restelli C, Benraiss A, Fraser RAR, Gravel M et al. Identification, Isolation, and Promoter-Defined Separation of Mitotic Oligodendrocyte Progenitor Cells from the Adult Human Subcortical White Matter. J Neurosci 1999; 19: 9986–9995.

53 Windrem MS, Roy NS, Wang J, Nunes M, Benraiss A, Goodman R et al. Progenitor cells derived from the adult human subcortical white matter disperse and differentiate as oligodendrocytes within demyelinated lesions of the rat brain. J Neurosci Res 2002; 69: 966–75.

54 Wang S, Bates J, Li X, Schanz S, Chandler-Militello D, Levine C et al. Human iPSC-derived oligodendrocyte progenitor cells can myelinate and rescue a mouse model of congenital hypomyelination. Cell Stem Cell 2013; 12: 252–264.

55 Goldman SA, Nedergaard M, Windrem MS. Modeling cognition and disease using human glial chimeric mice. Glia 2015; 63: 1483–93.

56 Lee MK, Stirling W, Xu Y, Xu X, Qui D, Mandir AS et al. Human alpha-synuclein-harboring familial Parkinson's disease-linked Ala-53 --> Thr mutation causes neurodegenerative disease with alpha-synuclein aggregation in transgenic mice. Proc Natl Acad Sci U S A 2002; 99: 8968–73.

57 Han SSW, Williams L a, Eggan KC. Constructing and deconstructing stem cell models of neurological disease. Neuron 2011; 70: 626–44.

58 Holmes C, Boche D, Wilkinson D, Yadegarfar G, Hopkins V, Bayer A et al. Long-term effects of Abeta42 immunisation in Alzheimer's disease: follow-up of a randomised, placebo-controlled phase I trial. Lancet (London, England) 2008; 372: 216–23.

59 Mertens J, Wang Q-W, Kim Y, Yu DX, Pham S, Yang B et al. Differential responses to lithium in hyperexcitable neurons from patients with bipolar disorder. Nature 2015; 527: 95–99.

Appendix

SUMMARY

Schizophrenia is a complex psychotic disorder to model. The first challenge arises from the complexity of brain physiology in which there are multiple distinct cell types: neurons, glia, microglia and pericytes, and their variety of intercellular signaling. The other main difficulty is the unfeasibility of examining living brain tissue from patients with schizophrenia. Mainly, schizophrenia research is based on genetics, postmortem studies, neuroimaging and animal models to investigate the etiology of the disorder. Until recently, there were no technologies available to investigate schizophrenia and other neuropsychiatric disorders using living human neural tissue. Therefore, the development of induced Pluripotent Stem Cell (iPSC) technology has offered a unique opportunity for studying living neural cells of individual patients. The aim of this thesis is to advance our knowledge of the etiology and pathophysiology of schizophrenia through the use of patient-derived iPSCs.

Chapter 1 of this thesis is an introduction to schizophrenia. Pathophysiological models to study schizophrenia, iPSC technology and different neural protocols are described.

Chapter 2 explains a detailed neural differentiation protocol that enables differentiation of human iPSCs into functionally mature neurons together with glia. Neurons derived from this protocol exhibited all the major physiological hallmarks expected from neurons that were assessed by both immunofluorescence and electrophysiological parameters. The protocol generated stable and reproducible results, showing low variability within and between lines. Moreover, the vast majority of cells were active and capable of firing repetitively in response to depolarizing current injections.

Chapter 3 focuses on designing a protocol for iPSC-derived oligodendrocyte lineage cells. Oligodendrocyte Precursor Cells (OPCs) are generated from human iPSC-derived Neural Precursor Cells by the sequential introduction of factors required for OPC development *in vivo*. iPSC-derived OPCs can proliferate, migrate and differentiate into myelin basic protein-expressing myelinating oligodendrocytes.

Chapter 4 describes a series of experiments, which yield novel insights into schizophrenia pathophysiology through a genetic and iPSC-based investigation of families with a high incidence of schizophrenia. Even though schizophrenia is a polygenic disorder, the heritability is high and families with a Mendelian pattern of disease inheritance are not infrequently observed. Therefore, we examined a family with a high incidence of schizophrenia in which healthy siblings were used as a control for the derivation of iPSCs. Using linkage-based exome sequencing, a missense mutation (A131T) in the *CSPG4* gene was found to segregate with schizophrenia. Multiple additional families were identified carrying rare variants in *CSPG4* segregating with schizophrenia, together highlighting *CSPG4* as a novel candidate gene for schizophrenia. The *CSPG4* gene encodes the membrane protein Neural/glial antigen 2 (NG2), which is highly expressed in OPCs. We therefore examined the functional impact of the $CSPG4^{A131T}$ mutation in iPSC-derived neural cells from patients with schizophrenia and their healthy siblings. Although no electrophysiological differences were observed between neurons of affected carriers and their unaffected non-carrier siblings, multiple abnormalities of OPCs were observed to segregate between iPSCs derived from affected versus unaffected siblings. In particular, patient-derived OPCs exhibited altered morphology, intracellular retention of NG2 and impaired post-translational modification of NG2 protein, together confirming the pathogenicity of the $CSPG4^{A131T}$ mutation and highlighting the importance of the oligodendrocyte lineage in schizophrenia pathophysiology. On the basis of these findings, diffusion tensor imaging was performed on affected and unaffected family members, and matched general population controls, which confirmed that the *CSPG4* mutation might result in a significant impairment of white matter integrity.

Chapter 5 is a general discussion about the current theoretical and technical challenges for iPSC-based neural disease modeling. In addition, future directions are proposed to further advance our understanding of the neurobiological mechanisms of schizophrenia.

SAMENVATTING

Schizofrenie is een complexe psychiatrische ziekte om te bestuderen. Allereerst door de mate van complexiteit van de fysiologie van de hersenen; verschillende celtypen zoals neuronen, glia, microglia en pericyten gaan interacties met elkaar aan waar nog maar weinig over bekend is. Daarnaast is het praktisch onmogelijk om levend hersenweefsel van patiënten te onderzoeken. Onderzoek naar schizofrenie centreert zich doorgaans rond genetica, hersenbeeldvorming, *postmortem* studies en diermodellen om te proberen de oorzaken van deze ziekte te achterhalen. De ontwikkeling van nieuwe technieken maakt het nu mogelijk om patiënt specifieke hersencellen te creëren uit geïnduceerde pluripotente stamcellen (iPSC). Dit proefschrift richt zich op het bestuderen van schizofrenie met behulp van iPSC technologie.

Hoofdstuk 1 van dit proefschrift is een introductie over schizofrenie en beschrijft de modellen die gebruikt worden om deze ziekte te bestuderen. Daarnaast worden de verschillende huidige protocollen om hersencellen van iPSC's te maken besproken.

Hoofdstuk 2 beschrijft in detail de ontwikkeling van een protocol dat gebruikt kan worden om efficiënt functionele en mature neuronale netwerken te differentiëren van iPSCs. De verkregen neuronen bezitten de voornaamste kenmerken van volwassen functionaliteit zoals wordt gedemonstreerd met immunofluorescentie en elektrofysiologische technieken. Door middel van dit protocol is het mogelijk om stabiele resultaten te verkrijgen met verschillende cellijnen. Bovendien is de meerderheid van de neuronen die elektrofysiologisch gekarakteriseerd werd in staat om voor langere tijd herhaald actiepotentialen te vuren als respons op depolariserende spanning.

Hoofdstuk 3 richt zich op het beschrijven van een protocol voor het deriveren van cellen in de lijn van oligodendrocyten. Oligodendrocyt voorloper cellen (OPC) kunnen van iPSCs gemaakt worden door factoren aan het medium toe te voegen die bekend zijn uit de embryonale ontwikkeling van oligodendrocyten. De verkregen OPCs bezitten de bekende OPCs markers en zijn in staat om te prolifereren, te migreren en kunnen in oligodendrocyten differentiëren die myeline produceren in *ex vivo* condities.

Hoofdstuk 4 beschrijft een serie genetische en iPSC-experimenten gericht op het ontrafelen van nieuwe inzichten in het ziektemechanisme van schizofrenie door families te bestuderen met een hoge incidentie van deze ziekte. Ondanks dat schizofrenie een polygene stoornis is, is de erfelijkheid van de ziekte hoog en zijn families met een mendeliaanse patroon van overerving van deze ziekte niet extreem zeldzaam. Deze studie richt zich op een Nederlandse familie met een mendeliaans overervingspatroon. Door het *sequencen* van de *exomen* van patiënten en gezonde familieleden hebben we een *missense* mutatie (A131T) in het *CSPG4* gen ontdekt. In verschillende Mexicaanse families met een hoge incidentie van schizofrenie hebben we andere mutaties in hetzelfde gen gevonden, wat suggereert dat mutaties in het *CSPG4* gen causaal voor schizofrenie kunnen zijn. Neural/glial antigen 2 (NG2) is het eiwitproduct van het *CSPG4* gen en is een van de kenmerkende eiwitten voor OPCs. In OPC's van patiënten uit de Nederlandse familie vinden we retentie van NG2 in het endoplasmatisch reticulum. Daarnaast wordt er minder van de gemodificeerde vorm van het NG2 eiwit gevonden in patiënten OPC's en hebben deze een andere morfologie. Al deze bevindingen suggereren een significant effect van de mutatie in *CSPG4* in relatie tot schizofrenie. Op basis van deze bevindingen zijn *diffusion tensor imaging* opnamen gemaakt van de hersenen van leden uit de Nederlandse familie die vergeleken zijn met gelijkwaardige beeldvorming van mensen uit de normale populatie. De resultaten hiervan bevestigen dat de mutatie in *CSPG4* correleert met een ernstig defect in de integriteit van de witte stof in de hersenen.

Hoofdstuk 5 is een algemene discussie over de controversiële onderwerpen en uitdagingen die komen kijken bij onderzoek naar schizofrenie met iPSC technologie. Daarnaast worden toekomstige onderzoeksrichtingen besproken die kunnen bijdragen aan meer inzicht in de neurobiologische mechanismen die ten grondslag liggen aan schizofrenie.

PhD Portfolio

Name:	Nilhan Günhanlar
PhD period:	November 2010- May 2016
Department:	Psychiatry
Promotor:	Prof.dr. Steven A. Kushner
Co-promotor:	Dr. Femke M.S. de Vrij
Research School:	Graduate School Neuroscience Amsterdam Rotterdam (ONWAR)

PhD training	**Year**
General and Specific courses (e.g. Research school, Medical Training)	
· Biomedical English Writing and Communication, Erasmus MC. Rotterdam, the Netherlands	2015
· Translational Approaches in Schizophrenia, ONWAR. Utrecht, the Netherlands	2015
· Neuro-Oncology/Glioma, ONWAR. Utrecht, the Netherlands	2015
· Research Integrity in Science, Erasmus MC. Rotterdam, the Netherlands	2015
Seminars and workshops	
· 8th Dutch Society for Stem Cell Research (DSSCR) Utrecht/ the Netherlands (poster presentation)	2015
· 10th Dutch Endo-Neuro-Psycho Meeting (ENP). Lunteren/the Netherlands	2012
· 9th Dutch Endo-Neuro-Psycho Meeting (ENP). Lunteren/the Netherlands (poster presentation)	2011
· Masterclass Prof. Oliver Brustle. Amsterdam/the Netherlands (oral presentation)	2014
· Annual Netherlands iPSCs meeting. Leiden/ the Nethlerlands	2011/2012
· Neuroscience carreer event. Amsterdam/the Netherlands	2015
Conferences	
· The XII European *Meeting* on *Glial* Cell Function in Health and Disease. Bilbao/Spain	2015
· 44th Annual meeting of Society for Neuroscience (SfN) Washington D.C./USA (poster presentation)	2014
· 5th Cold Spring Harbour Laboratory conference on Glia in Health and Disease. New York/ USA (poster presentation)	2014
· Graduate School Neurosciences Amsterdam Rotterdam (ONWAR) Retreat. Zeist/the Netherlands (poster presentation)	2013
· Cell Press, Stem Cell Symposia. Using Stem Cells to Model and Treat Human Disease. Los-Angelas/USA (poster presentation)	2013
· International Society for Stem Cell Conference (ISSCR) Regional Form. San Francisco/USA (poster presentation)	2012
· Cell Press, Stem Cell Symposia. Stem Cell Programming and Lisbon, Portugal (poster presentation)	2011
Teaching	
Minor students	2011/2012
Supervising master students	
Bas Lendemeijer	2012-2014
Maarouf Baghdadi	2013-2015

List of Publications

Oligodendrocyte precursor cells generated from induced pluripotent stem cells derived neural progenitors
Gunhanlar N*, *Lendemeijer B**, *Baghdadi M, Shpak G, Slump DE, Hoogendijk WJG, de Vrij FM# and Kushner SA#*
Manuscript in preparation

A robust differentiation protocol for human induced pluripotent stem cell derived neural networks with improved electrophysiological maturity
Gunhanlar N*, *Shpak G**, *van der Kroeg M, Gouty-Colomer L-A, Munshi ST, Lendemeijer B, Dupont C, Gribnau J, Borst JG , de Vrij FM# and Kushner SA#*
Manuscript in preparation

CSPG4 mutations implicate oligodendrocyte precursor cell dysfunction as a pathophysiological mechanism of schizophrenia
*de Vri FM**, *Bouwkamp CG**, ***Gunhanlar N****, *Shpak G, Lendemeijer B, Baghdadi M, Ghazvini M, Li TM, Quadri M, Olgiati S, Breedveld GJ, Coesmans M, Mientjes E, de Wit T, Verheijen FW, Beverloo HB, Cohen D, Kok RM, Bakker PR, Nijburg A, Spijker AT, Haffmans PJ, Hoencamp E, Bergink V, GROUP consortium, Vorstman JA, Amin N, Langen CD, Hofman A, van Duijn CM, Hoogendijk WJ, Ikram MA, Vernooij MW, Tiemeier H, Uitterlinden AG, Elgersma Y, Distel B, Gribnau J, Ophoff RA, White T, Bonifati V, Kushner SA.*
Manuscript in preparation

Epigenetic characterization of the FMR1 promoter in induced pluripotent stem cells from human fibroblasts carrying an unmethylated full mutation.
*de Esch CE, Ghazvini M, Loos F, Schelling-Kazaryan N, Widagdo W, Munshi ST, van der Wal E, Douben H, **Gunhanlar N**, Kushner SA, Pijnappel WW, de Vrij FM, Geijsen N, Gribnau J, Willemsen R.*
Stem Cell Reports. 2014 Oct 14;3 (4):548-55.

The pluripotency factor-bound intron 1 of Xist is dispensable for X chromosome inactivation and reactivation in vitro and in vivo.
*Minkovsky A, Barakat TS, Sellami N, Chin MH, **Gunhanlar N**, Gribnau J, Plath K.*
Cell Rep. 2013 Mar 28;3(3):905-18.

RNF12 activates Xist and is essential for X chromosome inactivation.
*Barakat TS, **Gunhanlar N**, Pardo CG, Achame EM, Ghazvini M, Boers R, Kenter A, Rentmeester E, Grootegoed JA, Gribnau J.*
PLoS Genet. 2011 Jan 27;7(1):e1002001.

* : Shared first authorship
# : Shared last authorship

Curriculum Vitae

Nilhan Günhanlar was born on August 25, 1985 in Nicosia, the capital of Cyprus and raised in the town called Alsancak/Karavas in the Kyrenia district. After graduating from 19 Mayis T.M. College in Kyrenia, she studied Molecular Biology and Genetics at Bilkent University, Ankara, Turkey between 2002 and 2007 and got her Bachelor of Science degree. During her bachelor studies, Nilhan completed her summer internships in different labs with various biological disciplines; in 2004 at Cyprus Institute of Neurology and Genetics, Nicosia, Cyprus under supervision of Dr. Stavros Malas, with a focus on the human SOX1 gene in Amyotrophic Lateral Sclerosis, in 2005 at Rikshospitalet, The National Hospital of Oslo, Norway in the group of Prof.dr. Arne Klungland about Base Excision Repair mechanisms in mitochondrial DNA and in 2006 at Kansas State University, Department of Physiology and Anatomy, Kansas USA in the group of Prof.dr. Philine Wangemann about Oxidative and Nitrative Stress in Pendred Syndrome in Inner Ear. For her bachelor graduation project in Bilkent University, she joined in the group of Dr. Cengiz Yakıcıer and was involved in the identification of internal tandem duplications in childhood acute myeloid leukemia. After her bachelor graduation, Nilhan worked as a research assistant at Medical College of Georgia, Augusta, Georgia, USA between 2007 and 2008 to investigate the molecular mechanisms of nuclear reprogramming and genomic imprinting in mouse stem cells in the group of Dr. Ali Eroglu's. In 2008, she started her master's degree studies in the Molecular Medicine master program at Erasmus MC, Rotterdam. She performed her master project at the department of Reproduction and Development, working in the group of Prof.dr. Joost Gribnau, focusing on the role of pluripotency factors in X chromosome inactivation. After graduating from the Molecular Medicine master program, Nilhan began her PhD in the department of Psychiatry at Erasmuc MC, Rotterdam, under supervision of Prof.dr. Steven Kushner and Dr. Femke de Vrij in November 2010. Her research focused on establishing Induced Pluripotent Stem cell-derived neural cells from a family with a high incidence of schizophrenia. At present, Nilhan is still working in the lab of Prof. dr. Steven Kushner.

Acknowledgements

Doing a PhD is a serious, controversial, hectic and glamorous process. It is composed of difficult times and easier times; sunshines and dark winters; statistically significant results and variability problems; dreaming having a Nobel prize and deciding never going to do science again... In these five (and a half) years, patience has been the aid, together with various people.

… Those people… this part is for you!

Thank you very much!

Firstly, I would like to thank to my promoter, Prof.dr. Steven Kushner. Dear Steven, thanks for this exceptional opportunity to allow me to do a PhD under your supervision, which was a life-changing event for me. Every conversation with you, whether scientific, philosophic or ordinary daily life discussion, was outstandingly inspiring. Thanks for always believing and supporting as a scientist, person and a friend. Going to be the first PhD graduate from "the coolest lab" is a premium position. Glad that these are not good-bye sentences and looking forward to the future times.

And my co-promoter Dr. Femke de Vrij... Dear Femke, thanks for all during different stages of my PhD; from iPSC to mature neurons, from supermix to organotypic slices, from showing how to take the best confocal images to correcting my thesis, from Lisbon to Los Angeles and more. I am so lucky that I did my PhD with such a humorous, caring and professional person. Now I know that it is possible to be a great scientist, mother and actress at the same time. Also, after five and a half years, I know how important it is to have a good lab journal. Hope to celebrate many papers, have more coffees/chats and meetings together.

I would like to thank to Prof.Dr. Joost Gribnau, Prof.Dr. Elly Hol and Prof.Dr. Ype Elgersma for kindly accepting to be in this thesis reading committee; and to Dr. Pim Pijnappel, Dr. Raymond Poot and Prof.Dr. Witte Hoogendijk for being this thesis committee member.

I would like to thank to the dearest-coolest Kushner lab people; Ane, Bas, Behi, Christian, Denise, Guy, Ineke, Ivo, Jay, Jeffrey, Kate, Maarouf, Marielle, Mark, Priyanka, Roberto, Shashini and Stefano.

Marielle, thanks for all the formal arrangements for my thesis with your patience and wisdom. Denizaa, thanks for all the mice work and loud music in the lab, without you this lab is so boring! Dear Behi, thanks for nice conversations, salt and chocolate supply! Hope you arrange the Iranian dinner soon (now this is a written proof ;)), we will have double PhD celebrations (may be in Iran!). Shashini, thanks for all the struggle to organize the cell culture world, without you everything would be a mess, and good luck with your PhD. Ane, sad to loose a fellow-late comer/leaver in the lab, however, happy to know that you have strong roots now in The Netherlands. Mark, thanks for

all your effort to teach me Dutch and good luck in designing the 3D cultures (Can I use some of the wells?). Hiii!! Priyanka, thanks for all the effort in explaining Image J and other programs ("search in google"). Can I call you when I finally do the Heat Map? I will miss you in the lab!!! Jay, thanks for your talk shows, music taste and your famous sentence "it could be worse". I will miss you too! Dear Guy, I am glad to have such a gentleman (and "dangerous") colleague =), hope to celebrate our paper soon! Christos and mIvo, it was great to know you guys! Million thanks for all your support, long conversations (mostly about psychology) and laughs during these years. I miss our long lab hours, jazz nights and dinners together. Annddd!!! my OPC guys, Bas and Maarouf… Without you this thesis would not be that perfect :P thanks a lot for your inputs and hard work. I know, one day, you are going to be great scientists and hire me as a postdoc, please remember me. Maarouf, you left me alone in immigrants' discussions!

And the ex-Kushner lab people, Jaime, Wouter, Cato, best neighbor-Laurie Anne, another 10euro Sander (I promise after my PhD, I will read "Kafka on the Shore"), and my gurbet Yagmur (I miss you when I wash the dishes), it has been an honor to have colleagues like you. Thousand thanks!

I would like to thank to Mehrnaz and Tracy, for the babies, without them this project could have never even started; next-door komsu Edwin, for all the troubleshooting helps (especially for Western Blots (jokes); Geeske, for the primary mouse neuron cultures; Elize, for the help in the histology lab and Leontine for migration experiments.

It has been 8 years that I have been researching in Erasmus MC. Thus, I also would like to thank to the people for their contribution to my research during my master years to the end of my PhD; especially to Prof.Dr. Dies Meijer and Dr. Martine Jaegle from the department of Cell Biology, Prof.Dr. Vincenzo Bonifati from the department of Clinical Genetics, Prof.Dr. Joost Gribnau, Prof.Dr. Anton Grootegoed, Dr. Willy Baarends, Christina, Catherine, Eveline, Stefan and Annegien, from the department of Reproduction and Development; Dr. Joke Tulen and Wai from the department of Psychiatry; Prof.Dr. Gerard Borst, Prof.Dr. Chris de Zeeuw, Prof.Dr. Hans van der Steen and the people of Elgersma's lab from the department of Neuroscience.

My paranimfs, Merih and Bas, thanks for accepting to be my paranimfs. Merikocum, in the Nieuwe Binnenweg, 14th and 23rd floors triangle; after tons of stories, dramas, happy hours, texts, emails, suggestions, ideas and comments, we made it! Thanks for always being there. Even though now we cannot share the daily life, I am glad to feel that we are connected. (For me, Nieuwe Binnenweg without you is like Rotterdam without the harbor). Basje, counting the annoying heterogeneous cultures (and other experiments too) was nicer with you (please let me know when FACS sorting will be ready :P). Thanks for everything, especially for our love for Rotterdam and daily walk in Erasmus (to touch the wall). Looking forward to the coming fun days in Kushner lab.

My sweet, traditional (!), expat family in The Netherlands, Iso, Beste, Merih, Nimet, Tunc, Rodos, Gorkem, Sinanagam, Soner,

Seda, Derya, Firat, Can, Ceyda, Safak, Ezgi, Ulas, Melike, Ekin, Yasemin, Oguz, Ozge, Fanny, Sofia, Umut, Angela, Aristea, Hegias, Zalihe, Nesrin and Iremom. I cannot explain how grateful I am to know you. It is difficult to fit here what you mean for me guys (destan olur). Thanks for all the holidays, parties, coffees, dinners, movies and endless support and love. Without you, for sure, I would not do this. (gurbet sizsiz cekilmez!). Looking forward to our future stories.

Speical thanks to Karin, life-long Bilkent buddies, Iremom (kaderimsin, kaderim kalacaksin), Seda (hayatimin bogasi senmissin yillar sonra anladim), Cansel, Gulino, Nilufer and Oyacim; and to the best journalists of “the Cyprus times” Verda, Hamis and Neri.

Ayrica, uzaklarda, hep yanimda olan Kibris’taki ailemin her uyesine tesekkur ederim. Erhan ve Unsel, sizin gibi kardeslerim oldugu icin cok sansliyim. Anne ve baba, sizin desteginiz ve sevgiliniz sayesinde asilamayacak zorluk yokmus. Siz bana hep guc verdiniz. Ne mutlu bana ki, sizin gibi bir ailem var. Her sey icin tesekkurler, sizi cok seviyorum.

Dear Stappers, needless to say, your breakfasts, big monitor and bitter chocolate Den Haag life are the main sponsors of this thesis writing process. Thanks for all zinho! Especially for the grammar critics, “finish it now!“ philosophy, cover design ideas, “trips to recover” holidays and power hugs. Kocham Cię...

Sincerely yours,

Nilhan